Mobile and wireless communications Enablers for the Twenty-twenty Information Society-II

# Deliverable D4.1
# Draft air interface harmonization and user plane design

Version: v1.0

2016-05-04

# Deliverable D4.1
# Draft air interface harmonization and user plane design

| | |
|---|---|
| **Grant Agreement Number:** | 671680 |
| **Project Name:** | Mobile and wireless communications Enablers for the Twenty-twenty Information Society-II |
| **Project Acronym:** | METIS-II |
| **Document Number:** | METIS-II/D4.1 |
| **Document Title:** | Draft air interface harmonization and user plane design |
| **Version:** | v1.0 |
| **Delivery Date:** | 2016-05-04 |
| **Editor(s):** | Malte Schellmann (Huawei ERC), Venkatkumar Venkatasubramanian (Nokia) |
| **Authors:** | Osman Aydin, Jens Gebert (ALUD), Jakob Belschner (Deutsche Telekom), Jamal Bazzi, Petra Weitkemper (DOCOMO Euro-Labs), Caner Kilinc, Icaro Leonardo Da Silva, Ali Zaidi (Ericsson), Malte Schellmann (Huawei ERC), Miltiadis Filippou, Ahmed Soud Salem (Intel), Marco Mezzavilla (New York University) Venkatkumar Venkatasubramanian, Patrick Marsch (Nokia), Milos Tesanovic, Yinan Qi (Samsung), Nandish Kuruvatti (Universität Kaiserslautern) Daniel Calabuig, Jose F. Monserrat (Universitat Politècnica de València) |
| **Keywords:** | air interface design, multi-connectivity, multi-service support, cellular protocol stack, 5G waveforms, user plane design |
| **Status:** | Final |
| **Dissemination level:** | Public |

# Abstract

The METIS-II project envisions the design of a new air interface in order to fulfil all the performance requirements of the envisioned 5G use cases including some extreme low latency use cases and ultra-reliable transmission, xMBB requiring additional capacity that is only available in very high frequencies, as well as mMTC with extremely densely distributed sensors and very long battery life requirements. Designing an adaptable and flexible 5G Air Interface (AI), which will tackle these use cases while offering native multi-service support, is one of the key tasks of METIS-II WP4. This deliverable will highlight the challenges of designing an AI required to operate in a wide range of spectrum bands and cell sizes, capable of addressing the diverse services with often diverging requirements, and propose a design and suitability assessment framework for 5G AI candidates.

# Executive summary

The METIS-II project envisions the design of a new air interface in order to fulfil all the performance requirements of the envisioned 5G use cases including some extreme low latency use cases and ultra-reliable transmission, xMBB requiring additional capacity that is only available in very high frequencies, as well as mMTC with extremely densely distributed sensors and very long battery life requirements. Designing an adaptable and flexible 5G Air Interface (AI), which will tackle these use cases while offering native multi-service support, is one of the key tasks of METIS-II WP4. This deliverable will highlight the challenges of designing an AI required to operate in a wide range of spectrum bands and cell sizes, capable of addressing the diverse services with often diverging requirements, and propose a design and suitability assessment framework for 5G AI candidates.

More specifically, in this deliverable we propose a unified way of describing 5G AI design proposals using a 5G service/frequency map, and capture different 5G AI design proposals. We then crucially propose a design and suitability assessment framework for 5G AI candidates. This framework focuses on "harmonization KPIs" and how to measure them (qualitatively / quantitatively). The deliverable proposes that evaluation of 5G AI candidates should, in addition to performance, include the "extent of harmonization", which is defined in this deliverable as a combination of features such as utilization of radio resources, implementation complexity, standardization effort, forward compatibility, and interaction with legacy systems. A comprehensive list of 5G AI design proposals, covering the entire envisaged range of 5G bands and services, is then provided. An initial evaluation of various AI design proposals using the described assessment framework is then carried out. Additionally, an initial overview of different User Plane aggregation approaches is provided. We then discuss the types of APIs which may need to be offered to higher layers to enable novel 5G radio resource management techniques. Additionally, under certain link conditions / deployment scenarios / traffic assumptions, some of the AI candidates may allow for better (in some but perhaps not all aspects) support of certain 5G Control Plane features – and this deliverable outlines the potential scope of these features.

# Contents

# List of Abbreviations and Acronyms

| | |
| :--- | :--- |
| **3GPP** | 3rd Generation Partnership Project |
| **4G** | 4th Generation of mobile networks |
| **5G-PPP** | 5th Generation Public-Private-Partnership |
| **AI** | Air Interface |
| **AIV** | Air Interface Variant |
| **AMC** | Adaptive modulation and coding |
| **API** | Application Programming Interface |
| **ARPU** | Average Revenue Per User |
| **BLER** | Block error-rate |
| **BMRS** | beam measurement reference signal |
| **BS** | Base Station |
| **CA** | Carrier Aggregation |
| **CAPEX** | Capital Expenditure |
| **CN** | Core Network |
| **CoP** | Control Plane |
| **CP** | Cyclic Prefix |
| **CSI** | Channel State Information |
| **CoMP** | Coordinated Multi-Point Transmission and Reception |
| **CTS** | Clear To Send |
| **D2D** | Device-to-Device |
| **DFTs-OFDM** | Discrete Fourier Transform spread OFDM (aka SC-FDMA) |
| **DL** | Downlink |
| **DSA** | Dynamic Spectrum Access |
| **E2E** | End-to-End |
| **eNB** | Evolved Node B |
| **EPA** | Extended Pedestrian A model |
| **ETU** | Extended Typical Urban model |
| **E-UTRAN** | Enhanced UTRAN |
| **EVM** | Error Vector Magnitude |
| **FBMC** | Filterbank Multi-Carrier |
| **FDMA** | Frequency Division Multiple Access |

| | |
| :--- | :--- |
| **FER** | Frame Error Rate |
| **FIR** | Finite Impulse response |
| **FFT** | Fast Fourier Transform |
| **FMT** | Filtered Multi-Tone |
| **F-OFDM** | Filtered OFDM |
| **FQAM** | frequency and quadrature amplitude modulation |
| **HW** | Hardware |
| **ICI** | Inter-Carrier Interference |
| **ISI** | Inter-Symbol Interference |
| **ISR** | Interference to signal ratio |
| **ITU** | International Telecommunication Union |
| **KPI** | Key performance indicator |
| **L2/L3** | Layer 2 (MAC + RLC + PDCP) / Layer 3 (RRC) |
| **LTE (-A)** | Long Term Evolution (Advanced) |
| **LTE-M** | Variant of LTE for M2M communications |
| **MAC** | Medium Access Control |
| **MBB** | Mobile Broadband |
| **MBMS** | Multimedia Broadcast Multicast Service |
| **MC** | Multi Connectivity |
| **MCS** | Modulation and Coding Scheme |
| **ML** | Maximum Likelihood |
| **MIMO** | Multiple-input Multiple-Output |
| **MMSE** | Minimum Mean Square Error |
| **mMTC** | Massive Machine-Type Communications |
| **NF** | Network Functions |
| **NGMN** | Next Generation Mobile Networks |
| **NR** | Next Generation Radio |
| **OOB** | Out-of-band |
| **OFDM** | Orthogonal Frequency Division Multiplex |

**Document:** METIS-II/D4.1      **Status:** final
**Version:** v1.0      **Dissemination level:** Public
**Date:** 2015-05-04

| | | | | |
|---|---|---|---|---|
| **OFDMA** | Orthogonal Frequency Division Multiple Access | | **SDMA** | Space Division Multiple Access |
| **OPEX** | Operating Expense | | **SDU** | Service Data Unit |
| **OQAM** | Offset QAM | | **SFN** | Single Frequency Network |
| **OSTBC** | Orthogonal space–time block code | | **S-GW** | Serving Gateway |
| **PAPR** | Peak-to-average power ratio | | **SSS** | Secondary Synchronization Signal |
| **PDCCH** | Physical Downlink Control Channel | | **SotA** | State of the Art |
| **PDCP** | Packet Data Convergence Protocol | | **SW** | Software |
| **P-GW** | Packet Gateway | | **TA** | Timing Advance |
| **PHY** | Physical layer | | **TDMA** | Time Division Multiple Access |
| **P-OFDM** | Pulse shaped OFDM | | **TeC** | Technology component |
| **PPN** | PolyPhase Network | | **TTI** | Transmit Time Interval |
| **PRB** | Physical Resource Block | | **UDN** | Ultra-dense Network |
| **RTS** | Request To Send | | **UE** | User Equipment |
| **QAM** | Quadrature Amplitude Modulation | | **UF-OFDM** | Universal filtered OFDM |
| **QoE** | Quality of Experience | | **UL** | Uplink |
| **QoS** | Quality of Service | | **uMTC** | Ultra-reliable Machine-Type Communications |
| **QOSTBC** | Quasi-orth. space-time block code | | **UP** | User Plane |
| **RAN** | Radio Access Network | | **UTRAN** | Universal Terrestrial RAN |
| **RAT** | Radio Access Technology | | **V2I** | Vehicle-to-Infrastructure |
| **RB** | Resource Block | | **V2V** | Vehicle-to-Vehicle |
| **RF** | Radio Frequency | | **V2X** | Vehicle-to-Anything |
| **RLC** | Radio Link Control | | **WF** | Waveform |
| **RRC** | Radio resource control | | **WLAN** | Wireless Local Area Network |
| **RS** | Reference Signal | | **W-OFDM** | Windowed OFDM |
| **SAP** | Service Access Point | | **WP** | Work Package |
| **SC** | Subcarrier | | **xMBB** | Extreme Mobile Broadband |
| **SC-FDMA** | Single-Carrier FDMA (aka DFTs-OFDM) | | **ZT** | Zero Tail |
| **SDN** | Software Defined Networking | | | |

# 1 Introduction

## 1.1 Objective of the document

A key question related to the 5G system design is how the different air interface (AI) candidate technologies, including LTE-A evolution, can be integrated into one overall 5G AI, such that this design maximally benefits from the wide landscape of bands, cell types etc., and such that both the complexity of the standard and that of the implementation are minimized, while the performance of individual technologies is not sacrificed. This question is address within METIS-II by Work Package 4 (WP4), and the present deliverable aims at answering some of the key underlying unknowns.

The main objectives of this deliverable are:

- to provide a first recommendation on which and how many novel air interface proposals are expected to be introduced in the 5G context;
- to collate initial views on which forms of air interface aggregation and user plane provisioning are foreseen for 5G;
- to open the discussion on which protocol level novel air interfaces should ideally be integrated among each other and with legacy technologies, and give examples of various options and underlying trade-offs.

## 1.2 Structure of the document

An adaptable and flexible 5G AI design is required to address the support for multiple heterogeneous services. Key METIS-II design principles are therefore agreed and formulated which enable this design.

Different 5G AI design proposals may contain different levels of similarities and differences between the different AI variants, or AIVs (characterized by tailored numerology and/or features for certain frequency ranges, services, or cell types and further discussed in Section 2.1); therefore an agreement is presented in Chapter 2 on a way to capture various AI design proposals using a unified framework. Chapter 2 then proposes a design and suitability assessment framework for 5G AI design proposals. This framework focuses on "harmonization KPIs" and how to measure them (qualitatively / quantitatively). In other words, evaluation in addition to performance includes the "extent of harmonization", which is defined in Chapter 2.

A single AI framework is the main goal of METIS-II WP4, but this does not mean a "one-size-fits-all" solution. Different use-cases will likely need some level of differentiation in the AI. How to achieve this differentiation is another key question. Additionally, current proposals differ in the technology components they are comprised of, and in the type and extent of harmonization they propose. Therefore Chapter 3 provides an overview of key physical layer considerations for 5G.

Building on top of this, Chapter 4 then captures all current METIS-II 5G AI design proposals and provides a first evaluation of harmonization criteria of these proposals.

METIS-II additionally investigates to which extent UP instances related to different bands / cell sizes etc. can be aggregated on certain layers, and beyond which layer there would be a single CoP instance. D4.1 aims to scope out these different possibilities and their impact on system design. As detailed in Chapter 4, some of the 5G AI design proposals pursue harmonization at different levels in the protocol stack: Some proposals rely on the harmonization of the lower layers of the different AIVs, while others rely on the harmonization of the higher protocol layers for the different AIVs (with a higher differentiation in the lower layer). Main types of aggregation being studied are therefore the MAC layer aggregation (with its potential to enable tighter integration features like cross-carrier scheduling, but may be challenging in the context of e.g. PHY layers with very different frame structure) and PDCP-level aggregation. It is worth noting that Issues are somewhat different when the discussion focuses on aggregation with legacy technologies. Chapter 5 discusses various trade-offs involved in different design decisions to do with UP aggregation.

We conclude the deliverable with Chapter 6 where we summarize the key findings and discuss open issues and future work.

# 2    Air interface design for 5G

## 2.1    General introduction and definitions

METIS-II considers the overall 5G AI to be comprised of multiple so-called AIVs, which may for instance be characterized by tailored numerology and/or features for certain frequency ranges, services, or cell types etc. As an example, an AIV tailored towards lower carrier frequencies, large cell sizes and high velocity will likely be based on a PHY designed to be more robust towards delay spread and Doppler spread, whereas an AIV tailored towards mmWave frequencies and used for short-distance communication with limited mobility may rather require robustness towards other impairments such as phase noise. Further, in order to support applications requiring very low latencies (in the order of 1ms) and/or very high data rates, some new 5G AIVs are expected to use new time-domain structure(s) based on shorter transmit time intervals (TTIs) and a wider bandwidth for radio resource blocks compared to the one specified for LTE-A [MET15-D24]. As another example, an AIV tailored towards a specific service may foresee a specific flavour of hybrid automatic repeat request (H-ARQ), or a specific form of packet data convergence protocol (PDCP) functionality. Finally, LTE-A and its evolution is likely to play a pivotal role in the overall 5G system, allowing this to maximally leverage on the installed base.

***Flexible single technical framework***

Altogether, the overall 5G AI is expected to cover all three main service types xMBB, mMTC and uMTC [MET2-WP], as only a common RAN that accommodates all will likely be an economically and environmentally sustainable solution. The same assumption has been captured by the recently approved Study Item on New Radio Access Technology in 3GPP [3GPP-160671], stating that a single technical framework should be targeted "addressing all usage scenarios, requirements and deployments scenarios defined in [3GPP16-38913] including xMBB, mMTC and uMTC". That has been translated in a consensus within METIS-II to have a single set of specifications for all 5G service types.

The number of distinct AIVs that are needed to jointly cover all services, bands and cell types that are expected to characterize the overall 5G system, the extent of difference between these AIVs, and how these AIVs or their sub-sets are integrated into overall 5G AI design proposals, those three aspects are the main topics of this deliverable. In this respect, different hypotheses for the overall AI design are being pursued. On one hand, one could consider to use one waveform family such as orthogonal frequency division multiplex (OFDM), and use different numerologies and slight modifications and enhancements of the waveform to cater to different services, bands, and cell types. On the other hand, one could consider a co-existence of different waveforms (e.g. OFDM and filter bank multi-carrier, FBMC) that jointly address the

overall space of services, bands and cell types. These two principal options are illustrated by way of two representative examples in Figure 2-1. Please note that beyond the two displayed dimensions (service type and frequency bands) there are also other dimensions of the requirements space (such as cell size, velocity etc.) that have to be covered, again with the option of utilizing one or multiple waveforms.
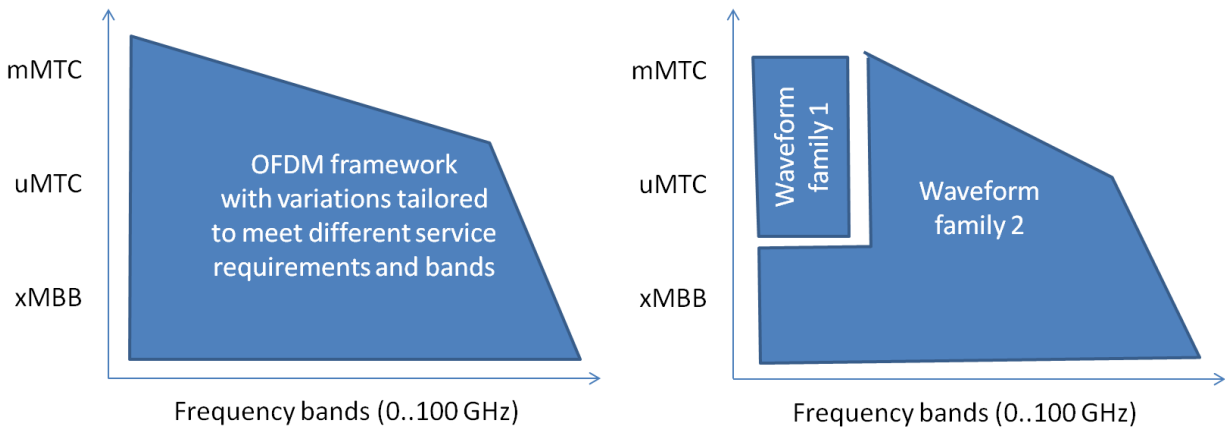


**Figure 2-1: High-level examples of potential AI design proposals addressing the 5G landscape.**

In an earlier phase of the project [MET215R41], METIS-II has selected a comprehensive set of AIVs which help meet one or more 5G KPIs, and conform to one or more 5G AI design principles. These KPIs and design principles were outlined in [MET215R41], and are described and furthered in the remainder of this chapter. Physical layer design considerations for the AIVs and underlying technologies which conform to these principles are then presented in Chapter 3. Proposals for overall AI design proposals, being the focus of this deliverable, and being composed of one or multiple AIVs, are then presented in detail (together with a preliminary evaluation) in Chapter 4.

## 2.2 Air interface evaluation criteria and key design principles

The METIS-II criteria, according to which the AI proposals – comprised of their component AIVs – can be classified, are split into the following categories:

- The suitability of an AI proposal to meet the overall 5G KPIs and directly related UP design requirements
- Additional UP-related AI design principles as identified by METIS-II
- Requirements posed from CoP considerations on the design of AIs
- The extent of harmonization across AIVs in overall AI considerations

## 2.2.1      5G KPIs and directly related design requirements

There is an industry consensus that the 5G architecture shall support multiple heterogeneous services; among these, of special importance are extreme Mobile Broadband (xMBB), ultra-reliable Machine Type Communication (uMTC), and massive Machine Type Communication (mMTC) [NGMN15-WP] [MET215-D11]. Within METIS-II, the KPIs to be used for benchmarking novel solutions for the 5G air interface are the following [MET215-R11]:

1. Traffic volume density, targeting values of 750 Gbps/km$^2$ in downlink (DL) and 125 Gbps/km$^2$ in uplink (UL),
2. Experienced end-user throughput, targeting values of 300 Mbps in DL and 50 Mbps in UL,
3. User plane latency, where ultra-low values < 1 ms shall be attained for selected use cases like the tactile internet,
4. Reliability, achieving values of up to 99.999% for end-to-end latencies < 5 ms, with the main application area being traffic efficiency and safety in the V2X context,
5. Availability and retainability,
6. Energy consumption (efficiency),
7. Cost (CAPEX, OPEX).

3GPP has recently proposed scenarios and requirements for the 5G AI (called the "next generation radio" (NR) access technologies) where some of the previously listed requirements have been captured and further detailed per scenario [3GPP16-38319]. Based on these performance requirements associated with xMBB, mMTC and uMTC, some potential improvements compared to LTE-A have been identified and the following requirements and/or assumptions for the UP design have been derived:

1. Both low-data and high data rate services should efficiently co-exist. It is envisioned that this will drive solutions such as flexible frame structures for the PHY layer design. In the low-data rate case (mainly mMTC services) a massive amount of devices will likely drive the data volume. The design shall also support very high-data rates for xMBB and some uMTC applications such as remote control of infrastructure with high quality video. Solutions have been proposed to improve LTE-A towards that direction (such as the introduction of MTC services) and more recently Narrow-band IoT (NB-IoT) [3GPP15-45820]. However the degrees of freedom available to the design of the new AI should be explored.
2. Efficient usages of the spectrum shall also be supported as spectrum is the most valuable and scarce resource for radio communication. That would require the design of Radio Resource Management (RRM) solutions that support mMTC, uMTC and xMBB service multiplexing on a time scale and with frequency granularity that is capable to capture the dynamics of the traffic, but also dedicated spectrum in extreme scenarios.
3. The design of reference signals should allow a high level of configurability, possibly exploring even more the definition of UE-specific reference signals. Some of the LTE

signals, such as cell-specific reference signals (CRSs), are provided for all users regardless the signal conditions they are experiencing. Considering the much broader range of envisioned scenarios, there will be cases where the pilot grid is oversized, while in other cases (e.g. very high mobility) it may be too sparse. Another example is the physical downlink control channel (PDCCH) in LTE, which multiplexes the control elements of all users (i.e. in a broadcast manner). Two main disadvantages can be noted: 1) fixed formats for the control channel elements will have no possibility to introduce refined formats designed for specific scenarios; 2) further transmissions following the broadcast principle suffer from the fact that the transmission format has to be chosen to allow the weakest user to detect it properly, which leads to strong inefficiencies. Breaking away from this latter paradigm may lead to improvements of physical control channels.

4. The design of reference signals should allow energy efficient mechanisms and avoid the transmission over the entire bandwidth and all subframes. In LTE-A CRS signals are transmitted all the time, over the entire band and in all directions. As stated earlier the definition of more UE-specific reference signals (possibly configurable per service) has the potential to reduce the energy in scenarios without any traffic. The configurability of these signals also avoids the transmissions over the entire band, which may facilitate the further introduction of new physical channels if needed.

5. Low UP latency at the radio access should be supported, being in the order of 1ms in selected scenarios. Low latency is enabled by the frame structure and some control plane procedures. When it comes to the UP design, low latency requirement will drive solutions such as flexible frame structures / frequency domain numerology in the physical layer design of the new 5G AI.

6. Ultra-high reliability within a comparatively short time frame should be supported for selected services. This will drive more flexible frame structures since current systems have been designed for delay-tolerant services: The targeted block error rate (BLER) for the first transmission lies at 10%, as it is assumed that consecutive retransmissions based on HARQ process can compensate for information losses and finally achieve the desired reliability by extending the transmissions over time. This paradigm needs to be reconsidered for ultra-high reliability.

7. Device-to-device (D2D) mechanisms should be defined and efficiently exploited to provide coverage. This may be used to enable the availability and retainability required for ultra-reliable 5G services like those from the V2X context.

8. The UP design should support sensors or other low cost devices. The importance of considering that issue from the beginning in the design process can be acknowledged by the fact that 3GPP started a work item to reduce complexity in MTC devices, e.g. by eliminating the use of control channels (e.g. PCFICH, PDCCH) for MTC devices in LTE, see [3GPP-141865].

9. The UP design should cope with a high range of frequencies (both below and above 6 GHz, all the way up to 100 GHz). In the particular case of higher frequencies,

beamforming is an essential feature that needs to be supported. In that case the design should support the beamforming of reference signals and data channels.

## 2.2.2    Additional METIS-II AI design principles

As elaborated in the previous section, 5G will offer support for multiple heterogeneous services; among these, of special importance are extreme Mobile Broadband (xMBB), ultra-reliable Machine Type Communication (uMTC), and massive Machine Type Communication (mMTC) with their evolved requirements and more ambitious KPIs than 4G is able to meet today. The KPIs which will be used for benchmarking novel solutions for the 5G system were detailed in the previous section.3GPP has achieved remarkable data rates through the LTE and beyond set of standards, making LTE/LTE-A and their evolution well suited for MBB, and well placed to meet many of the xMBB requirements. When it comes to other  services foreseen to be addressed by 5G, there is a large amount of ongoing work in 3GPP to standardize, for example, the support for V2X and MTC solutions for traffic comprising short data packets and transmitted in quick bursts, which can be confirmed by the study item on Narrow-Band IoT (NB-IoT).

Despite these achievements and ongoing work to advance them, METIS-II recognizes that there is a demand for a new AI to fulfil the complete set of performance requirements of the envisioned 5G use cases including some extreme low latency use cases, ultra-reliable transmission and extreme MBB requiring additional capacity that is only available in very high frequency, as well as massive MTC with extremely densely distributed sensors and very long battery life requirement.

An adaptable and flexible 5G AI design should address these issues by providing the required flexibility for multi-service support and non-traditional applications, such as the IoT, V2X, Tactile Internet, to name a few. For that reason 3GPP has started a study item for a new radio [3GPP-160671]. Following this study item, it is assumed that the new AI as designed by 3GPP should also be tightly integrated at a RAN level with the evolution of LTE. As explained in this Chapter, METIS-II 5G AI framework goes significantly beyond the one currently discussed in 3GPP – while ensuring awareness of and alignment with work in 3GPP – and is expected to be able to strongly influence 5G concepts, study and work items, and assessment methodologies in 3GPP.

In this section we outline key METIS-II design principles which govern our own work in producing 5G AI proposals suitable for providing this required flexibility and achieving all the 5G KPIs which LTE and its evolution cannot fulfil in their entirety.

1. Flexibility by design: 5G AI needs to be adaptable and flexible in order to provide the required flexibility for multi-service support and non-traditional applications. A single but sufficiently wide harmonized AI would allow this flexibility.

2. 5G AI should be forward-compatible: This is needed to ensure future-proofness for upcoming services. Such a future-proof design needs to allow the introduction of new physical channels.

3. 5G AI should offer easy interworking with evolution of LTE: It is assumed in METIS-II that the 5G RAN should allow to integrate LTE-A evolution and novel 5G radio technology on RAN level, though integration need not always take place on this level. The exact mechanics of this interworking are still under study. More light will be shed on possible approaches to this issue in Chapter 6.

4. Design of 5G AI should be lean, minimizing signaling overhead and unnecessary transmissions. As one example of a system design under study, one could strive to avoid transmitting reference signals over the entire bandwidth, but instead use self-contained transmissions (i.e. transmissions should be well confined in time and frequency and payload should possibly have their own reference signals and synchronization sequences if necessary).

5. 5G AI design should take into account the latest information on available bands (or to be made available shortly) to IMT2020 [ITU14]: In all likelihood 5G systems will operate across a wide range of mm-wave and cm-wave frequencies. 5G AI design should therefore consider the beam-centric approach, i.e all control and user plane signals should be possible to be transmitted in beams instead of omnidirectionally. This is essential in frequencies above 6GHz where beamforming is used to combat propagation losses. Additionally, better support for operation in unlicensed bands should be examined.

6. 5G AI design should take into account terminal complexity.

7. 5G AI design should enable APIs so as to facilitate the implementation of network slicing.

8. 5G AI design should from the beginning assume the usage of multi-connectivity features inspired by Carrier Aggregation and/or Dual Connectivity from LTE, but not only cover the aggregation of multiple links from the same AIVs, but also different AIVs, including the evolution of LTE.

In the following, we describe additional criteria which enable us to evaluate specific conditions imposed by CoP design considerations and which allows us to estimate the extent of harmonization.

## 2.2.3 Requirements posed by control plane design considerations

The previously stated criteria for the evaluation of proposed AIVs and AIs were all related to the evaluation of the (predominantly UP) related concepts as such.

However, in order to develop an efficient overall 5G RAN, it is important to ensure that UP concepts also fit together with the considered 5G control plane concepts. In this section we list

potential requirements posed by control plane aspects on the air interface design, as additional criteria that can be used in the context of the 5G AIV and AI assessment.

Note that all these requirements are to be seen as "soft requirements" for now, as it is either not possible to find consensus on certain control plane design aspects as such in this initial phase of 5G work, or because there may be different alternatives to solving certain problems in 5G. Consequently, it is not possible yet to agree on one single set of strict requirements posed towards the AI and AIV design.

The following soft requirements on the AI design due to **synchronous** control function considerations have been identified:

- **AIVs should offer a certain extent of resource granularity** covering a diversity of resource block formats tailored to different services (e.g. small subset of spectrum, but long codeword lengths for mMTC, large bandwidths but short blocks in time for xMBB etc.). In particular, AIVs should allow support for:
    - o variable TTI size configuration,
    - o Contiguous and non-contiguous allocation in the frequency domain,
    - o a dynamic control of the size of each allocation in time and frequency per scheduling instant,
    - o and the option that users can be scheduled (both control and data) on a fraction of the bandwidth.

- **A HARQ round trip time (RTT) in the order of 1 ms** should be supported in 5G for mission-critical services [3GPP16-38913] [ITU14]. Further, 5G HARQ design should support asynchronous and asymmetric link operation.

- **In order to support scheduling purposes, AIVs should be able to allow UEs and BSs to do frequency-selective channel / interference estimation, also including cross-links between devices or between BSs, and also on unlicensed bands.** In more detail,
    - o Cross-link interference measurements, i.e. UE-to-UE and BS-to-BS, should be supported. This is relevant in scenarios with dynamic TDD and also for D2D, e.g. to know the interference coupling between devices (cellular and D2D) for resource reuse decisions.
    - o The license-assisted operation in unlicensed band is seen one of the objectives of the study item for next generation radio [3GPP-160671]. Accordingly, for the effective and efficient utilization of the unlicensed spectrum, AIVs should allow interference estimation also on the unlicensed bands.

- **The physical layer design should allow for efficient interference mitigation and enable interference-resistant design considering cross-link interference** (e.g. from UEs to UEs or BSs to BSs), i.e.

- o AIVs should support efficient MIMO processing for widespread usage of techniques such as interference rejection combining.

- o AIVs should enable the efficient and reliable estimation of interference covariances for the application of e.g. interference rejection combining, which for instance implies that receivers need to be able to rely on the fact that certain interference characteristics remain close to constant during the process of estimation.

- o AIVs should be able to perform interference cancellation efficiently within each sub-frame and supported by network assistance.

- **The physical layer design should aim at minimizing energy consumption**, considering in particular that

  - o Reduced physical layer latency can be utilized to reduce device energy consumption. Maximizing UE's sleep time is essential to improve the battery lifetime.

  - o The time duration of the synchronization and transfer states, and therefore the total energy consumption, are directly related to the latency and frame length.

  - o The short physical layer latency enabling fast transitions between sleep and active modes brings significant gains in terms of power consumption.

  - o In concrete terms, the requirement could be formulated as: the overall time that a UE has to keep its receiver/baseband processing circuitry on to receive a single PDU (e.g under the condition of being in connected state) should be minimized.

Identified soft requirements on the AI design due to **asynchronous** control function considerations are:

- Allow the design of synchronization signals that are possible to be superimposed and still be detected individually and with good autocorrelation properties. These could encode information such as beam ID, cell ID, or some sort of index encoding system information configurations.

- Support for Multicast Broadcast Single-Frequency Network (MBSFN) transmission of CoP information e.g. via system information blocks or equivalent

- Support for flexible standalone operation in narrow band channels (e.g. similar to NB-IoT)

- Support for fast AIV switching between low and high frequencies. This can for example be achieved by using the same MAC layer for the high and low frequency AIVs.

- Support for self-contained transmissions as discussed in section 2.2.2.

- Support for lean design schemes as described in section 2.2.2.

## 2.2.4 Extent of harmonization across AIVs in overall AI designs

METIS-II envisions that the overall 5G AI should ideally be characterized by a large extent of **protocol harmonization across the AIVs used for different bands, services and cell types.** Harmonization addresses finding an optimal compromise between potentially highly specialized solutions for specific services and/or frequency bands, and the broader goal to only have one AIV supporting multiple services and bands. As an example, user equipment (UE) and network procedures (such as initial access and mobility) should ideally be as similar as possible in the different carriers such as mmWave and lower frequency bands, bearing in mind the existence of technology tailored to each of these bands (such as e.g. narrow-band beamforming for the mmWave bands). Such specific technologies may in fact be quite disparate, making harmonization highly challenging. A harmonized PHY, as an example, could mean the choice of the same waveform family or reference frame structure for different bands, such that different PHY variants for different bands can be derived from the same framework simply through parameterization (e.g. through adjusting the PHY numerology) or through (de-)activation, addition or removal of certain functionalities, such as, e.g., an additional Discrete Fourier Transform (DFT) in the processing chain for some PHY variant. Note that while a large extent of lower-layer harmonization among novel 5G AIVs may already be considered in their design phase, the lower-layer harmonization of novel AIVs with evolved legacy technology may be challenging or not even desirable: Here, the benefits of harmonization have to be weighed against the potential legacy constraints imposed towards novel AI technology.

Ultimately, it is clear that the final choice of a particular 5G AI design has to be based on a careful trade-off between the potential benefits of a large extent of harmonization (e.g. from standards and implementation complexity point of view) vs. the potential performance benefits of AIVs that are comparatively more highly specialized for certain services, bands and cell types.

Overall 5G AI proposals developed within METIS-II consider harmonization at different levels in the protocol stack. Some proposals rely on the harmonization of the lower layers of the different AIVs, while other solutions rely on the harmonization of the higher protocol layers for the different AIVs (with a higher differentiation in the lower layers). Each proposal presented in Section 4.1.2 is a single framework comprised of multiple AIVs selected to fulfill the performance of the different use cases and scenarios.

In order to evaluate the different AI proposals, KPIs specifically related to the extent of AIV harmonization within the AI proposals have been defined so that not only performance but other equally important aspects (e.g. cost and complexity as well as switching delay) are taken into account. These harmonization KPIs are described in the following:

### Ability to dynamically utilize radio resources

The KPI assesses in which time scale the proposed AI can utilize the frequency bands in a given location. The highest level is achieved when multiple services with similar latency requirements possibly relying on the same AIV numerology (e.g. frame structure) can be

scheduled in the fastest possible time scale (i.e. on a TTI-basis) in order to capture the dynamics of the traffic demands of these services and maximize the resource utilization.

The lowest level is attained when a dedicated portion of the spectrum is quasi-statically allocated and can be reallocated in a large time scale (higher than minutes / hours) only, so that no other service can utilize the spectrum portion due to design reasons. In the case of using multiple numerologies, one should assess the ability to schedule multiple shorter TTIs within longer TTI periods.

## Support of UP aggregation among new AIVs

The KPI assesses the ability of aggregating multiple AIVs in different layers of the protocol stack to support UP aggregation. UP aggregation is further detailed in Chapter 5. The maximum level would be attained when the solution allows for any kind of aggregation, e.g. carrier aggregation, dual connectivity and core network CN aggregation, i.e. multiple flows aggregated at a core level (more details in Chapter 5). The second highest level is attained when the solution allows dual connectivity with UP flow split (translating into the possibility to define a common PDCP layer). The third highest level is when the solution allows multi-flow dual connectivity i.e. without flow split (translating to the case where different PDCP layers are defined, but a common CN exists). The lowest possible level of UP aggregation is when a common CN cannot be defined so that UP aggregation needs to rely on TCP/IP level solutions e.g. multi-path TCP (see more details in Chapter 5). Below this level, aggregation is not possible at all.

## Ability to reuse SW and HW components among new AIVs

The KPI assesses the ability of reuse SW and HW components by the different AIVs for both the UE and the network equipment.

For networks with a heterogeneous set of AIVs supported by the UEs and the network, there will be variations in the number of devices using a particular AIV. This is caused by fluctuations in the number of users in the network as well as by the requirement to use AIVs that are simultaneously supported by the network and the UE.

For AIV requiring specialized HW or SW, these resources need to be dimensioned such that they match the peak load expected for that particular AIV. For the case of AIV-specific components, this will result in overdimensioning, since the system has to be dimensioned to handle high loads in one or another AIV, whereas most of the time normal load conditions are experienced, where a large share of resources remain unused. For the case of reusable components, however, resources can be shared, and only the total system load is decisive for the resource utilization..

The UE will have to adapt to varying AIVs, since not all AIVs will be available at all locations at all times. Reusing components is beneficial, because it avoids implementation of multiple independent radio chains when only a single chain is used at a time.

HW overdimensioning of in the UE and network sides translates into costs for consumer devicess, operators and infrastructure vendors.

### Standardization effort and product development of AIs (time to market)

This KPI assesses the amount of work needed to standardize and develop the different AI proposals. This effort translates into costs, as more effort will require more time, which will increase the time to market for a new feature, a new scenario or a new service. The amount of effort can be measured approximately by the number of features / protocol layers that can be reused by multiple AIVs.

### Ability to integrate new AIVs with LTE-A

This KPI assesses the ability of a proposal for the integration with LTE-A. There is a consensus within METIS-II that the new 5G AIVs should not be constrained to be backwards compatible with LTE-A. It should be noted that 3GPP has decided that its own design of 5G RAN should strive for a tight integration of LTE-A and the new 5G AIVs.

Some benefits exist in harmonizing at least a few 5G AIVs with the LTE design, such as the possibility to reuse HW components and perform HW load balancing, so that parts of the equipment could be reused by LTE-A and new AIVs. The same reasoning can be considered for standardization effort where the reuse of LTE protocol functions would save time and effort to standardize the new AIVs.

### Forward compatibility

The new 5G AI must be future proof, i.e. enable an efficient introduction of new features and services without the need of redesigning the AI. This is a difficult KPI to measure, since the future is uncertain. However, from past experience with legacy systems, we can see design choices that could be changed in order to improve future-proofness, such as the transmission of reference signals continuously over time (which forbids the introduction of new physical channels in new releases).

# 3 Physical layer considerations for 5G

This chapter elaborates on physical layer considerations for the 5G air interface design pursued in chapter 4. In particular, a set of technology components is described, which can favorably address the 5G KPIs and fulfill 5G AI design principles, as presented in the previous section. These technology components comprise all waveform candidates that are discussed in METIS II for the 5G AI design (presented in the first subsection), and other promising physical layer techniques and design considerations (presented in the second subsection). These components are the main building blocks used by the harmonized AI proposals provided in the succeeding chapter.

## 3.1 Waveform considerations for 5G AI design

### 3.1.1 OFDM-based solutions

OFDM is the underlying waveform for different wireless standards such as WiFi, WiMAX and LTE. With the use of cyclic-prefix (CP), OFDM provides numerous advantages such as an efficient implementation through FFT, easiness to combat severe multipath fading and its good affinity with MIMO systems. Because of low baseband complexity, OFDM based solutions can well utilize advanced multiple antenna technologies such as higher order MIMO and massive MIMO for beamforming as well as spatial multiplexing. OFDM is well-localized in time which is vital for TDD systems and delay critical applications. CP-OFDM is a flexible waveform; the subcarrier spacing (or bandwidth) and the cyclic prefix length can be optimized to meet a wide range of 5G requirements.

On the other hand, classical CP-OFDM has its disadvantages. The comparatively high out-of-band (OOB) leakage induces high sensitivity towards frequency distortions like Doppler and phase noise and poses the need to use large guard bands. The use of the cyclic prefix introduces a signaling overhead to the system. In the cases of asynchronous or high mobility users, the resulting inter-carrier interference may degrade the overall system performance. Moreover, high PAPR is an issue for any multi-carrier waveform. Currently, a number of research activities are ongoing to identify enhancements of OFDM and alternative waveforms to address the requirements for 5G wireless systems and to enable a more flexible adaptation to the needs of the diverse services to be provided. Such solutions are listed in the following. A discussion on the comparison among waveforms can be found in Section 3.1.3.

## Enhanced OFDM-based solutions

One approach is to enhance OFDM-based solutions in order to have only minor changes compared to existing systems. The reason is that OFDM is well-understood, easy to implement and much research effort has been spent already to design a system based on OFDM, e.g. with respect to MIMO schemes. These enhanced OFDM-based solutions include harmonized/flexible CP-OFDM, advanced SC-FDMA schemes, filtered OFDM-based solutions and OFDM with windowing / pulse shaping.

### *Harmonized/flexible CP-OFDM*

CP-OFDM is a multi-carrier waveform, currently used in LTE for downlink transmissions. OFDM has been widely studied in the literature. It is well-known to provide high spectral efficiency, an easy integration with MIMO, very simple transceiver design, and robustness against frequency selective channels. Moreover, OFDM is well-localized in time domain and due to the presence of cyclic-prefix, OFDM is also robust to time synchronization errors. The drawbacks of OFDM include high PAPR  (inherent to all multi-carrier waveforms), sensitivity to phase noise, and low frequency localization. Moreover, tight synchronization in time and frequency is required. However, CP-OFDM offers high flexibility to combat the above mentioned drawbacks, which is discussed in Appendix A.

### *Advanced SC-FDMA schemes*

OFDM can also be tailored and modified for a variety of use cases such as machine type communication (MTC) without adding significant baseband complexity. For example, single carrier solutions such as zero-tail (ZT)-DFT-s-OFDM [BTS +13] [BTS +14] can be achieved as simple add-ons for OFDM. ZT-DFTs-OFDM is a modification of single carrier frequency division multiple access (SC-FDMA), the latter is already being used in 4G systems. SC-FDMA uses a DFT spreading before the IFFT at the transmitter to achieve a single carrier property (thus also known as DFTs-OFDM). ZT-DFTs-OFDM uses zeros within the pre-DFT data samples of DFTs-OFDM to achieve better spectral containment (for details of ZT-DFTs-OFDM, refer to Appendix A).  Hence, while both SC-FDMA and ZT-DFTs-OFDM can be used to achieve lower PAPR, ZT-DFTs-OFDM can further yield higher spectral containment by reducing OOB emissions for certain use cases.

### *Filtered OFDM-based solutions*

Filtered OFDM based solutions build on an OFDM system where the individual sub-bands (i.e. aggregation of of a set of subcarriers) are filtered. This allows maintaining full compatibility with the OFDM signal structure, i.e., in particular, a clear separation of the symbols in time domain (there may be negligible symbol overlap due to the filter tails, though) and the strict orthogonality of the subcarrier signals). Two candidates for filtered OFDM are currently under discussion, namely F-OFDM, which builds on a CP-OFDM system, and universal filtered (UF-)OFDM. Detailed description of both these waveforms can be found in Appendix A.

### Windowed-OFDM (W-OFDM)

The main reason for the slow "1/f" decay of OFDM spectrum is signal discontinuities at OFDM symbol boundaries: Since OFDM symbols are independent from each other, amplitude and phase at the end of OFDM symbol *n-1* are different from amplitude and phase at the beginning of OFDM symbol *n* leading to a signal discontinuity. This signal discontinuity is largely responsible for the slow spectrum decay in OFDM. Windowing can be applied at Transmitter (TX) and/or Receiver (RX) side independent of each other to improve the spectral shape of OFDM. In Appendix A, we describe both transmitter and receiver windowing.

### Pulse shaped OFDM (P-OFDM)

Pulse-shaped OFDM (P-OFDM) follows the idea to fully maintain the signal structure of CP-OFDM, but allowing for the use of pulse shapes other than the rectangular pulse to balance the localization of the signal power in time and frequency domain. Pulse shaping translates to a subcarrier-wise filtering as in FBMC, but thanks to the CP-like overhead used per symbol, complex-field orthogonality can be maintained for the signal space, so that all schemes developed for OFDM can be reused without adaptations, including all MIMO algorithms. The complex-field orthogonality together with the reuse of the signal structure from CP-OFDM renders P-OFDM fully compatible with conventional OFDM.

To allow for a good spectral containment of the signal in frequency domain, the pulse shape is allowed to extend over the symbol interval T, yielding successively transmitted symbols to (partially) overlap. The overlap is characterized by the so-called overlapping factor K, which can be any rational number specifying the number of successive symbols the pulse shape spans over. For a value of K close to one, P-OFDM coincides with the well-known windowed-OFDM. While a value of K close to one maintains the time localization of the symbols as in CP-OFDM, chosing K equal to two and larger creates signal properties that resemble those of an FBMC system. P-OFDM can thus be considered a hybrid solution capable of creating any compromise between a time-localized OFDM system (small K) and a frequency localized FBMC system (large K).

A more detailed description of P-OFDM is given in Appendix A as well as in [ZSW+15].

## 3.1.2    FBMC-based solutions

FBMC represents a multi-carrier system where the single subcarrier signals are individually pulse shaped with a pulse that may extend over several symbol intervals of duration T, yielding an excellent spectral containment of the multi-carrier signals. The use of such a pulse results in overlapping pulses if several FBMC symbols are transmitted successively in time. However, an orthogonal (or bi-orthogonal) pulse design ensures that the overlapping pulses can be (near to) perfectly reconstructed without creating any mutual interference. Thanks to the orthogonal pulse design, FBMC does not require a cyclic prefix, and thus is capable to achieve the maximum

spectral efficiency of all multi-carrier schemes. This increases the degrees of freedom for the system design, as the overhead of the CP, which is usually dictated by the channel, does no longer represent a decisive design constraint. Since each of the FBMC subcarrier signals are individually filtered with the pulse, each individual subcarrier signal exhibits excellent spectral containment properties, and thus a sub-band of any size can be defined fulfilling strictly a desired spectral mask.

Main FBMC candidates under discussion for 5G are FBMC Offset-QAM (OQAM-FBMC) and QAM-FBMC. While OQAM-FBMC relaxes the orthogonality to the real signal field only to attain the best possible time/frequency localization, which requires some redesign of selected signal processing schemes like some MIMO algorithms, QAM-FBMC maintains the orthogonality in the complex field, enabling a reuse of all algorithms developed for OFDM, at the price of compromised time/frequency localization. Further details on both these FBMC candidates are given in Appendix A.

### 3.1.3 Conclusions on the waveforms analysis

In this chapter, we have considered several multicarrier and single carrier waveforms that are candidates for 5G air interface. The multi-carrier waveforms include CP-OFDM, W-OFDM, F-OFDM, UF-OFDM, P-OFDM, QAM-FBMC, and OQAM-FBMC. The single carrier waveforms include SC-FDMA and ZT-DFTs-OFDM. All multi-carrier waveforms have high spectral efficiency and there are not significant differences among them in terms of their spectral efficiency. All multi-carrier waveforms have good compatibility with MIMO, except OQAM-FBMC, which has issues with some non-linear MIMO detection schemes. CP-OFDM is localized in time and has the lowest baseband complexity, but high OOB emissions. The OOB emissions can be reduced by additional filtering/windowing/pulse shaping, as enabled by F-OFDM, W-OFDM, UF-OFDM, P-OFDM, ZT-DFTs-OFDM, QAM-FBMC-QAM, and OQAM-FBMC. The improved frequency localization, however, comes at the cost of additional complexity and a compromise on time localization. Time localization is important for TDD and to achieve low latency, whereas frequency localization is important when spectrum is fragmented and asynchronous communication is desired, for instance for D2D communications. CP-OFDM is robust to synchronization errors only as long as synchronization errors stay within the CP duration. For completely asynchronous FDMA communication, one can either use waveforms with improved frequency localization (F-OFDM, W-OFDM, UF-OFDM, P-OFDM, QAM-FBMC, OQAM-FBMC, ZT-DFTs-OFDM) or use CP-OFDM by inserting guard bands (leading to inefficient spectrum utilization). The common disadvantage of all multi-carrier waveforms is their high PAPR, which scales with the number of subcarriers of the transmitted signal, affecting mainly the battery consumption at the terminal side. The single carrier waveforms, such as SC-FDMA and ZT-DFTs-OFDM, have lower PAPR and can be useful when high power efficiency is desired.

# 3.2 Other physical layer considerations for 5G AI

***Non-coherent reception, differential decoding and Grassmannian constellations***

Most of the current cellular technologies are based on coherent reception where channel state information (CSI) should be estimated for equalization, demodulation, etc. The CSI can be obtained by inserting reference or pilot signals in the transmitted data, which clearly implies increased signaling overhead. The required signaling overhead in current wireless communication networks is not yet significant simply because the number of antennas is still small. However, Massive MIMO, envisaged as one of the key enabling technologies in 5G to satisfy the extremely high data rate demand, requires huge number of antenna elements installed at least in 5G base stations (BSs). The signaling overhead due to channel estimation will increase with the number of equipped antennas and can easily reach a prohibitive level. Moreover, channel estimation errors can degrade the performance of MIMO techniques substantially. On the contrary, non-coherent reception, which performs data detection without any knowledge of the channel coefficients, has already been identified as a potential enabler for 5G and a good complement to coherent communication in some scenarios [RCC+14]. These techniques are also referred to as blind detection schemes. With non-coherent reception pilot signals are no longer needed and multi-point coordinated transmission is fully exploited, provided that different columns of the equivalent codeword matrix can be transmitted from a distributed antenna system. Given that no pilot signal is needed, the assistant transmission points act like phantom transmitters from the end user point of view, which is only aware of the existence of the main base station. This phantom cell concept, widely discussed in the 3GPP forum, fits perfectly with the blind transmission mode studied in METIS-II. In the following, we give some minor details on the two non-coherent reception schemes under discussion.

***Differential Unitary Space-Time Modulation (DUSTM)***

In order to eliminate the pilot symbols, two modulations for non-coherent reception will be considered. The first one is Differential Unitary Space-Time Modulation (DUSTM), in which data (typically at least $M$ symbols) is encoded into $M \times M$ unitary matrices, where $M$ is the number of transmit antennas [HS00]. Before transmission, the unitary matrices are multiplied by the previous transmitted signal, and are then transmitted through the $M$ antennas in $M$ channel uses. In this context, a channel use is the time-frequency grid used by one waveform pulse. In particular, the signal transmitted during the $t$-th period (consisting in $M$ channel uses, i.e., waveform pulses) is $X(t) = V(t)X(t-1) \in \mathbb{C}^{M \times M}$, where $V(t)$ is the unitary matrix with the encoded data. The channel uses can be arranged in the resource grid in time, frequency, or both. Assuming that the channel matrix, $H$, is constant during two consecutive periods, i.e., $2M$ channel uses, the received signal during the $t$-th period is $Y(t) = X(t)H + Z(t) = V(t)X(t-1)H + V(t)Z(t-1) - V(t)Z(t-1) + Z(t) = V(t)Y(t-1) + \sqrt{2}Z'$, where $Z(t)$ is the additive noise matrix during the $t$-th period and $Z'$ is a random matrix with the same distribution as $Z(t)$. The last equality follows from the independence of $Z(t)$ and $Z(t-1)$ and the fact that multiplying $Z(t-1)$ by a unitary matrix does not change the probability distribution. As a consequence, the receiver sees the desired signal transmitted through a channel which coefficients equal the previous

received signal and with twice the noise power. The performance of DUSTM depends on how data is encoded into the unitary matrices $V(t)$. The best known proposal builds diagonal unitary matrices, whose main drawback is that it uses only $M$ out of the $M^2$ Degrees of Freedom (DoF) of the unitary group.

### Grassmannian constellations

The second modulation for non-coherent reception is based on Grassmannian constellations [Fou15]. The points of these constellations are selected from the $G(M, \mathbb{C}^T)$ Grassmann manifold, i.e., the set of al $M$-dimensional linear subspaces of $\mathbb{C}^T$. Hence, data is encoded into subspaces, and transmitted using an orthonormal basis of the corresponding subspace, say $Q \in \mathbb{C}^{T \times M}$, which is signaled through the $M$ antennas during $T$ channel uses. Assuming that the channel, $H$, is constant during the $T$ channel uses in which $Q$ is transmitted, the received signal is $Y = QH + Z$, where $Z$ is the additive noise. The product $QH$ represents linear combinations of the basis elements, which form a new basis of the same subspace. Hence, the subspace spanned by $Q$ is the same than the one spanned by $QH$, and, for a sufficiently small noise $Z$, the encoded data can be retrieved. It can be shown that both the Grassmann manifold $G(M, \mathbb{C}^T)$ and the block fading channel with $M$ antennas and a block length $T$ have $2(T - M)M$ DoF.

### Relaxed synchronism

In current cellular systems, like LTE, the communication between base station and the devices is enabled by high synchronization levels. Relaxation of these levels is rapidly reflected in non-negligible efficiency losses and higher interference levels. In order to avoid these negative effects, and hence to achieve the required synchronism, current systems use synchronization signals that reduce spectral efficiency, and devices have to consume certain time and resources in the synchronization procedures. Although this is acceptable in current systems, the new services, like mMTC with limited-power devices, and link types, like D2D, envisioned for 5G exhibit the need of a new air interface that allows communication with relaxed synchronization requirements. Research is being conducted to select the best physical layer configuration to address the requirements related to this relax synchronism. For instance, numerology is adapted, waveforms are dynamically configured depending on the delay of sources, being also possible via software-defined radio to switch from one waveform to another in the time domain.

## 3.2.1    Harmonization aspects for V2X communications

Another important enabler of the 5G is V2X, i.e. Vehicular to Vehicular (V2V) or Vehicular to Infrastructure (V2I), communications. The main characteristic of the communications in which transmitter and receiver are moving at high relative speeds is that the channel varies rapidly. In this case, it is expected that channel estimation with pilots and coherent reception becomes highly suboptimal. METIS-II is considering the use of non-coherent reception techniques that save the resources used by the pilot signals and allows reliable and high data rate transmission with high relative speeds.

METIS-II will study new DUSTM and Grassmannian constellation designs (cf. Chapter 3.3) to be harmonized with modulations for coherent reception, e.g. QAM modulation, Alamouti codes, Orthogonal Space-Time Block Codes (OSTBC) and Quasi-OSTBC (QOSTBC). One of the questions that METIS-II should answer is when non-coherent reception should be used. This answer is affected by two main factors: the relative speed between transmitter and receiver that affects the Doppler frequency and hence the channel coherence time, and the frequency band that affects the delay spread and hence the channel coherence bandwidth. These factors also affect the density of pilot signals for coherent reception. In particular, it can be shown that there should be a pilot signal for each antenna port every $1/(2f_D)$ seconds, where $f_D$ is the maximum Doppler frequency, and every $1/(2\tau)$ Hz, where $\tau$ is the delay spread, to retrieve all the channel coefficients variations. However, in some scenarios, fewer pilots can be used if some inaccuracy in the fading coefficient estimation can be tolerated. Or conversely, because of various practical constraints, such as phase noise (which becomes even more of an issue in above 6 GHz bands), a denser distribution of pilots may be required. The non-coherent reception techniques are relevant for scenarios where the density of pilots is significantly high, or, in other words, where $1/(4f_D\tau)$ is low. Figure 3-1 shows an initial proposal of the reception technique mapping into frequency bands and relative speeds.
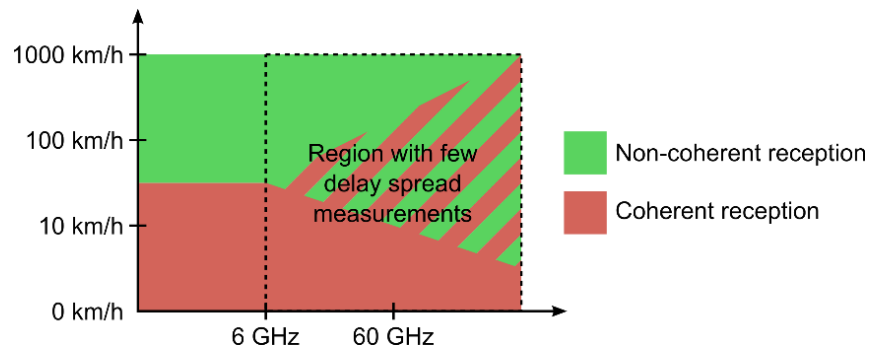


**Figure 3-1: Reception technique mapping into frequency bands and relative speeds.**

In Figure 3-1, it was assumed that non-coherent reception is beneficial for $1/(4f_D\tau) \leq 256$ pulses, which results in, at least, 30 km/h below 6 GHz. It is important to note that this figure may evolve in the future due to the lack of public delay spread measurements in the higher bands (above 6 GHz). The few available measurements show that the delay spread is reduced with the frequency band due to the low multipath effect. However, the extent of this reduction and whether this reduction is able to counteract the Doppler frequency increment is still unclear. Due to this, Figure 3-1 depicts a region above 6 GHz with some uncertainty about the most beneficial reception technique.

With respect to the harmonization possibilities of non-coherent and coherent reception techniques, METIS-II will focus on constellation designs for non-coherent reception that are based on constellations for coherent reception, like QAM modulation, in such a way that most of the functional blocks implemented for coherent reception communications could be reused for non-coherent reception communications. This will reduce implementation costs and standardization efforts.

# 4 Harmonized air interfaces and UP design aspects

This chapter elaborates on harmonized air interface solutions, building on the waveform variants that have been described in Chapter 3.  From a very broad perspective, the following two types of harmonization approaches are followed here:

- OFDM framework with variations tailored to meet different 5G service requirements and bands

- Multiple waveforms to cover the overall 5G landscape

The envisioned overall 5G landscape comprises of multiple services with very diverse requirements, as well as multiple carrier frequency bands up to 100 GHz.  A short description of the characteristics and requirements of the 5G service landscape to be supported by the harmonized air interface(s) is listed below.

1. Enhanced Mobile Broadband (eMBB):
    - very high data rate in the range of Gbps per user
    - high coverage
    - reliable communications with moderate data rates in crowded scenarios.
    - high mobility
    - broadcast multimedia service for lower frequencies

2. ultra reliable machine type communication (uMTC)
    - extreme requirements on availability, latency, and reliability
    - spectral efficiency is of lower importance
    - MTC for vehicular applications (V2X): resilience against Doppler effects and robustness against asynchronicity
    - other scenarios such as industrial control applications

3. Massive Machine-Type Communication (mMTC)
    - support for a very large number of devices,
    - high coverage,
    - long battery-life per device: energy efficiency is of high priority
    - low signaling overhead

# 4.1    Particular design proposals

The objective of METIS-II is the design of a "single air interface framework for 5G". This has been derived from an overall 5G system requirements assumed in METIS-II to avoid ending up with very different RAN designs and architectures considering each service type separately and building a 5G network accordingly. However, we believe that only a common RAN that accommodates all three service types will likely be an economically and environmentally sustainable solution (the service categories should comprise the envisioned 5G use cases but also others that may emerge in the future).

One way to achieve that differentiation is by defining dedicated core network instances, often called CN network slicing instances [MET2-WP], as shown in Figure 4-1. When it comes to the 5G RAN, the impact of network slicing is currently being investigated [MET2-WP]. The previous assumption of a common RAN within METIS-II is also being considered by 3GPP where a common RAN basically leads to one single protocol stack framework for the overall 5G air interface that is capable of fulfilling the requirements of 5G use cases in an economically viable manner.
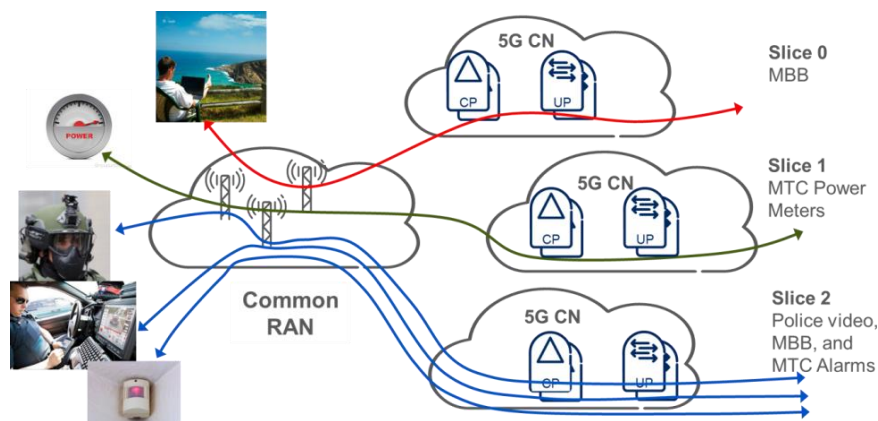


**Figure 4-1: Network slicing enabling dedicated CN functions and a common RAN**

In order to be capable to differentiate services and/or use cases this *single protocol stack* framework needs to be *highly configurable* so that traffic can be differentiated and certain procedures can be tailored to different frequency bands, services and/or deployment scenarios.

In the following subsections, different solution proposals for a harmonized air interface design covering the entire 5G landscape are presented. At the beginning of each sub-section, a list of keywords is presented, which characterizes the key features of each of the proposals. Before venturing into these specific proposals, it is worth mentioning that all proposals have in common that the PHY numerology, i.e. aspects such as subcarrier spacing, cyclic prefix length (where applicable) etc., typically have to be adapted to the carrier frequency, cell size and services envisioned to be supported. Considering that the 5G RAT is envisioned to operate from sub-1 GHz to 100 GHz for a wide range of deployment options, it is clear that there cannot be a one-size-fits-all numerology.

In particular, subcarrier spacing and cyclic-prefix (where applicable) should be chosen keeping in view channel delay spread, phase noise, and Doppler effect. The robustness of systems towards phase noise and Doppler shift typically increases with subcarrier bandwidth. Since the effect of both impairments increases with carrier frequency, the required subcarrier bandwidth typically has to increase with carrier frequency. Where a CP is applied, this must be designed based on the expected delay spread and is thus determined by the deployment. Wider subcarriers imply shorter symbols despite a constant cyclic prefix length per symbol. Hence, the "ideal" subcarrier bandwidth has to keep the CP overhead as low as possible, while being wide enough to provide sufficient robustness towards Doppler and phase noise.

A side effect of increased subcarrier spacing (at the same number of subcarriers) is that the symbol duration is shortened, which may be a good solution for achieving lower user plane latency. This property can be used for flexible and fast link direction switching between uplink, downlink and device to device communications, also known as flexible TDD.

## 4.1.1 A harmonized L1/L2/L3 solution based on CP-OFDM for sub-1 GHz to 100 GHz carrier

**Keywords:** Scalable CP-OFDM, Harmonized PHY/MAC/PDCP, Candidate 5G Layer2 Design, Candidate 5G transport channels, Candidate 5G contention based access

### Scalable CP-OFDM and common higher layers

The proposed overall air interface is based on CP-OFDM (for all link types such as uplink, downlink, sidelink, backhaul, fronthaul), where each AIV is mainly defined by its PHY layer numerology (adapted to the different 5G use cases and frequency bands) and its set of protocol features, device capability, network capability, etc. Some use cases may need multi-connectivity (so the feature must be standardized), others may not. This differentiation needs to be implemented in the network (and standardized) so that it can be instantiated during the connection setup or when performing a state transition from RRC inactive state to RRC connected state.

To handle the wide range of carrier frequencies and deployments, a scalable numerology flexible CP-OFDM is considered, where the parameters such as subcarrier spacing, cyclic prefix, and subframe duration scales as a function of frequency depending on the service type. For example, a local-area, high-frequency node uses larger subcarrier spacing and shorter cyclic prefix than a wide-area, low-frequency node. To support very low latency, one of the important requirements for 5G use cases, a significantly short subframe can be used (with the possibility for subframe aggregation for less latency-critical services). Detailed numerology to support these are provided in further sections.

**Why OFDM?**

OFDM is considered due to its suitability for MIMO, low complexity, and robustness against frequency selective channels and timing synchronization errors thanks to the cyclic-prefix. Importantly, OFDM is very well-localized in time, and thus suitable for TDD systems (envisioned mostly above 3 GHz) and low delay applications.

**Numerology design: addressing a wide frequency range and multiple services**

CP-OFDM numerology refers to choice of subcarrier spacing and cyclic prefix length, which, for a given bandwidth, determines the FFT size.

In Table 4-1, we propose a set of CP-OFDM numerologies that can be enabled at different frequencies for different services. We define a base numerology, and the other numerologies are derived from that by scaling the base numerology. The proposed base numerology is based on LTE numerology (15 KHz subcarrier spacing).

**Table 4-1: Proposed CP-OFDM Numerology**

| | Numerology 1 | Numerology 2 | Numerology 3 |
| --- | --- | --- | --- |
| Sub-carrier bandwidth | 15 KHz | 30 KHz | n×15 kHz |
| Clock frequency | $f_s$ = 61.44 MHz = 2 · 30.72 MHz | $f_s$ = 2×61.44 MHz = 122.88 MHz | $f_s$ = 2n×30.72 MHz |
| Number of Symbols per subframe, $N_{sf}$ | 7 | 7 | 7 |
| FFT size, $N_{ofdm}$ | 4096 | 4096 | 4096 |
| CP samples, $N_{cp}$ | 288 | 288 | 288 |
| Subframe duration, $T_{sf}$ in µs | 500 | 250 | 500/n |
| OFDM symbol duration, $T_{ofdm}$ in µs | 66.67 | 33.33 | 66.67/n |
| CP duration, $T_{cp}$ in µs | 4.76 | 2.38 | 4.76/n |
| $T_{ofdm} + T_{cp}$ in µs | 71.43 | 35.71 | 71.43/n |

Numerologies with shorter delay spreads can be enabled in low dispersive environments. At very high frequencies (above 40 GHz), CP-OFDM with Peak-to-average power ratio (PAPR) reduction is a promising candidate. The air interface may also enable DFTs-OFDM for the reason of low PAPR.

For some use-cases, mixing of different OFDM numerologies may be beneficial, e.g., to support different services with different latency requirements. Mixing of OFDM numerologies can either be done in time-domain or frequency domain. If the numerologies are mixed in frequency domain, one possibility is to use some guard band in between different numerologies to suppress inter-numerology interference (since sub-carriers are not orthogonal between two different numerologies). Another alternative is to apply low complexity windowing in time domain, i.e., Windowed-OFDM. Nevertheless, the window size should be limited to one OFDM

and may use few samples of CP, in order to allow TDD and low latency transmissions. Short window is also preferred for FDD. The window can either be applied at the transmitter or at the receiver or at both places, depending on the system design.
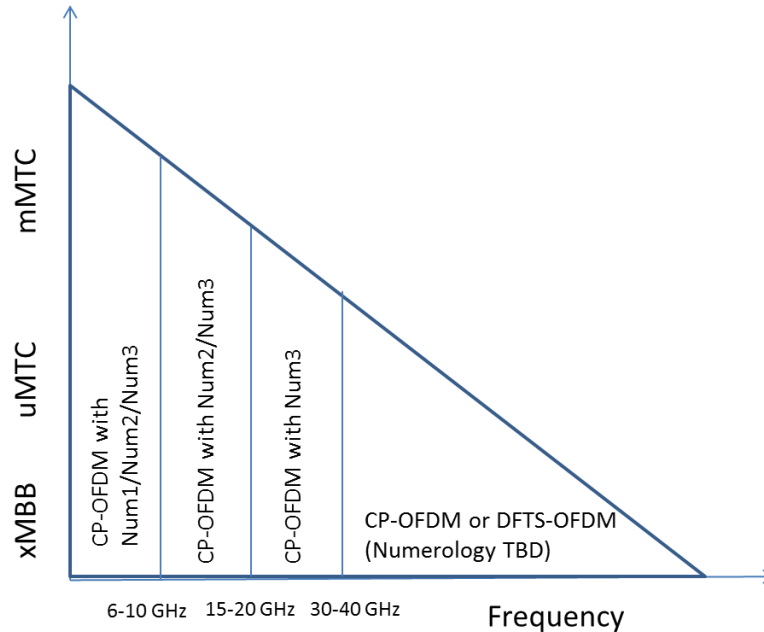


**Figure 4-2: Mapping of services and frequencies**

## 4.1.2 Harmonized CP-OFDM for multiple bands with enhancements for multi-service support

**Keywords:** CP-OFDM with scaling/flexible numerology, Advanced SC-FDMA, Flexible TDD

The **purpose of the harmonization in METIS-II** is the design of a "**single air interface (AI) framework for 5G".** At a high level, the approach described here is to utilize a CP-OFDM, with slight modifications to cater for multiple service types in the 5G air interface. These service types will encompass the multiple 5G use cases. The single waveform family approach will also be applied for harmonization as much as possible above and below 6 GHz. Figure 4-3 shows the waveform flexibility considerations using OFDM waveform covering the use cases. This solution proposal builds on CP-OFDM by using slight modifications to CP-OFDM and SC-FDMA. More description and additions to the preferred design in Figure 4-3 is discussed in the text.
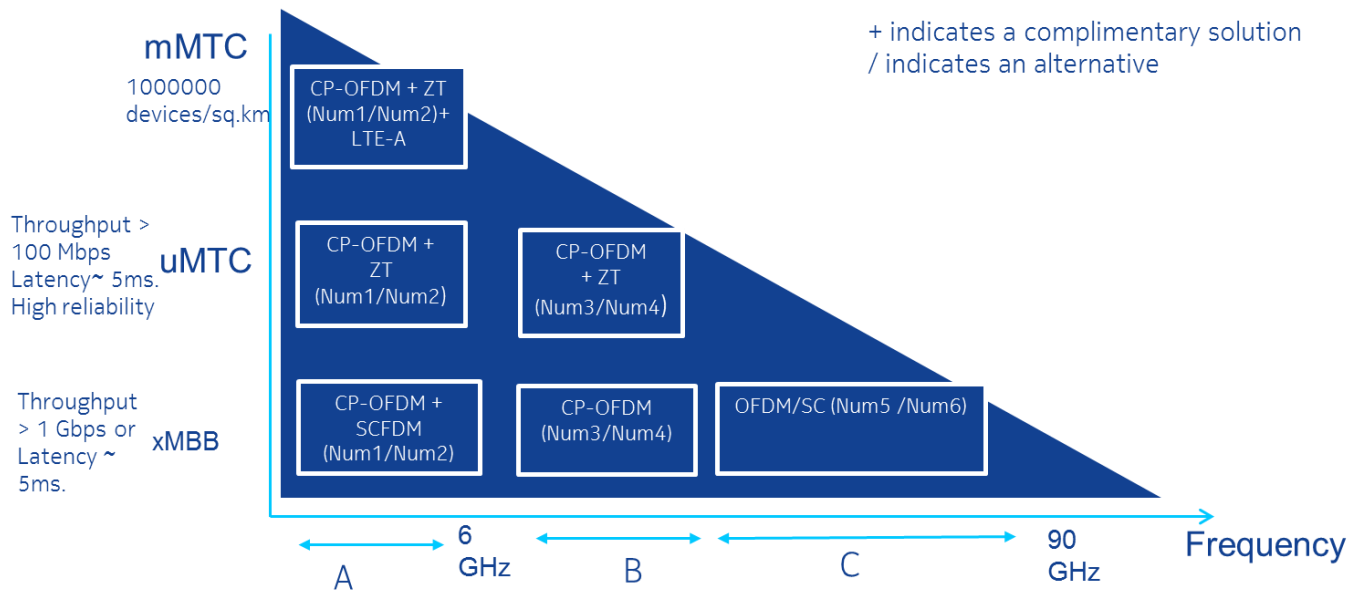
**Figure 4-3: Mapping of services and frequencies using harmonized OFDM**

As seen in the figure above, the main technology components are derived from OFDM and enhancement in order to make use of lower complexity, while also harmonizing the AI characteristics such as sub-frame structure across different frequency ranges. Please see the appendix A for a more detailed description of the CP-OFDM, SC-FDMA and ZT-DFTs-OFDM, which are the main technology components within the harmonization.

A bandwidth dependent numerology is proposed as below for an example FFT size of 2048:

**Table 4-2: CP-OFDM and ZT-DFTs-OFDM numerology examples for the mapping in Figure 4-3**

| | **Num 1** | **Num 2** | **Num 3** | **Num 4** | **Num 5** | **Num 6** |
|---|---|---|---|---|---|---|
| **Subcarrier spacing** | 15 KHz | 30 KHz | 60 KHz | 120 KHz | 480 KHz | 960 KHz |
| **FFT size** | 2048 | 2048 | 2048 | 2048 | 2048 | 2048 |
| **OFDM symbol length** | 66.67 us | 33.33 us | 16.67 us | 8.34 us | 2.08 us | 1.04 us |
| **Sub-frame duration** | 0.5 ms | 0.25 ms | 0.125 ms | 0.125 ms | 0.125 ms | 0.125 ms |

We now provide discussions on frequency to service type mapping for harmonized OFDM solution below. In the table above the CP length is assumed to introduce around 7% overhead in the presence of delay spread.

## Frequency range A

The illustration for frequency range A shows waveforms for use cases in frequency bands below 6 GHz. The frequency range A will support heterogeneous deployments, i.e macro cells and small cells.

xMBB :

CP-OFDM(A) for DL and SC-FDMA for UL are the preferred waveforms for xMBB use cases for very large cells, akin to LTE-A systems. The intention is to make use of CP-OFDM(A) in order to support MIMO, and thus achieve high throughput that is required for xMBB services. The CP-OFDM numerology can be bandwidth dependent. It can thus be optimized for a new harmonized sub-frame structure (please see Appendix A.2 ) where a bi-directional control is embedded within each sub-frame. Such a combination of numerology and sub-frame structure can be used for providing low latency for some applications even within xMBB. Sub-carrier spacing, FFT size are important design parameters that have to be carefully chosen in order to achieve robust performance while keeping a tolerable overhead, please see Table 4-2. Note that a CP overhead of 7 % is assumed in the table to tackle delay spread.

uMTC:

uMTC requires low latency as well as higher reliability. CP-OFDM and SC-FDMA are again good candidates to support such services with high reliability requirements for mobile users because of good time localization which leads to robust channel equalization (because of channel coherence time). The shortened sub-frame duration of 0.25 ms (please see Num 2 in Table 4-2) reduces the UP latency on the AI as well as reduces the RTT for HARQ. D2D communications can be further utilized for certain uMTC scenarios such as V2V communications. Here, ZT-DFTs-OFDM waveform with good spectral containment as well good time localization is seen as a good candidate.

mMTC :

mMTC type services will support a multitude of devices with typically low payload. Low synchronization effort and longer sleep times are the main design choices for these applications. For low synchronization, ZT-DFT-OFDM is a good choice because of good spectral containment, and hence mMTC users do not generate asynchronous interference to xMBB and uMTC users. The mMTC users can be supported with the same numerology as the xMBB users in order to allow for flexible TDD UL-DL switching of the xMBB and uMTC users. mMTC services can be further supported by integration to legacy LTE-A technologies LTE-M and NB-IoT which target supporting a large number of mMTC users.

**Frequency range B**

Frequency range B corresponds to the middle range of frequencies above 6 GHz, in the centimeter wave band(s). xMBB and uMTC are the main foreseen use cases in these band(s) where a larger bandwidth support is expected as compared to frequency range A.

xMBB and uMTC :

The same harmonized sub-frame structure is used with support for xMBB and uMTC. CP-OFDM is the preferred waveform for xMBB both UL and DL because of local area cells, i.e. smaller cell sizes. Furthermore an even smaller sub-frame size of 0.125 ms with bi-directional control can support low latency for uMTC. For D2D communications, ZT-DFTs-OFDM is again the preferred choice for spectral containment for in-band multiplexing of D2D and xMBB.

**Frequency range C**

Frequency range C corresponds to the higher range of frequencies in the millimeter wave band(s). xMBB is the main use case in these band(s) where a very large bandwidth support is expected. The millimeter wave frequencies can utilise single carrier transmissions by using zero-tail single carrier waveform for lower PAPR. Millimeter wave beamforming is a key technology at these frequencies.  On the other hand, multi-carrier waveform such as OFDM can also be used depending on the implementation, cost and performance trade-off.

## Harmonization aspects:

1) The favored approach is to make use of one numerology for all three services types, so that scheduling degrees of freedom can be fully exploited for dynamic TDD with bi-directional control sub-frames. This means that the xMBB, uMTC and mMTC users can be prioritized on a sub-frame basis (with the sub-frame sizes meeting uMTC latency requirements) without affecting the UL-DL switching time, and thus also minimising the RTT in the UP. A multi-numerology co-existence approach is also possible aiming at co-existence of multiple numerologies to support multiple users in a band. This approach can optimise the numerology and PHY performance for each of the three service types and cell sizes. While this may optimise the PHY layer performance, the design benefits have to be considered carefully in a dynamic TDD system from a MAC perspective as given below:

   o If the sub-frame definitions are done based on the longest OFDM symbol (for mMTC in wide area cells), the UL-DL switching time will span a longer sub-frame size. This will affect the latency performance of the low latency services because of longer UL-DL switching time, while the wide area users can be flexibly scheduled.

   o To avoid the above issue, the mMTC users requiring longer symbol lengths can be scheduled at fixed positions in the frequency domain to somewhat mitigate in-band emissions, and use semi-full-duplex communications. This

will reduce the MAC layer scheduling degrees of freedom for mMTC users, while still providing low latency for xMBB and uMTC users.

On the other hand, one could consider multi-numerology co-existence only for FDD scenarios, where the UL-DL switching time issue does not arise.

2) The implementation of filtering and windowing, along with zero-tail waveform needs further investigations to better understand the trade-offs in terms of performance and complexity. It has to be studied what percentage of functional blocks can be harmonized above and below 6GHz thus reducing implementation complexity.

### 4.1.3 Multi-service support with UF-OFDM

**Keywords**: Increased waveform configurability and reconfiguration, Possible use of CP and zero postfix, Strong frequency and time confinement
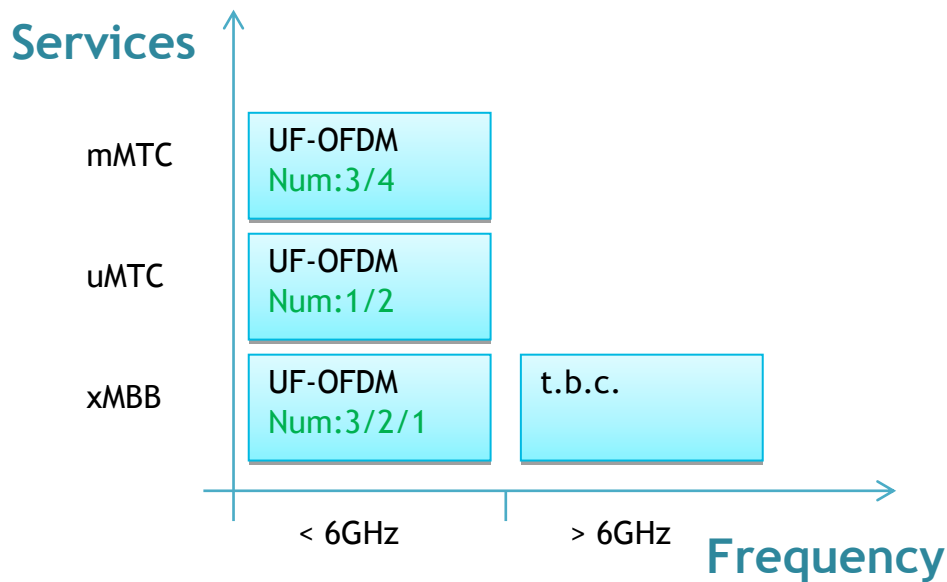


**Figure 4-4: UF-OFDM numerology options tailored for different 5G services**

We target to design a framework allowing parameterization and reconfiguration depending on the respective characteristics imprinted by the carrier frequency, network deployment setting and use case requirements (in the following called 'scenarios'). In the following we focus our air interface descriptions, which uses multi-carrier technology, on the macro cell layer version of the air interface for below 6 GHz with UF-OFDM numerology options as exemplary shown in Figure 4-4. As an example for xMBB service, the numerologies listed are according to

Table 4-3 with the priority having numerology 3 (TTI length=1ms) as the standard case for typical transmissions. Numerologies 2 and 1 are special cases with shorter subframe lengths (e.g. to support the slow-start of TCP).

However, the key components of the discussed air interface proposal (e.g. waveform) can be adapted to e.g. higher frequencies.

## Waveform considerations

In general, the family of waveforms being proposed here is taken from the OFDM-family. Depending on the scenario, sub-band-wise filtering has been shown to be beneficial as given in numerous publications and project reports (e.g. within [MET15-D21], [MET15-D22], [MET15-D2.3], [MET15-D24], [5GN15-D31], [5GN15-D32], [5GN15-D33] and discussed currently in FANTASTIC-5G). Means to fit the waveform characteristics to the characteristics of the scenario (e.g. frequency range, UC, deployment setting) are available such as reasonable scaling of the subcarrier bandwidth, choice of the filter design. In more detail, dedicated waveform adaptations (in combination with respective adaptations of related design aspects such as frame design, TTI definitions etc.) are envisioned for low latency cases, coverage extension for low power devices, high Doppler scenarios, massive access, broad- and multi-cast services, big cell scenarios (e.g. in low Average Revenue Per User (ARPU) areas ).

The research community has provided a plethora of options for designing the waveform. General motivation for us related to this are as follows (key driver is not to overdesign the solution, i.e. only apply reasonable means):

- Practical allocations happen in groups of adjacent subcarriers. So, for support of relaxed time-frequency alignment it is sufficient to confine the side-lobe levels outside of the respective allocations [SW14]. It is not required to confine the sidelobes within the respective allocations. Additionally, frequency domain blanking is improved by applying subband filtering.
- Filters need to be comparatively short to prevent strong overlap or the need for symbol staggering [SWC14] (Note: Shorter filters (time domain characteristic) are wider in frequency domain). Main reason for this is to keep the overhead for very short bursts in check (similar reasoning holds for the design of control/reference characteristics) and to maximize the available degrees of freedom to match the AI characteristics to the respective scenario.
- Spectral decay rate are needed only as far as they generate impact on system level and can be sustained with practical power amplifier hardware

## Design options for UF-OFDM:

- The subcarrier inputs are typically scaled according to the frequency response of the filter to achieve a flat passband [5GN15-D33].

- Implementations with lower complexity are available for e.g. devices having heavy constraints on cost [SW15]
- Either the use of a cyclic prefix or a zero postfix is possible. The former with filter length equal to 1 transforms UF-OFDM to classical CP-OFDM [VV16].
- Related signal processing functionalities (e.g. channel estimation [WWS+15], PAPR reduction techniques [5GN15-D33] etc.) may reuse techniques being designed for CP-OFDM. This simplifies the standardization process and the development of respective products.
- The filter may be designed according to the respective scenario (e.g. transmissions from low-end devices being constrained to lower modulation orders are benefitting from choosing long filter responses reducing inter-subband-interference while introducing tolerable inter-symbol interference levels (NB: it is not anticipated to allow the system to freely design the filters on the fly. Instead the use of a codebook of filter options is reasonable to avoid to AI design to be overcomplicated and to ease testing.)
- 'True' zero-tail (achieved using filters with length shorter than the respective zero postfix) and 'almost' zero-tail (zero-tail DFT-spreading: UF-OFDM extension of [BTS+13]) are means to increase the robustness against intersymbol interference (e.g. in case of high delay spread channels)

## Numerology design: addressing a wide frequency range and multiple services

Numerology design can address on physical layer the harmonization approach for different AIVs. Following waveform numerology adaptations are identified as the optimal waveform parameterization for the different cases [SW15] and [SWA16]. For mMTC traffic the PAPR can be kept low by using a wider spacing which allows to reduce the number of subcarriers within a given allocation width (in kHz) (PAPR depends on the number of subcarriers a burst is consisting of). For achieving low end-2-end latencies the TTI length is a key contributing factor. So, by allowing the system to make use of adaptive subcarrier bandwidths (again no free running parameterization, but codebook of options) we increase the degrees of freedom to design short TTIs (number of symbols and length of the single symbols), see Figure 4-5. Network deployment scenarios with very large cells (e.g. in low ARPU regions) or the introduction of broad- and multicast services (based on single-frequency networks (SFN)) are both potentially introducing higher delay-spreads. Longer symbols and connected to this smaller subcarrier bandwidths may be used in response to this. UE mobility is considered in case of high Doppler scenarios (e.g. high speed train communication at 3-6 GHz carrier frequency) with the waveform configuration providing shorter symbols and wider spacing to reduce Inter-Carrier Interference (ICI) which improves channel estimation for a given pilot placement setting which may depends on channel coherence time.

**Table 4-3: Numerology options for 5G tailored for different propagation environments and use cases.**

| TTI length | 1/8 ms | 1/4 ms | 1 ms<br>LTE-like case | 2 ms | 4 ms |
| --- | --- | --- | --- | --- | --- |
| | Num | Num | Num | Num | Num |
| Subcarrier spacing | 60 kHz | 30 kHz | 15 kHz | 7.5 kHz | 3.75 kHz |
| #symb/TTI | 7 | 7 | 14 | 14 | 14 |
| Samples /symb | 512 + X | 1024 + X | 2048 + X | 4096 + X | 8192 + X |
| Guard time (overhead) | 1.17 µs<br>X = 36<br>(6.6%) | 2.38 µs<br>X = 73<br>(6.6 %) | 4.76 µs<br>X = 146<br>(6.6%) | 9.52 µs<br>X = 292<br>(6.6%) | 19 µs<br>X = 584<br>(6.6%) |

Latency demands,
User velocity $\longleftrightarrow$ Coverage demands,
channel delay spreads

Hence, the UF-OFDM waveform proposal emphasizes the requirement to provide configurability in both frequency and time [SWA16], as it should be targeted by all other 5G waveform candidates. The configurability on time and frequency dimension for multi-service service support is exemplarily illustrated in Figure 4-5 for frequency spectrum smaller than 6 GHz case.
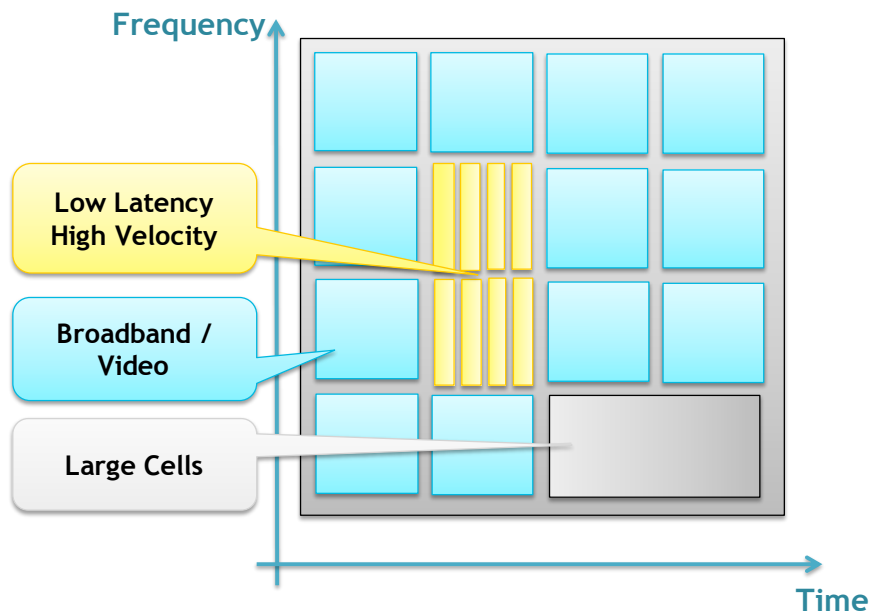


**Figure 4-5: Exemplary Multi-service air interface achieved by increased waveform configurability**

## 4.1.4 A qualitative, feature-driven AIV design for the 5G landscape

**Keywords**: assessment study, AIV mapping, waveform features
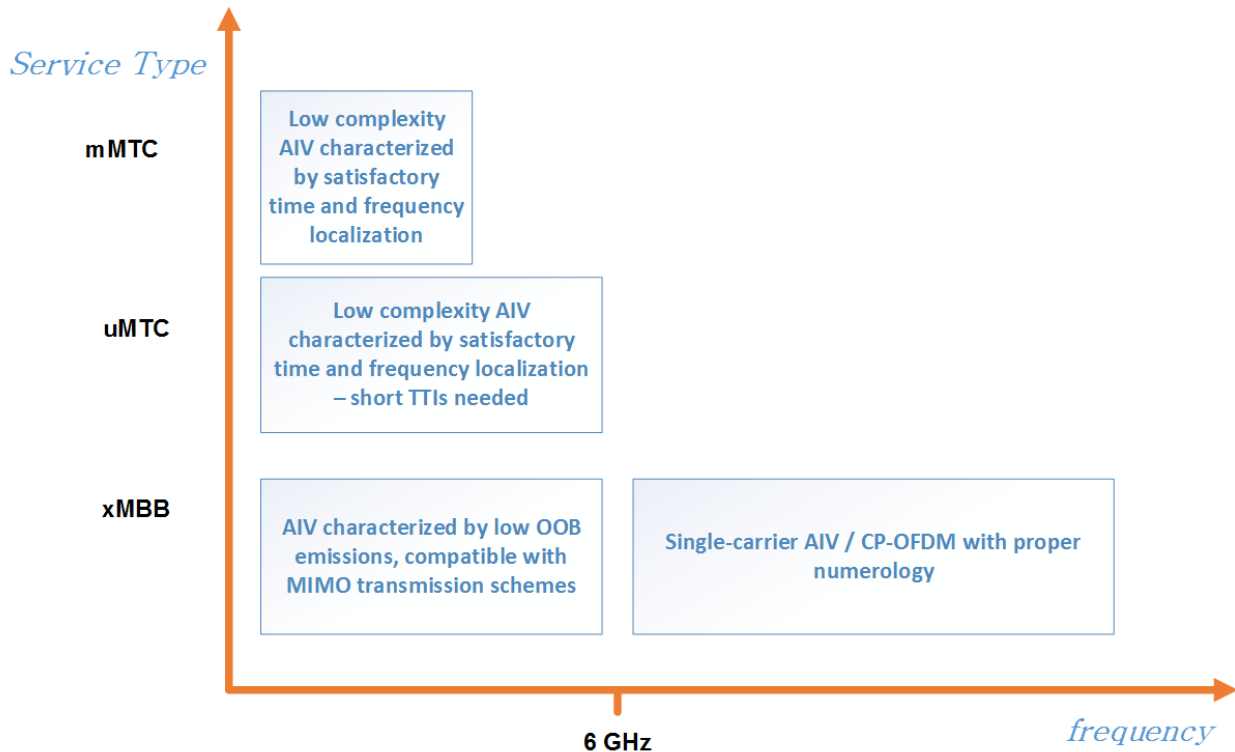


**Figure 4-6: Mapping of frequencies and services**

**xMBB service type**

**Frequencies below 6GHz**

The use of an AIV having the following essential features is required:

i. Low Out-of-Band (OOB) emissions in the frequency domain, in order to avoid the excessive use of guard bands, which would shrink the (already) short available bandwidth at such frequencies.

ii. Support of MIMO transmission techniques under a low complexity regime in order to achieve high throughput.

**Frequencies above 6GHz**

The selection of an appropriate AIV should be based on the following characteristics:

iii. Single carrier AIVs are promising due to the lower Peak to Average Power Ratio (PAPR) as compared to multi-carrier ones.

iv. Compatibility with massive MIMO transmission architectures is mandatory (via beamforming), in order to achieve high data rates, focusing on outdoor small cell as well as indoor deployments (i.e., short range communications). As an example, a CP-OFDM specific AIV can be used, under a suitable numerology.

v. The choice of the FFT size, the subcarrier spacing and the CP size (when a CP-OFDM based AIV is investigated) need to be carefully selected.

vi. High data rate requirements, in the existence of largely available bandwidths in such frequencies bring up the need for certain numerologies, where, high subcarrier spacing is going to be considered. Correspondingly, shorter sub-frame durations are obtained, which are essential in terms of achieving low end-to-end (E2E) latencies.

## uMTC & mMTC service types

### Frequencies below 6GHz

Tailoring one of the proposed AIVs to these specific service types, should be driven by the following observations:

vii. Good frequency localization is essential in order to enable asynchronous multiple access transmissions specifically needed for mMTC & uMTC service types. For example, focusing on OFDM based AIVs that could be achieved by filtering / windowing.

viii. Low complexity implementation should be considered for a subset of the mMTC related devices.

ix. Good time localization (as foreseen in OFDM-based AIVs) of the nominated WF is needed, in order to enable features like dynamic TDD (e.g., when fast switching between uplink (UL) and downlink (DL), is needed, in the coexistence of cross-service type deployments). Also, decent time localization of the selected AIV is beneficial for high mobility scenarios. Such a characteristic is essential regarding dense terminal deployments, in the existence of very short channel coherence times (envisioned for high mobility scenarios). For instance, when a TDMA approach in terms of access is applied, good time localization of the WF tailored to the selected AIV leads towards low multi-terminal interference and, as a consequence, higher spectral efficiency.

x. Regarding the uMTC specific use case, the numerology should be adjusted in order to sustain short TTIs which, in turn, lead towards low achievable RTT.

**Harmonization aspects**

**Harmonizing multiple AIVs**

In case more than one of the proposed AIVs is seen to co-exist in the same frequency range, then, harmonization between them should be first investigated, starting from the PHY layer. If this is not feasible even under parameterization, then the harmonization problem can be tackled at the MAC layer.

**Harmonization assessment study**

i.  Integration with LTE-A shall be considered, because it will lead to faster 5G initial deployments – LTE-A-Pro is envisioned to coexist with 5G (at least at an initial stage).

ii. In order to have the capacity to facilitate easier integration for future service types that are not yet defined, strong frequency and time confinement for the selected AIV(s) is required.

## 4.1.5    Air interface design based on P-OFDM

**Keywords**: Flexible numerology & frame structure, Adaptive pulse shape filter, Asynchronous multiple access, improved resilience against Doppler

To respond to the large variety of requirements from new use cases and services in 5G, a flexible air interface design supporting different PHY configurations (incl. numerologies and frame structures) in the same frequency band is targeted. The concept of waveform configurability as detailed in section 4.1.3 and illustrated in Figure 4-5 is adopted in this proposal, however, it is built on the waveform variant of P-OFDM (see section 3.1.1). Pulse shaping is used to balance the distribution of the signal power in time and frequency domain, and thus it does not only provide a spectral containment of the sub-band signals as in filtered OFDM, but further yields better robustness against signal distortions like Doppler and timing misalignment. P-OFDM uses a CP like in CP-OFDM, and it allows symbols to have a tail that may overlap with successive symbols, the latter providing improved robustness against timing and frequency mismatches. However, the overlapping factor, specifying the extent of overlap between succeeding symbols, is a free design parameter and needs to be carefully chosen dependent on the signal conditions. For most scenarios, it is favourable to chose the overlapping factor small, so that only small amounts of the symbols are overlapping (from 5 to 30 per cent), such that the temporal containment of the signal is close to the one of CP-OFDM and thus satisfying the conditions detailed in section 4.1.1. However, in some scenarios (in particular FDD), longer symbol durations can be afforded, opening the door for facilitation of highly robust signal transmission, which could be beneficially utilized for selected uMTC applications. In particular, one of the favourable features of P-OFDM in this context is its capability to enable asynchronous multi-user access of the same frequency resources, which could be realized by space division multiple access (SDMA) or superposition coding (for some

evaluation results on asynchronous access, refer to Appendix B.3). Compared to CP-OFDM, pulse shaping constitutes an additional degree of freedom for the system design: Together with the numerology, defined by the subcarrier spacing F and the symbol interval T (incl. cyclic prefix), P-OFDM thus offers three system design parameters in total to adapt the waveform to requirements from new use cases and services.

The problem space constituted by the 5G services, targeted frequency bands and cell sizes is covered by P-OFDM with different PHY configurations, where each of these PHY configurations will respond the needs of the particular problem area. The 5G landscape as covered by P-OFDM is depicted in Figure 4-7, where further details on the design parameters are given thereafter.
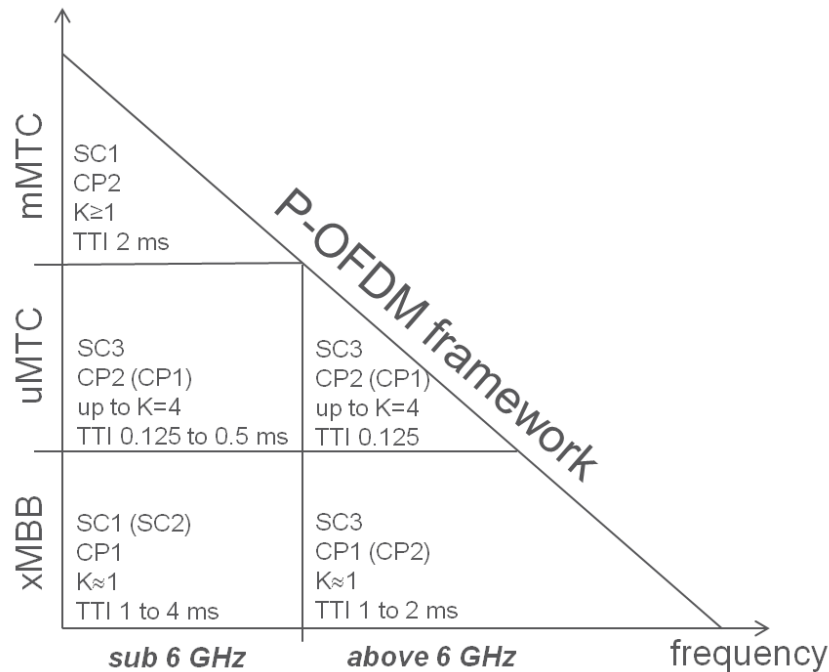


**Figure 4-7: Configurations of P-OFDM covering the 5G landscape of frequencies and services**

The solution based on P-OFDM offers the following PHY configuration options:

## Numerology

### Subcarrier spacing

As in the proposal in section 4.1.1, different subcarrier spacings are considered to allow adapting to larger subcarrier spacing in cases of high mobility or if very large bandwidth is available (like in the high frequency bands) to keep complexity to a reasonable level. The subcarrier spacing starts with 15 kHz as a basis, and is then scaled by integer multiples to allow

for compatibility of the corresponding frame structures. The following three configurations are supported:

- SC1: 15 KHz (basis)
- SC2: 30 KHz
- SC3: n*15 KHz (integer multiples)

where SC1 and SC2 are supported in LTE-like deployments, where SC2 is chosen for high mobility. SC3 is chosen for new services and use cases, like uMTC / mMTC services and broadband transmission in the high frequency bands.

**Symbol interval**

As in LTE, we consider to use two different CP lengths, which can be selected according to the channel environment (the larger CP to be chosen for large delay spread channels, as, for example, in Multimedia Broadcast Multicast Service (MBMS) scenario)

- CP1: 7% overhead (basis)
- CP2: 25% overhead (optional)

## Pulse shape

**Length**

The length of the symbol, specified by the overlapping factor K being a rational value describing the amount of symbol intervals T the symbol spans over, should be chosen depending on the desired signal conditions. In TDD scenarios, strict temporal containment of the symbols is desired, as detailed in preceding subsections. Hence, a small value for the overlapping factor close to one (K≈1) should be chosen, basically extending the symbol duration by up to half of the symbol interval at maximum. Thus, for TDD, the overlapping factor may be chosen to lie in the range K $\in$ [1, 1.5].

In FDD scenarios, however, the temporal containment of the symbols is not a strict requirement, since the overlap of succeeding time-domain symbols dedicated to different users does not create any mutual interference as long as they use the same pulse shape fulfilling the complex orthogonality constraint. An issue may occur only if the pulse shape is supposed to be changed during operation, but if properly considered by the system design, such changes may occur only seldomly. For FDD, much larger overlap factors up to K=4 are therefore allowed, which offer the favourable property to support time asynchronous transmission for FDMA as well as superposition access (like in SDMA, where more than one user access the same time/frequency resource). This property of asynchronous access is particularly beneficial in selected scenarios for MTC and V2X transmission, e.g. for low latency transmission, as the time-consuming connection setup phase can be omitted completely.

- K $\in$ [1, 1.5] for TDD scenarios and xMBB service
- K $\in$ [1.5, 4] for FDD scenarios and selected scenarios for MTC and V2X service

**Dynamic pulse shaping**

A set of useful pulse shapes, each one realizing a different distribution of the signal power in the time/frequency plane, can be provided by the system. These can be selected for particular scenarios and use cases, yielding improved robustness for signal transmission and thus better performance. For a given frequency resource, the pulse shape may be changed dynamically according to its allocation to a service or use case. However, for longer pulse shapes (overlapping factor K ≥ 2), reconfigurations may require some transition time, and hence changing the pulse shape is not considered to happen on a very fast time basis going down to the frame level in that case, but rather infrequent, yielding semi-persistent PHY configurations. For overlapping factor K close to one, this constraint is significantly relaxed, though.

## Frame structure

**TTI length**

Different TTI length are considered to allow adapting to strict latency requirements as well as adjusting to larger available bandwidth in the higher frequencies. For MBMS services, large TTI length is supported, which may reach up to 4 ms. For a scalable design, a minimum TTI length of 0.125 ms is considered, which is then doubled subsequently up to reaching the maximum TTI length of 4 ms. The symbol interval T should be chosen such that a TTI is always constituted of an integer number of OFDM symbols. Pilot structures should be designed such that they will also scale with the TTI length.

- 6 TTI length supported: {0.125, 025, 0,5, 1, 2, 4} ms

## UL/DL design

- We target a symmetric design for UL and DL; however, this has not yet been finally decided.
- DFTs-OFDM also works with P-OFDM, hence a single-carrier transmission may also be considered.

## 4.1.6 QAM-FBMC and OFDM Harmonized Solution

**Keywords**: QAM-FBMC, OFDM, beamforming
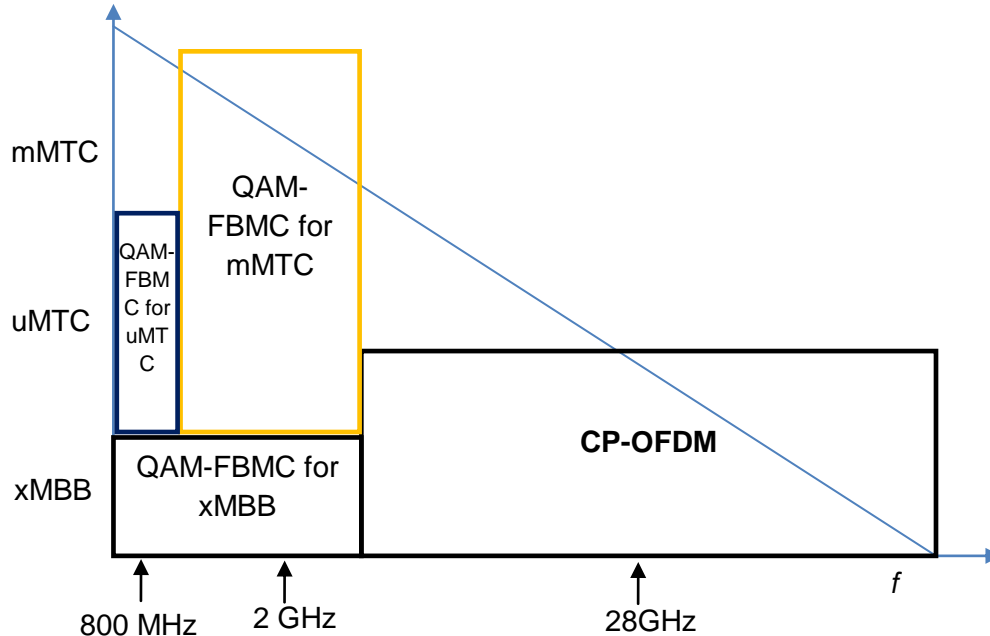


**Figure 4-8: Mapping of frequencies and services with fast beam switching for xMBB in mm-wave bands**

The proposed multi-WF harmonization can be reflected in Figure 4-8. Basically, from carrier frequency perspective,  lower bands are expected for coverage purposes and therefore suitable for both MTC services and outdoor xMBB services in a large area with larger cell sizes where the speed of terminal is expected to be from medium to high. On the contrary, higher bands, e.g., 28 GHz, with large contiguous bandwidth are more suitable to cope with the traffic capacity of xMBB services for indoor and outdoor in small cells and the expected low speed of terminals. Two AIVs with different PHY features will need to be harmonized to support heterogeneous services that have quite different requirements.

QAM-FBMC enhances the fundamental spectral efficiency because of the well-localized time/frequency traits adopted from a pulse shaping filter per subcarrier, thus reducing the overhead of guard band required to fit in the given spectrum bandwidth, while meeting the spectrum mask requirement. Furthermore, the effectively increased symbol duration is suitable for handling the multi-path fading channels even without CP overhead. Consequently, the FBMC system can reduce the inherent overheads such as CP and guard-bands in CP-OFDM.

In addition to higher spectral efficiency, QAM-FBMC is also well-localized in the frequency domain so that the OOB is very low, which makes it suitable to be employed in the lower end of the frequencies, e.g., 800 MHz or 2 GHz, where available spectrum bandwidth is highly limited.

It is also regarded as a natural candidate for asynchronuous scenarios, including Coordinated Multi-Point Transmission and Reception (CoMP), Dynamic Spectrum Access (DSA) in a fragmented spectrum. Furthermore, application of multiple prototype filters for different subcarriers provides an extra degree of design freedom so that complex domain orthogonality can be achieved, which makes it straightforward to apply conventional pilot designs and corresponding channel estimation algorithms as well as MIMO schemes as in CP-OFDM systems.

The performance of QAM-FBMC is compared with OFDM over Extended Pedestrian A model (EPA) and Extended Typical Urban model (ETU) channels in a 2×2 MIMO system and the results are presented in Figure 7-20 of Appendix A. In summary, in EPA channel, which is less frequency selective, the MIMO receiver in QAM-FBMC show similar performance with the receiver in CP-OFDM. Especially in ETU channel, which is more frequency selective, the minimum mean square error (MMSE) receiver in QAM-FBMC shows even better performance than that in CP-OFDM because MMSE equalization in oversampled domain and filtering can exploit frequency diversity in QAM-FBMC. . Even if we cannot see much frequency diversity gain as in MMSE receiver, noniterative per-tone Maximum Likelihood (ML) receiver in QAM-FBMC shows similar performance to ML in CP-OFDM in ETU channel. For further details the reader is referred to the Appendix B.

**CP-OFDM**

CP-OFDM achieves perfect orthogonality of subcarrier signals in the complex domain that allows trivial generation of transmit signal through IFFT, trivial separation of the transmitted data symbols at the receiver through FFT, and trivial adoption to MIMO channels. It is well-localized in time domain and thus suitable for delay critical applications and Time Division Duplexing (TDD) based deployments. Even though the spectral efficiency of CP-OFDM in terms of TF with T and F representing symbol duration and subcarrier spacing, respectively, is less than FBMC and it has comparatively high out of band (OOB) leakage, which can be tackled with enhanced solutions, these disadvantages can be easily compensated by the large available bandwidth in millimeter wave bands, e.g., 28 GHz.

## Harmonization Considerations

It is expected that the harmonization of multi-WF AIVs requires any modifications of the AIVs, especially in cases of approaches 3 and 4. However, it is unlikely that the fundamentally PHY layers of different AIVs will be changed, but changes in functionalities of higher layers resulting from harmonisation may impact the performance of said PHY layers.

- Waveforms, modulation and coding: even though multiple waveforms are chosen, they share the same modulation (QAM) and coding schemes (LDPC).
- Reference signals, baseband signal processing related to detection, equalization etc.: For CP-OFDM, pilot can be used to spread reference signals in the time and frequency grid and simple LS estimation and interpolation can be used at the receiver for frequency domain channel estimation. For QAM-FBMC, a similar approach could be implemented

with minor modifications. A harmonized channel estimation approach could be easily designed in such a case. Furthermore, same one tap equalization can be applied to both waveforms.

**Numerology, frame timing and time-frequency-space resource utilisation**

Another important issue to be considered for harmonization is the frame structure and numerology. Robust and efficient numerology and frame structure design are needed to achieve high throughput and reliable communication. Coexistence of data, control and measurement signals in the frame should also be supported by flexible and efficient design to achieve optimization at implementation and deployment, considering the antenna and RF configuration, hardware capability, the offered services, possibility of carrier aggregation, etc. Scalable measurement signal design is needed to efficiently support various MIMO/SDMA/hybrid beamforming configurations and beam scheduling and to minimize increase in hardware complexity. In addition to high throughput, other key KPIs of 5G, e.g., much lower latency compared with LTE/LTE/A, should also be supported with scalable design approaches.

As for most other air interface proposals, it is required to adapt the PHY numerology to a wide range of frequency bands and services. Here we focus on CP-OFDM AIV proposed for higher bands; details of QAM-FBMC AIVs are under investigation.

 In particular, two different numerologies are proposed for higher bands CP-OFDM AIV and these are detailed in Table 4-4 below.

**Table 4-4: Numerology for CP-OFDM**

| Parameter | LTE | Numerology 1 | Numerology 2 |
|---|---|---|---|
| **Carrier frequency** | 3GPP operating band | 28 GHz | 28 GHz |
| **Waveform** | OFDMA / SC-FDMA | OFDMA | OFDMA |
| **Subcarrier spacing** | 15 kHz | 150 kHz | 75 kHz |
| **TTI duration** | 1 ms | 0.1 ms | 0.2 ms |

| **TDD period** | 5 ms / 10 ms | Dynamic | Dynamic |
|---|---|---|---|
| | | | |

Frame structure design for TDD systems should be self-contained and flexible. Four exemplary data subframe types are shown in Figure 4-9.
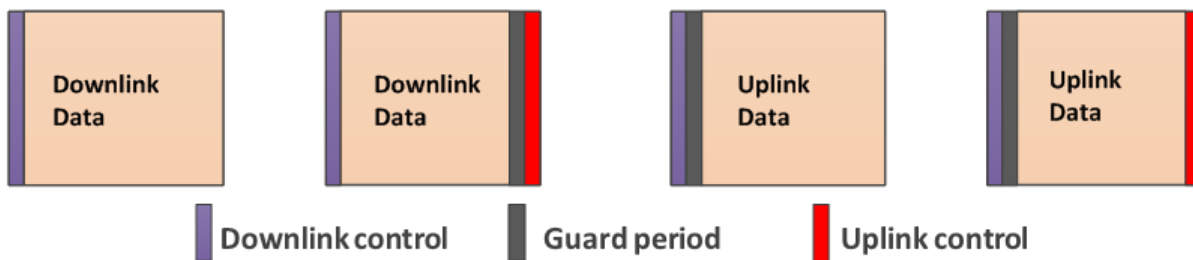


**Figure 4-9: Four types of subframe**

Time synchronization is the very first step for connection and synchronization for mm-wave is different from below 6 GHz systems because of beamforming as shown in Figure 4-10.
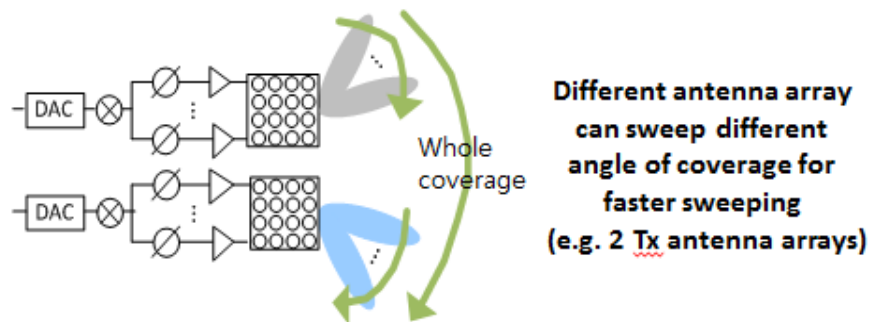


**Figure 4-10: Beam sweep for synchronization.**

There are two types of timing: symbol and subframe. Unlike LTE, subframe boundary cannot be known by SSS because beam sweeping symbol by symbol is needed during synchronization procedure. So, new SS is added to provide the function to tell the subframe boundary. Three signals for time synchronization are defined:

- Primary SS to achieve OFDM symbol timing and cell ID group
- Secondary SS for cell ID detection
- Extended SS to detect subframe boundary.

Fast and flexible periodic channel measurements should be supported by frame structure design, tailored for one of the most crucial enabling techniques for mm-wave - hybrid beamforming. In order to achieve maximum rate, beam measurement is needed to align Tx and

Rx beams. Beam measurements can be conducted by BS repeatedly transmitting beam measurement reference signal (BMRS) in an interval while at the same time UE measures with Rx sweep in the same interval as shown in Figure 4-11.
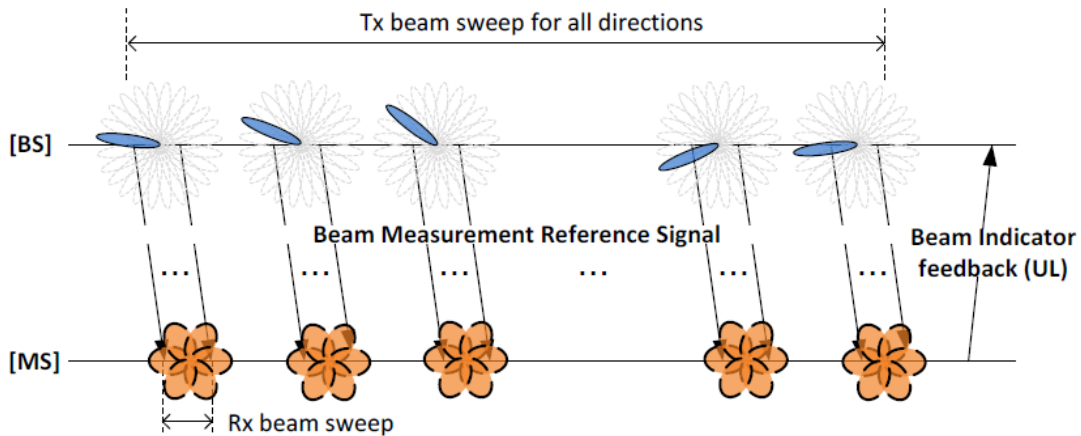


**Figure 4-11: BMRS transmission.**

In order to accommodate various measurement activities with different cycles due to the implementation of beamforming, three levels of notations are defined for frame structure: radio frame, subframe and slot. Synchronization, broadcasting and random access signals could be transmitted in the same subframe periodically. BMRS can be conducted once per radio frame or several radio frames depending on the variation of the environment. The position switching from UL to DL within a radio frame could be flexibly adapted to required DL/UL data rates. An exemplary TDD frame structure is illustrated in Figure 4-12, where 1 ms target air-latency can be achieved.
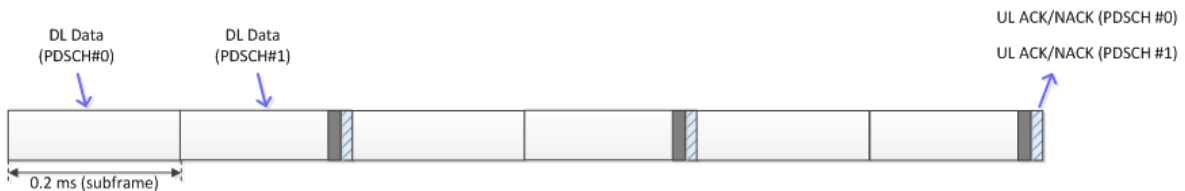


**Figure 4-12: Frame structure.**

The frame structure and numerology for QAM-FBMC is expected to be different because of the different symbol architecture and duration. However, the details still need further investigation.

## 4.1.7 OFDM based solution with flexible numerology and frame structure

**Keywords**: OFDM, frequency and quadrature amplitude modulation (FQAM), beamforming, flexible frame structure
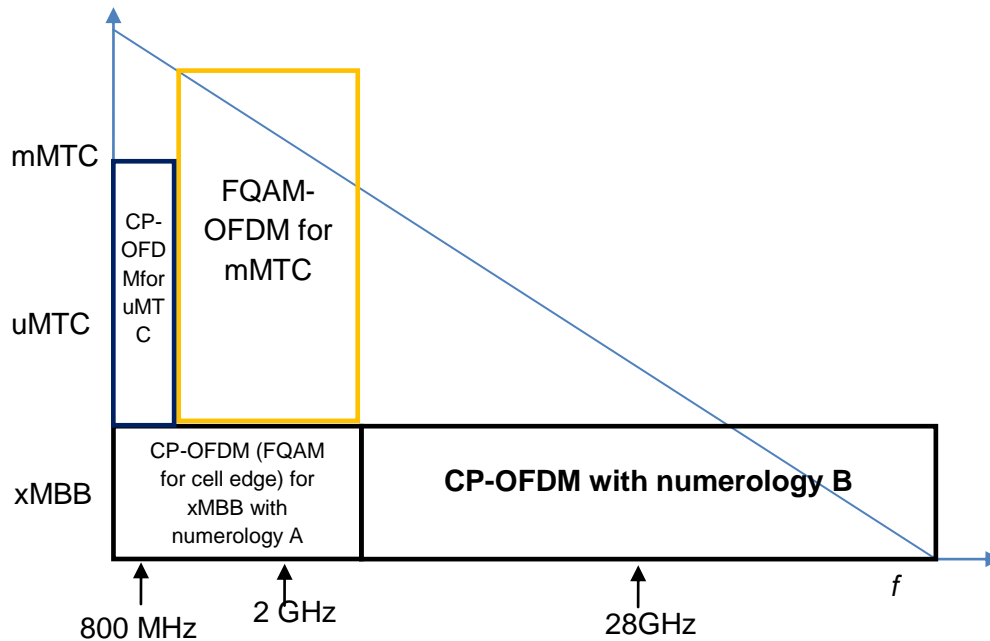


**Figure 4-13: Mapping of frequencies and services with fast beam switching for xMBB in mm-wave bands**

This solution is based on CP-OFDM and possibly its enhancement. CP-OFDM is used for xMBB services but different numerology and frame structures will be used for below and above 6 GHz. For example, shorter TTI and larger subcarrier spacing will be employed for above 6 GHz bands to explore the potential of more available spectrum bands and achieve much shorter latency. FQAM-OFDM could potentially be used for mMTC because of its reduced PAPR, leading to improved energy efficiency [Hyu14]. FQAM can also be used for xMBB to enhance the experiences of the cell edge users. It is worth mentioning that FQAM can also be integrated with other waveforms, e.g., QAM-FBMC.

Similar numerology and frame structure consideration in the previous solution, e.g., QAM-FBMC and OFDM Harmonized solution, can also be applied in this solution.

## 4.1.8 Multi AIV (OQAM-FBMC, CP-OFDM) harmonisation aspects for above PHY layer

**Keywords**: OQAM-FBMC, CP-OFDM, MAC/RLC/PDCP commonalities, adaptive beamforming
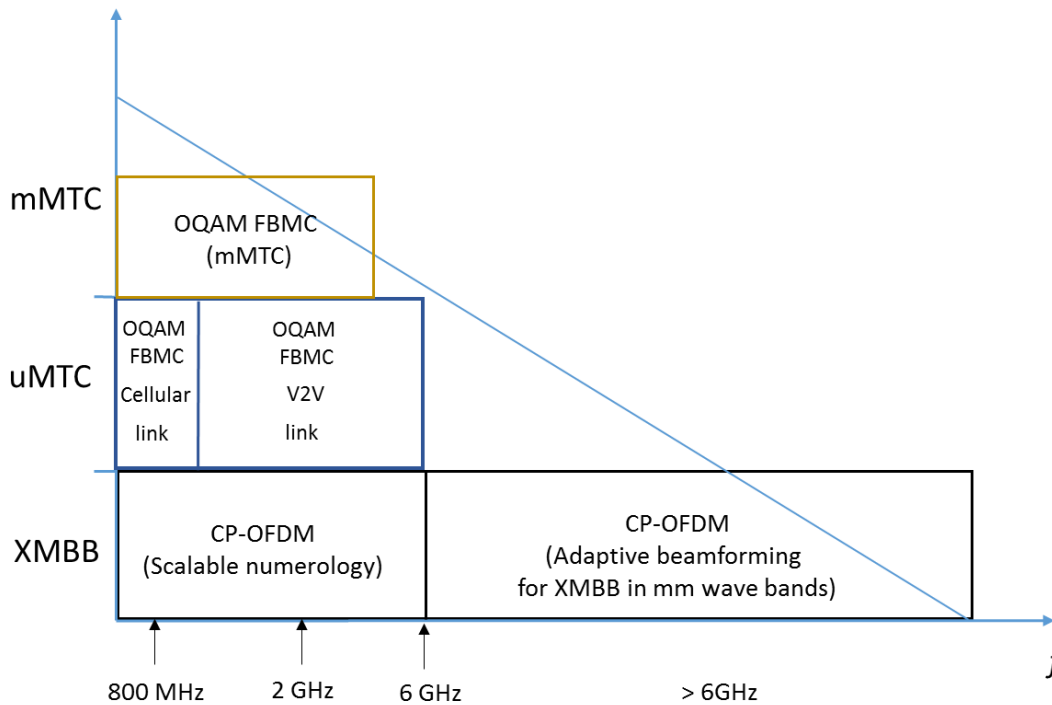


**Figure 4-14: Mapping of frequencies and services**

- For XMBB, CP-OFDM with scalable numerology is envisioned for frequency bands < 6 GHz. Although OQAM-FBMC has gains over CP-OFDM because of no cyclic prefix, due to CP-OFDM's ease of use with MIMO, it is favored over OQAM-FBMC. OQAM-FBMC would require modifications for its use with MIMO.
  For frequency ranges in mm-wave bands, CP-OFDM with adaptive beamforming targeting high data rates and short E2E delay is picked.

- For uMTC, OQAM-FBMC is chosen at low frequencies enabling long distance coverage and asynchronous transmission. uMTC also spans for some high frequency bands, i.e. at carrier frequency of 5.9 GHz. For the uMTC scenario, especially for V2X communications, one link from cellular network to each connected car is not sufficient to support the ultra-reliable requirement. Thus, another link to form the V2V direct communication is necessary to be added and that link can use a higher frequency band. For mMTC, OQAM-FBMC is selected to support wide service specific adaptations and efficient spectrum sharing.

## 4.1.9    Adaptive Filtered OFDM with Regular Resource Grid

**Keywords**: Massive MIMO, beamforming, flexible numerology, asynchronous multiple access, regular resource grid.
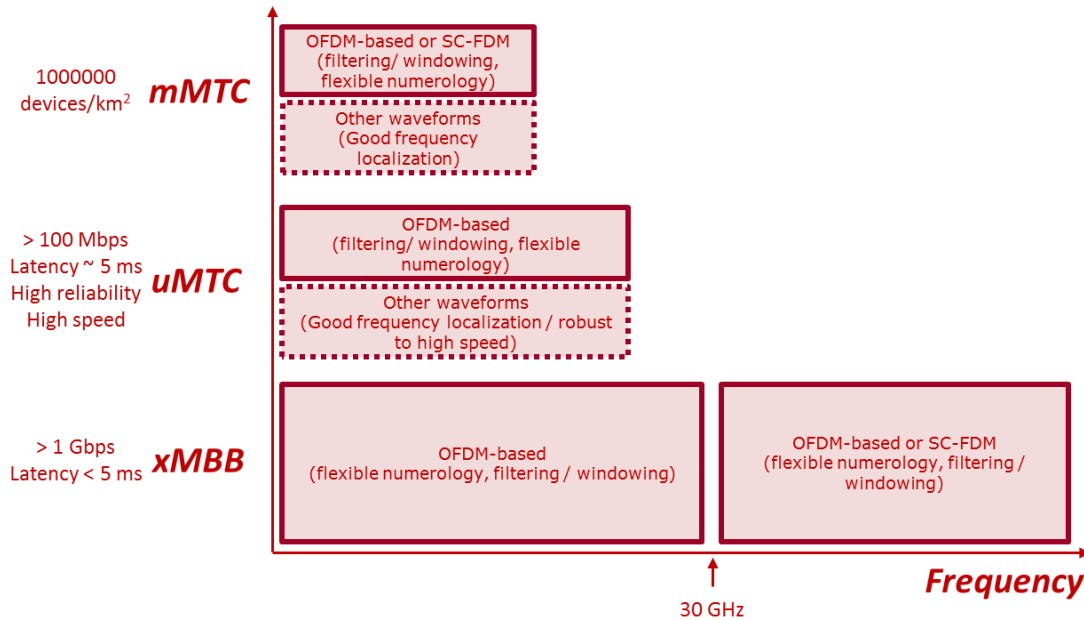


**Figure 4-15: Mapping of frequencies and services**

For xMBB, OFDM based AIV with flexible numerology (e.g. subcarrier spacing, CP length) and shorter TTI is envisioned for frequency bands < 30 GHz. Massive MIMO and beamforming are key technologies to provide fundamental gain so they should be easily supported by the new AIV. Filtering/ windowing could be applied for better coexistence of different numerologies or flavors in the same band/carrier.

For frequency ranges in millimeter wave bands, single carrier OFDM based AIVs (e.g. with DFT precoding) are promising due to the lower PAPR. Good frequency localization can be achieved by applying advanced CP (e.g. zero CP) and/ or filtering/ windowing.

For uMTC and mMTC, lower frequencies and optionally single carrier are envisioned to ensure wide area coverage. This is very crucial to guarantee high reliability (for uMTC) for example.. OFDM based AIV with additional filtering/ windowing could be used in such scenarios. Filtering/windowing is essential to achieve good frequency localization enabling asynchronous multiple access transmissions. Other AIVs from other waveform families (e.g. OQAM-FBMC) could be worth to consider in such scenarios due to their very good frequency localization enabling asynchronous multiple access transmissions and their robustness to high mobility.

## Harmonization considerations

In a classical OFDM system like LTE downlink the subcarriers are orthogonal to each other as long as the signals are received synchronously and the channel is static and therefore does not introduce inter-carrier interference (ICI). In case of a time-varying channel the ICI depends on the Doppler spread and may degrade the performance. But also asynchronicity between different users in uplink or different subcarrier spacing on different subbands introduce ICI. In such cases, F-OFDM can significantly reduce the interference between different subbands. Basically, the filtering of a subband of an OFDM system does not violate the orthogonality between the subcarriers within one subband but can theoretically completely avoid ICI between subbands if the filter would be a perfect bandpass filter. In practice, perfect bandpass filters are not suitable as they would require an infinite length of the filter impulse response. Therefore, filters are used that show a compromise between filter length and OOB suppression. This leads to filters that do not perfectly suppress the ICI, but keep it at a reasonable level. Nevertheless, even if the OOB radiation is reasonable for a setup with equal power users, the interference may become unacceptable if the interfering user has much higher power. This situation can occur if no proper power control is applied, e.g., as expected for Internet of Things (IoT) applications. In such a case, additional guard bands may be needed to achieve an acceptable level of interference. The width of the required guard bands highly depends on the specific circumstances including modulation scheme, power of neighboring users and filter shape. In order to have an efficient system, such guard bands should be chosen flexibly for any particular transmission.

## Regular resource grid

Many communication systems use a regular resource grid, meaning that the entire resource space in the time and frequency is divided into several sub-blocks of mostly same size. One example is LTE, where a slot is divided into a number of physical resource blocks (PRBs), each of them containing 14 symbols and 12 subcarriers. Based on these blocks, many signaling information refers to one or more resource blocks rather than to individual symbols or subcarriers. In this way, the amount of signaling overhead that are related to resource allocations and scheduling can be significantly reduced. So the granularity of the measurements and signaling of the resource grid plays a crucial role for the efficiency of a system; trade-off between quality of measurement reports and signaling overheads. While some granularity is needed as certain parameters should be adapted to the specific condition on a certain subband, the most efficient way would be to go for a regular resource grid, as any kind of irregular grid would lead to the need for extra signaling of the position of a certain subband within the entire resource space. Therefore, it is highly desirable to keep a regular resource grid also in future systems.

## 4.1.10    Harmonization aspects for D2D communications

One of the key enablers for 5G is the possibility of direct Device to Device (D2D) communications. In the case of mMTC, these can be used to gather the messages of many power-limited devices by one central device that, afterwards, sends an aggregated message to the base station. In the case of uMTC, D2D communications are very relevant in a vehicular scenario in which vehicles share critical safety information. Finally, in the case of xMBB, D2D communications can be used to share large amounts of data between close devices, like, for instance, sharing a high definition video between a smartphone and a smart television.

Although the devices are synchronized with the serving base station, i.e., they know the Timing Advance (TA), they are not synchronized with each other. This implies that, in a 4G system, the devices should estimate their own TA before any data transmission takes place, consuming non-negligible amounts of resources for synchronization signals and delaying the transmission. METIS-II is looking at other possibilities for addressing this problem in a 5G system. In particular, the good behavior of certain waveforms (and their corresponding numerologies) against certain lack of synchronism may be used to reduce (or even eliminate) the amount of synchronization signals. Considering the aspects described in the following paragraphs, it is proposed to follow the waveform mapping of Figure 4-16 for D2D communications.
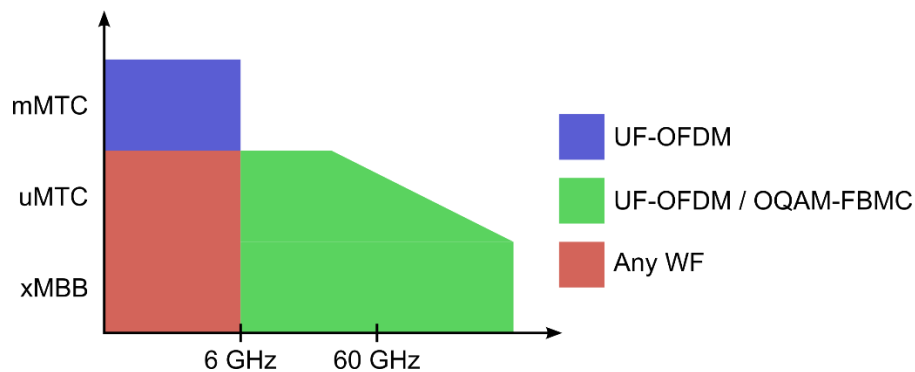


**Figure 4-16: Waveform mapping into frequency bands and services for D2D communications.**

METIS-II has conducted a first waveform study using a hardware testbed in the 5.9 GHz band. In particular, two devices located in the same angular direction with respect to the base station and separated from 0 to 225 meters transmitted to each other with their TAs (estimated with respect to the base station) using 16-QAM and different waveforms. The results show that all waveforms can be configured to adapt to the different levels of asynchronism. However, the way CP-OFDM is adapted is based on larger CPs that reduce the amount of resources that can be used to transmit data. Due to this, UF-OFDM and OQAM-FBMC seems to be the most promising waveforms for communications with lack of synchronism.

The need of robust waveforms against lack of synchronism is more doubtless in higher frequency bands in which the symbol periods are expected to be almost proportionally reduced with respect to the frequency.

Taking all this into account, it is proposed to use the waveform mapping of Figure 4-16 for the following reasons:

- UF-OFDM and/or OQAM-FBMC are proposed for the medium to high frequency bands due to the short distance at which CP-OFDM is degraded with a low CP.
- mMTC are expected to be constituted of very short bursts of sporadic transmissions for which the synchronization process may take large amounts of resources (as compared with the data transmission). At the same time, the long pulse tails of FBMC (for high K factors) delay the data transmission/reception and make devices to be active during a non-negligible amount of extra time. Thus, it is proposed to use UF-OFDM in the lower frequency bands for mMTC.

## 4.2 Analysis of commonalities

The following table presents an overview on the commonalities of the solution proposals as described in Section 4.2, based on a tentative set of features extracted from those descriptions. The proposals are presented in the columns in the order of their presentation in Section 4.2, while their descriptive name has been shortened for brevity. An X in the table highlights that the feature is supported by the proposal, while an (x) means this feature is covered only partially, as it applies as an option for selected use cases or a subset of the frequency bands only. In the first row, the approach is assigned to one of the categories introduced in the beginning of Chapter 4, i.e. either the approach building on an „OFDM framework with variations tailored to meet different 5G service requirements and bands," or the approach building on "multiple waveforms to cover the overall 5G landscape."

| | Harmonized L1-L3 with CP-OFDM | Harmonized CP-OFDM | UF-OFDM | Qualitative AIV design | P-OFDM | Harmonized QAM-FBMC & OFDM | OFDM with flex. numerology | Harmonized OQAM/FBMC & OFDM | Adaptive Filtered OFDM | Harmonization for D2D comm. |
|---|---|---|---|---|---|---|---|---|---|---|
| OFDM framework (O) or Multiple WFs (M) | O | O | O | M | O | M | O | M | O | M |
| Time localized symbols for xMBB | X | X | X | | X | (x) | X | X | X | (x) |
| Time localized symbols for uMTC | X | X | X | X | | | X | | (x) | (x) |
| Time localized symbols for mMTC | X | X | X | X | (x) | | X | | (x) | X |
| Scalable numerology over frequency bands | X | X | X | X | X | X | X | X | X | X |
| Symmetric waveform for UL/DL for xMBB | X | | (x) | | X | (x) | (x) | X | (x) | |
| Symmetric waveform for UL/DL for uMTC | X | | (x) | (x) | X | X | X | X | (x) | |
| Symmetric waveform for UL/DL for mMTC | X | | (x) | (x) | X | X | X | X | (x) | |
| Asynchronous communication for xMBB | | | X | | (x) | (x) | | | X | (x) |
| Asynchronous communication for uMTC | | X | X | X | X | X | | X | X | (x) |
| Asynchronous communication for mMTC | | | X | X | X | (x) | X | | X | X |

## 4.3　　　First evaluation of harmonization criteria

In this part we present the results of an initial qualitative evaluation of the harmonization criteria for both the approaches followed by the air interface design proposals.

The requirements of the 5G system are captured by the five METIS II use cases, where for each of those particular KPIs with corresponding target values are specified (see Table 4-5, for further details, refer to [MET216-D11]).

Table 4-5 shows the 5G use cases studied by METIS-II and some of their characteristics such as KPIs that needs to be fulfilled. These are certainly not the only 5G use cases but certainly a significant sample that maps to KPIs that are general enough so that new unpredictable uses cases will likely be covered by these.

**Table 4-5: Use cases and requirements for evaluation**

| Use Case (UC) | Key Performance Indicator (KPI) | Requirement |
|---|---|---|
| UC1 Dense urban information society | Experienced user throughput | 300 Mbps in DL and 50 Mbps in UL at 95% availability and 95% reliability |
| | E2E RTT latency | Less than 5 ms (augmented reality applications) |
| UC2 Virtual reality office | Experienced user throughput | 5 (1) Gbps with 20% (95%) availability in DL 5 (1) Gbps with 20% (95%) availability in UL both with 99% reliability |
| UC3 Broadband access everywhere | Experienced user throughput | 50 Mbps in DL and 25 Mbps in UL at 99% availability and 95% retainability |
| UC4 Massive distribution of sensors and actuators | Availability | 99.9% |
| | Device density | 1 000 000 devices/km$^2$ |
| | Traffic volume per device | From few bytes per day to 125 bytes per second |
| UC5 Connected cars | E2E one-way latency | 5 ms (traffic safety applications) |
| | Experienced user throughput | 100 Mbps in DL and 20 Mbps in UL (service applications) at 99% availability and 95% reliability |
| | Vehicle velocity | Up to 250 km/h |

## 4.3.1    Common evaluation of OFDM based solutions

**Performance fulfillment**

By referring to the KPIs specified for the use cases in the table above, it is described in the following that the OFDM based solutions exhibit favourable waveform-specific features that can be beneficially utilized to address those KPIs.

- **User throughput**: for extreme data rates, transmission in higher frequencies is mandatory (where spectrum is available). Consequently, the *massive usage of beamforming* is a key aspect. OFDM based schemes combine very favourably with multi-antenna schemes, such as beamforming. Other features will be essential such as *carrier aggregation*, *multi connectivity* and the usage of *unlicensed spectrum access*. By LTE-A evolution, it has been proven that CP-OFDM can support UP aggregation features such as carrier aggregation, dual connectivity and access to unlicensed spectrum, all of those being important features to achieve 5G data rate requirements.

- **E2E RTT latency**: There are many ways to achieve low latency such as the usage of *shorter TTIs*, *smarter ACK schemes*, *optimized state transition*, etc. There are also other aspects out of the scope of the RAN design such as the placement of CN and Service layer NFs closer to the access sites. For the OFDM based schemes, each symbol is very well localized in time, resulting in well confined TTI lengths being constituted of a small number of OFDM symbols only, as in the case of short transmission bursts prevailing in various MTC applications.

- **High availability use cases**: the most straightforward way to increase availability is to provide coverage and provide mechanisms to enable the UE to detect the network. *Usage of both low and higher frequency AIVs, including evolution of LTE*, are relevant technologies to be used within the AIVs where high availability is needed. Multi-antenna technologies are also a key aspect such as the usage of beamforming. Multi-antenna technologies developed for OFDM are very mature, rendering OFDM a suitable choice to support high availability use cases.

- **High speed use cases:** The AIVs used for that use case need to provide robustness against Doppler in a combination with other KPIs (depending on the C2C use cases) such as shorter delays and/or high data rates.

**Ability to dynamically utilize radio resources**

OFDM based solutions achieve perfect or near perfect orthogonality of subcarrier signals in the complex domain that allows trivial generation of transmit signal through IFFT, trivial separation of the transmitted data symbols at the receiver through FFT, and trivial adoption to MIMO channels. The time-frequency grid resource space formed by OFDM is in nature suitable for

dynamic radio resource utilization. The solutions proposing the use of OFDM to address all 5G services facilitates the usage of a common resource management framework in a short time scale where for each TTI, transport blocks can be scheduled for one service or another, depending on the traffic demands of each service. This might be a bit more challenging in the case of scheduling services with different numerologies, which may pose some constraints on the time scales. For xMBB services, millimeter wave bands, due to the large available spectrum bandwidth, are considered as one of the most promising approaches to significantly boost the capacity. However, due to the hostile propagation condition in millimeter wave radio channels, e.g., severe path loss, vulnerability to blockage, etc., large antenna gains at both transmitter and receiver sides are required to overcome propagation losses. In this regard, very large scale antenna arrays are needed that enable highly directive transmit and receive beamforming, which can be easily implemented for OFDM based solutions. Because of the utilization of beamforming, a new degree of freedom is created for radio resource utilization in the spatial domain. This integrated with beam scheduling and beam steering can provide coordinated transmission to exploit the spatial degree dynamically to greatly enhance the network capacity.

The proposed OFDM based solutions with strict time localization of symbols allow both for a common multi-service scheduler and a multiple coordinated multi-service scheduler, operating on a fast time scale (TTI basis). Such a scheduler can prioritise a service (or a user) on a sub-frame basis without 'semi-statically' reserving a longer time duration for one particular service. In addition, the symbol and frame structure of OFDM can be flexibly adjusted to be adapted to very diverse service requirements.

**Support for UP aggregation among new AIVs**

By LTE-A evolution, it has been proven that CP-OFDM can support the highest level of UP aggregation features, such as carrier aggregation. In the case of AIVs being deployed in different sites, it can also support multi-connectivity. Another feature that has been proven to work with OFDM is the usage of unlicensed bands.

**Ability to reuse SW and HW components among new AIVs**

The usage of OFDM for all bands and services allows the reuse of most of the HW components, since a simple SW parameterization can be used if different bands are being supported by a single baseband processing board. On the network side, this maximizes the HW utilization in scenarios where different carriers or services do not exhibit the same amount of traffic. In other solutions where dedicated components (such as pulse-shape filters) are used for specific services or carrier only, there may be some sub-utilization of selected HW/SW components in case the specifc service or carrier exhibits low traffic.

On the device side, a harmonization based on OFDM is particularly valuable for multi-service devices that might not be using multiple services simultaneously or devices capable of supporting carrier aggregation / dual connectivity, where components can be reused to switch from one to another.

**Standardization effort and product development of AIs (time to market)**

The usage of OFDM for all bands and services allows more simplified implementations based on SW parametrization for most of the cases. This enables standardization to treat different use cases addressing distinct services in a single track. Otherwise, the usage of different PHY layer technologies per service may lead to their treatment in parallel tracks, which may increase the amount of effort required to standardize features as well as the time to introduce new services into the market. In particular, the use case differentiation aspect in the lower layers of the protocol stack may propagate to the higher layers and thus increase the amount of standardization efforts. If changes occur in the higher layers For a harmonized PHY layer, as provided by the OFDM based solutions, the work on the lower layers can still be reused, minimizing the efforts to standardize new services.

The usage of OFDM allows to some extent the usage of similar PHY protocols for coverage detection, synchronization, cell search, etc. for the different services, despite the fact that there could be differences for the different bands.

The RAN4 efforts to define requirements for measurements may also be different if substantially different PHY technologies are defined for different services and bands.

Additionally, the usage of OFDM in higher bands is already being trialed, with further multiple trials announced (e.g., trial for PyeongChang Winter Olympics 2018) Therefore the technical feasibility of product development in higher bands based on OFDM has already been proven; additionally, this system design is well-aligned with the current 3GPP Study Item on New Radio [3GPP16-38913].

**Ability to integrate new AIVs with LTE-A**

CP-OFDM is already used in LTE-A, so an integration becomes much easier if the 5G system is solely based on OFDM. When it comes to the protocol stack, it is possible to at least integrate on a PDCP level and, depending on the numerology being used and the deployment, even consider some sort of common scheduler in the case of dual connectivity. When it comes to implementation, some HW components could be reused in the case that both LTE-A and 5G are implemented in the same site.

**Forward compatibility**

OFDM based solutions are forward compatible since the design of OFDM can be highly flexible and the design parameters of CP, frame structure and numerologies can be easily modified for expected different service requirements in the future.

## 4.3.2　　Evaluation of specific solutions based on OFDM variants

**Harmonized CP-OFDM for multiple bands with enhancements for multi-service support**

**Performance fulfillment**

As illustrated in section 4.1.2, the single waveform family can be optimized for service types and use cases based on parameterizable parameters such as zero tail, zero head length, filter length. OFDM waveform parameters such as subcarrier spacing and guard bands in the time frequency grid can be chosen for optimized performance in a band. A shortened sub-frame duration with bi-directional control is a main enabler for supporting low latency services. At the same time, a reasonable CP overhead is targeted by the careful choice of numerology for high throughput. The time localization property of OFDM and OFDM enhancements such as ZT-DFTs-OFDM makes it a good choice for high speed use cases and ultra-reliable use cases. The spectral containment property is useful for certain asynchronous scenarios. The support of massive machine type communication is envisaged to be enabled via ZT-DFTs-OFDM which has good spectral containment property, as well as through integration with LTE-A.

**Ability to dynamically utilize radio resources**

Utilizing MAC layer scheduling degrees of freedom with a single numerology is an appealing aspect of the proposed harmonization approach. In the case of TDD (and dynamic/flexible TDD) this suggests that a reduced switching duration from UL to DL (and also a flexible switching) is possible by using a compatible numerology for CP-OFDM and its enhancements.  This benefit comes from the fact that good time localization (without long filter tails or longer symbols) can be achieved with enhancements such as ZT-DFTs-OFDM, thus allowing flexible TDD switching to happen. A key aspect of the solution is embedding of downlink and uplink control signals within each subframe which allows for fast scheduling of different service types based on priority.

**Ability to reuse SW and HW components among new AIVs**

In addition to the reuse of most of the hardware components in the LTE/LTE-A systems for the CP-OFDM based downlink described already in section 0, user equipments can use ZT-DFTs-OFDM without new significant hardware design by reusing SC-FDMA design.

**Standardization effort and product development of AIs (time to market)**

The usage of OFDM based waveform is especially relevant to 5G standardization for application to new carrier types and support multiplexing of different services. Thus approaches based on slight modification to OFDM can be used  to achieve a lean standard for fast and low complexity baseband implementation at both user equipments and base stations.

**Multi-service support with UF-OFDM**

**Ability to integrate new AIVs with LTE-A**

The close relation between UF-OFDM and CP-OFDM enables 5G (if applying the former) to be tightly integrated with LTE-A. As extreme case, LTE-A and 5G may even share the band and trade frequency resources according to the actual needs. Though, a more simple integration may e.g. follow the principle of carrier aggregation.

**Forward compatibility**

The strong frequency and time confinement (by applying techniques like UF-OFDM and in-resource control channels) helps to ease the integration of future use cases not even yet anticipated.


## 4.3.3 Evaluation of solutions based on multiple waveforms

**QAM-FBMC and OFDM Harmonized Solution**

**Ability to dynamically utilize radio resources**

QAM-FBMC is well-localized in the frequency domain so that the OOB is very low, which makes it suitable to be employed in the lower end of the frequencies, e.g., 800 MHz or 2 GHz, where available spectrum bandwidth is highly limited. It is also regarded as a natural candidate for asynchronized scenarios, including Coordinated Multi-Point Transmission and Reception (CoMP), Dynamic Spectrum Access (DSA) in a fragmented spectrum. When considering xMBB services with certain coverage requirements, e.g., urban macro deployment, lower frequency bands are also needed and because of the more efficient usage of the spectrum bandwidth due to low OOB, QAM-FBMC is favorable in such cases. CP-OFDM is well-localized in time domain and thus suitable for delay critical applications and Time Division Duplexing (TDD) based deployments. Even though OFDM has comparatively high out of band (OOB) leakage, which can be tackled with enhanced solutions, this disadvantage can be easily compensated by the large available bandwidth in mm-wave bands, e.g., 28 GHz.

**Support of UP aggregation among new AIVs**

Design parameters of CP-OFDM can be highly flexible and QAM-FBMC has additional design degree of freedom, e.g., filter design so that both AIVs are capable of meeting different service requirements, which makes UP aggregation possible for both AIVs.

**Ability to reuse SW and HW components among new AIVs**

The implementation complexity and cost of CP-OFDM are low. Additionally, the QAM-FBMC system can be efficiently implemented using M/2-point inverse fast Fourier transform (IFFT), 2K-times repetition, and time domain filtering, where M and K representing FFT size and

overlapping factor, respectively. The complexity of IFFT is actually reduced from O(Mlog2(M)) to O(Mlog2(M/2)) due to the reduced IFFT length. The repetition will only add negligible complexity. The time domain filtering is implemented by element-wise multiplication. At the receiver side, polyphase network (PPN)-FFT scheme can be used with minor complexity addition. The time domain filtering is implemented by element-wise multiplication. The FFT/IFFT, time domain filtering parts can be easily reused by other new AIVs where the subcarrier is shaped using time domain filtering. The channel estimation/equalization algorithms can also be reused with negligible modification.

**Standardization effort and product development of AIVs  (time to market)**

The solutions based on multiple WFs do not have the traction as those based on OFDM, at least for the time being. In the short-term, 3GPP is focused on OFDM-based solutions; nevertheless 3GPP is open to solutions based on other WFs, which indicates an openness to exploring various options including those in this section. It should further be noted that FBMC is not a newcomer to the telecommunications history. In the 1990s, advancements in DSL technology motivated more activity beyond discrete multitone (DMT), the equivalent terminology often used in DSL literature instead of OFDM. Early development in this area is an American National Standards Institute (ANSI), which was later expanded and called discrete wavelet multitone (DWMT), which is closely related to FBMC. The research on FBMC has gained lots of attention recently because FBMC offers the right balance between 'shorter-term' (standards-linked work) and longer-term, more open-ended research required of 5G.

**Ability to integrate new AIVs with LTE-A**

For below 6 GHz bands, QAM-FBMC is compatible with OFDM (in terms of transceiver architecture), and for above 6 GHz band, OFDM as used and experienced from 3GPP standardization can be reused.

**Forward compatibility**

For QAM-FBMC, application of multiple prototype filters for different subcarriers provides an extra degree of design freedom so that it is possible to efficiently introduce new features and services by modifying the prototype filters in terms of overlapping factor, filter shape, etc.

## 4.3.4 End-to-end evaluation of CP-OFDM and flexible sub-frame structures

In this section, we describe an end-to-end 5G mmWave-aided simulative framework [mmW_ns3], which can beneficially be used to evaluate different CP-OFDM-based numerologies over different UCs and bands, such as those that have been proposed in harmonized AI proposal in section 4.2.1. We aim at evaluating the harmonization approach of a CP-OFDM waveform to ensure a good coexistence among numerologies, which are adaptively

mapped onto different use cases. Our main goal is to evaluate the impact of mmWave bands in a full stack next generation cellular system. Thanks to the high LTE-compatibility, along with a full customizability of the adopted waveform and frame structure, we will evaluate the overall performance at lower frequencies including numerologies such as those provided in section 4.2.1.

Some initial results, highlighting the capabilities of the evaluation framework, are presented in Appendix B.5.
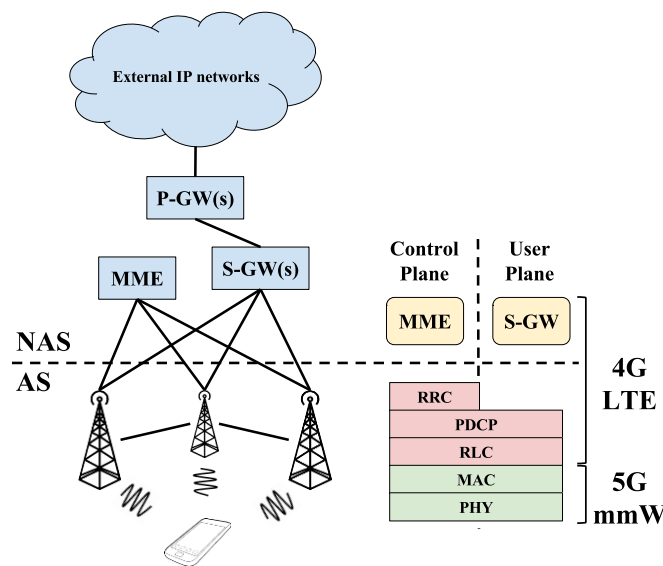


**Figure 4-17: End-to-end mmWave-aided simulation framework.**

The end-to-end simulation framework [MDZ+15] [FZD+16] shown in Figure 4-17 includes:

(i)    a detailed characterization of the millimeter wave bands plus BF capabilities at the **PHY layer**,

(ii)    a flexible sub-frame for millimeter wave communications with CP-OFDM, as defined in Chapter 3 (+ HARQ + dynamical TDD) at the **MAC layer,**

(iii)    all the main functionalities of the 4G LTE stack, from the **RLC layer above** (including EPC [LENA_ns3]).

# 4.4    MAC Layer Harmonization

This section presents a L2 concept for the 5G radio interface(s) including new contention based access physical control channels, a new access scheme and a scheduling entity as part of the harmonized MAC framework. Furthermore, the MAC layer harmonization is built on OFDM waveform with different numerologies in order to cater to different future services. Additionally, when designing L2 for 5G we have used a few key design principles that are important to keep in mind when examining the solutions in this section. Some key design principles and how they impact the L2 design are given in Appendix B.1.

Since 5G targets a number of different use case specific AIVs which may be different in terms of TTI and numerology, it is essential that the 5G RAN is designed so that the scheduler is aware of all AIVs, considers the different available resources and different services to allow the flexible resource sharing between different services.

5G user plane (UP) instances related to different frequency bands can be harmonized on certain layers, and there also would be a single control plane (CoP) instance. Therefore, the assumption is that for the integration between multiple novel 5G AIVs, UP harmonization could take place at MAC layer which is proposed by [MET2-WP].  Moreover, where the MAC layer harmonization is not feasible, a packet data convergence protocol (PDCP) level harmonization can be way out such as dual connectivity of LTE is.

Using the same waveform with different numerologies is a key element of many PHY design considerations as described previously. Thus, the proposed MAC layer harmonization is built on OFDM waveform family, and using different numerologies to cater to different future services, bands, and cell types, etc.  Indeed, mixing of xMBB and extremely latency-critical uMTC data on the same carrier (mixing of OFDM numerologies) is beneficial in case of radio resource management. The harmonized MAC aggregates the service specific MAC schemes and its scheduler assigns available radio resources to different use case specific MACs at UPs by considering each of the services.
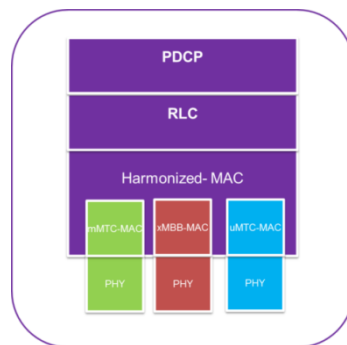


**Figure 4-18: UP MAC layer harmonization for novel 5G AIVs**

The proposed MAC layer harmonization towards a single specification that supports the usage of CP-OFDM waveform with multi numerology, where windowing is benefical, on PHY layer as described above and as well as illustrated by Figure 4-18 .

**Physical Channels of 5G**

Unlikely LTE, 5G needs to be sufficiently flexible henceforth we would like to define two novel data channel concepts; a data channel will be either direct or re-transmittable and both channels are able to carry user-plane and control-plane data. Basic harmonized 5G MAC channel structure is illustrated on Figure 4-19 where the direct channel is denoted dPDCH (direct Physical Downlink Channel) and the re-transmittable channel is donated rPDCH (re-transmittable Physical Downlink Channel) as example. The structure of having a direct and a re-transmittable channel is equally applicable to both uplink and downlink transmissions. The direct channel may e.g. be designed for a BLER of 10-3 without soft HARQ combining while a re-transmittable channel may target 10% BLER and support several HARQ retransmissions with soft combining in the receiver. The above two types of channels can be used to support different services e.g. MTC and MBB. The difference between such channels will primarily be that they are optimized for different operational points.

Furthermore, we want to avoid defining separate control channels for different purposes unless it is absolutely necessary. Because, control channels have a tendency to rely on frequency diversity as well as separate demodulation reference signals and thus the resource space can quickly become cluttered. We may also need a bootstrapping resource e.g., to be used for scheduling initial channel use. For this purpose we also propose to define a physical downlink control channel, is named as PDCCH, where the receiver blindly searches for it in a pre-defined or semi-statically configured search space.

**Table 4-6: Configurations of PDCHs**

| L1/L2 control information and CSI | Mapped on dPDCH. |
|---|---|
| Paging and random access response | Mapped on dPDCH. |
| MBB | Mapped on rPDCH. |
| u-MTC | Mapped on dPDCH or rPDCH. |
| Contention-based | Configured to enable contention-based access |

In Figure 4-19, a downlink example is illustrated where two PDCHs are configured. The dPDCH does not use soft combining of HARQ re-transmissions and it can only carry a single transport block (TB1), while rPDCH does support HARQ and supports transmission of up to two transport blocks (TB2 and TB3). In addition the downlink PDCCH can transmit DCI and possibly based on the use cases e.g. uMTC or xMBB also some harmonized MAC-control elements embedded into one transport block TB0.

On the other hand, a corresponding example for the uplink is depicted in Figure 4-20. Note that the uplink does not have any scheduler but instead a priority handler entity that selects data from the logical channels and controls the harmonized MAC Multiplexing within the grants provided. Since there is no scheduler there is no need for any PDCCH channel either. Instead the UL transmitter has a contention based channel (cPDCH).  The main difference between cPDCH and the other two uplink physical data channels (dPDCH and rPDCH) is that they are granted differently.  cPDCH uses a semi-persistent grant that may be assigned also to other UEs. Therefore the UE identity needs to be encoded onto the channel whenever cPDCH is used. In case the UE does not have a sufficiently sized grant then it may send a scheduling request (i.e. a buffer status report) on cPDCH. Depending on the size of the grant on the "contention-based channel" cPDCH the UE may also include user-plane data when transmitting on that channel.

The "direct channel" (dPDCH) and the "re-transmittable channel" (rPDCH) are typically scheduled in a dynamic fashion. When using granted resources on these channels it is assumed that the receiver knows who is transmitting and hence no UE identity needs to be embedded. Note that these are just examples used to illustrate that the basic PDCH structure in Figure 4-19 works for both UL and DL for a typical xMBB use case. For other use cases such as uMTC the UL and DL radio links can be configured slightly differently, e.g. we may not have any second "re-transmittable" data channel.

Different channel coding schemes exist for PDCH. For example, convolutional codes can be used for small payloads with high reliability requirements e.g. critical MTC, while higher performing channel codes are used for code-words with typical larger payload sizes and lower reliability requirements (e.g. MBB). PDCH uses the same numerology as used by the scheduling grant. MBB can use different MIMO modes, e.g. reciprocity-based MIMO vs. feedback-based MIMO. In addition, MBB data can be mapped to rPDCH, while the uMTC data is mapped to rPDCH or dPDCH due to strict latency requirements. For low latency communication, e.g. for uMTC, it is possible to send a scheduling assignment for downlink data and the data transmission in the same subframe as shown by Table 4-6. The scheduling assignment can be transmitted on the PDCCH at the beginning of a subframe and the data transmission can be done in the same subframe.

For the uplink we note that all non-system access related channels are scheduled in some manner (semi-persistent; dynamic; or implicit). So called "contention based channels" are not special in any particular way. When resources can be spatially separated, time/frequency resources need to be "dedicated" and consequently the important thing is to ensure that the receiver in the base station is able to derive who the transmitter is. Hence, on contention based channels a UE identity is embedded in the channel and on dedicated channels this is not needed. The key idea is that different physical channels may have different properties where each different channel can be harmonized by one MAC layer. Different channels may use different sub-set of a large common transmission format table (e.g. different channel encoders)

based on whether it is MTC or MBB uses cases and KPIs. Continuing with the example in Figure 4-20, we may configure three PDCHs as follows:

- **cPDCH**: Optimized for "contention use". For example a small grant may be available every 2 ms for transmissions of a buffer status report when needed. The UE is allowed to not use this grant. Normally, if a UE is scheduled on the UL and has no data to transmit, it needs to fill the granted resource with padding but for this channel the UE may simply refrain from transmitting anything at all in that case. The channel encoder may be configured to be a small block code. A "UE identity" and a packet sequence number needs to be signaled when this channel is used.

- **dPDCH:** Does not support soft-combining of re-transmissions; uses robust transport formats; optimized for embedded control information such as "HARQ feedback", "CSI feedback", and "RS measurement feedback".

- **rPDCH**: Carries 1 or 2 transport blocks of UL data; uses soft-combining of re-transmissions based on HARQ feedback; optimized for efficient transport of MAC SDUs (Service Data Units) (i.e. user data).
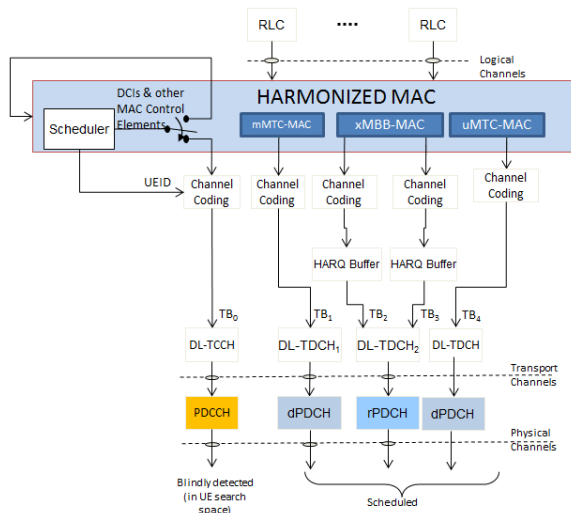


**Figure 4-19: Downlink channel structure and Harmonized MAC for 5G.**
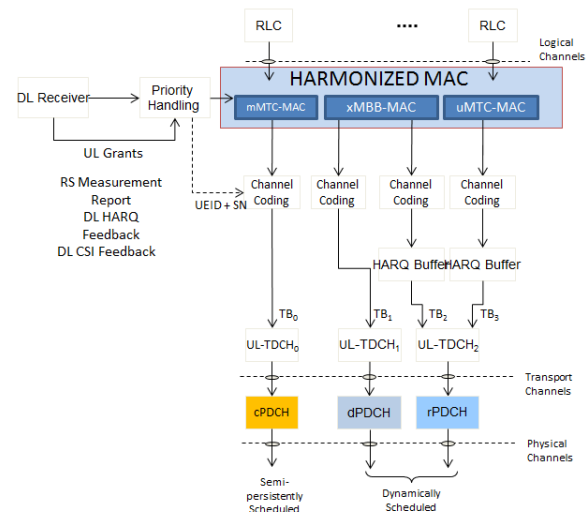
**Figure 4-20: Uplink channel structure and Harmonized MAC for 5G**

**Contention Based Access for 5G**

In order to avoid over-provisioning of resources for not-so-frequent traffic in uMTC use-cases, a cPDCH could be made available. However, the bandwidth of the contention based resource is allocated according to the scenario (i.e. number of devices in the network and the generated traffic etc.) so that the latency requirements for uMTC applications are fulfilled.

In high load scenarios the default transmission modes are based on maintaining coordination by means of a resource scheduler. However, as depicted in Figure 4-21 where the top is illustration of scheduled based access which is contention free and the performance is superior in high load scenarios; while bottom illustrates the contention based access can provide lower delay for initial uplink transmissions and in relay-nodes with a large delay to a central scheduling unit.
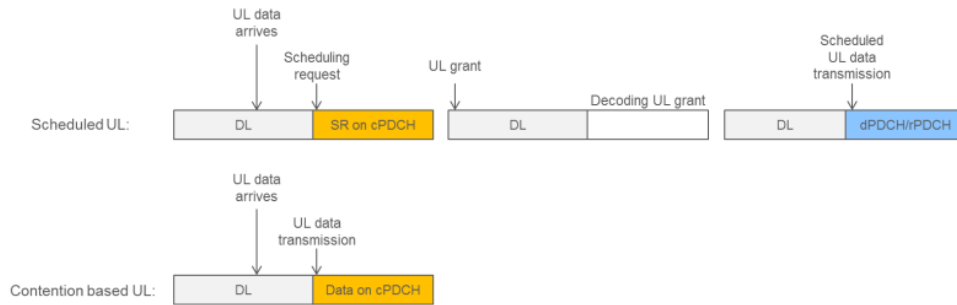


**Figure 4-21: Scheduled based access (top) and contention based access (bottom)**

The contention based uplink channel cPDCH is not very different from the normal contention free uplink channels dPDCH and rPDCH. A UE needs a grant to transmit on the cPDCH but it is not forced to use the grant in case it does not have any uplink data to transmit (in case the UE has a grant for a dPDCH/rPDCH and it has no data then it must fill the grant with padding).

When utilizing a cPDCH the UE need to include a temporary UE identity so that the receiving base station knows who the transmission originates from. The UE also need to add a sequence number to indicate the HARQ buffer.

In a dedicated spectrum we may for example want dynamically scheduled transmissions (dPDCH/rPDCH) to be prioritized. To efficiently enable both transmission principles (i.e. scheduled and contention based access) 5G is therefore designed to prioritize scheduled access over contention based as shown by Figure 4-22. Prioritization between scheduled data and contention based data access is enabled by having the scheduled data starting earlier than contention based data. This enables the contention based access to detect the scheduled data transmission using carrier sense.
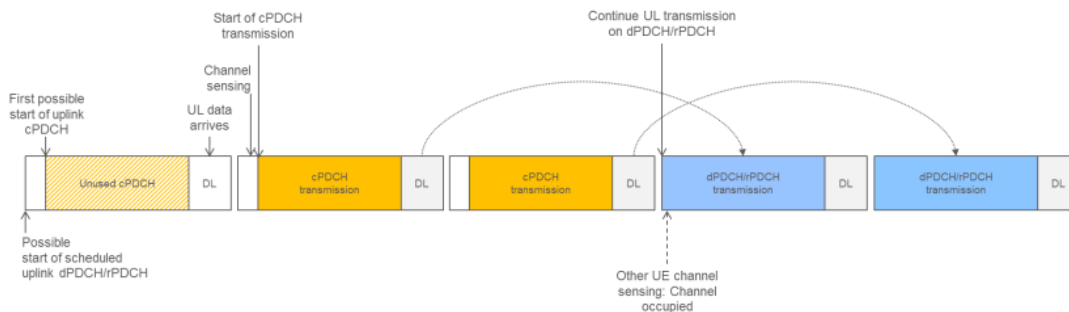


**Figure 4-22: Prioritization between scheduled data and contention based data access.**

The 5G concept is needs to be designed to allow flexible sharing of the radio resources between services with diverse requirements on, for example, delay and reliability. Therefore, we propose to have the dynamic resource sharing between different services by considering the various service requirements. To be able to support different UE configurations, the following concept of harmonized MAC level is presented.

This is in line with the stay in the box key principle (see appendix B) for Layer 2 and the basic idea is to assign the available radio resources for a user case specific MAC behavior. Numerous types of services can exist within the same network, and combinations of these may have to be served at the same time. Different performance requirements of these services translate into various radio resources usage requirements (TTI, Resource block size, Prioritization…).

In a network the scheduling must be aware of nodes and their use cases as well as link conditions to perform efficient decisions. On the other hand the scheduled resources also need to be known by all the concerned nodes in the system as well. Thus, the different MACs of AIVs can be operated by a harmonized MAC layer. The harmonized MAC layer provides one single protocol framework and acts as orchestration functionality between various use case specific AIVs which means that the harmonized scheduler aims to assign the most suitable radio resources for each service. Such cases can include, for example:

- When the physical resources have different properties, such as different numerologies;
- When service has very strict delay requirements (e.g. access delay so short that it needs a constant resource grant), such as in C-MTC;
- When the scheduling/signaling is handled in multiple nodes (D2D, distributed MAC…)

For a given UE or service, a harmonized MAC behavior can be partially configured following specific requirements. Different service specific MAC behaviors can be related to

- different MAC schemes, e.g. contention based versus scheduled based,
- different algorithms for a scheme, e.g..RTS/CTS (Request-To-Send/Clear To Send) versus listen before talk,
- different parameters used, e.g. timing, prioritization, resource location…

The resource assignment and MAC mode selection can be done for a single cell or among a cluster of cooperating cells and handled for different MAC behaviors on different level of scopes and updated with different frequencies. For instance, it can be done within a single cell or among a cluster of cooperating cells; and with short or long term resource partitions. Furthermore, the resource assignment of different MAC behaviors needs to be dynamically handled by harmonized MAC scheme. In other words, the scheduler should be able to assign all available resource dynamically for one use case specific MAC when it is needed.

The assigned service specific MAC schemes are aggregated as part of harmonized MAC which is illustrated on Figure 4-23, where we propose that the scheduler considers each service specific MAC behavior as subset of harmonized MAC scheme. By doing that, the overall MAC solution is optimized only for the requirements that are relevant in that particular special case

and the physical radio resources are dedicated to each particular MAC. Following the stay in the box concept as elaborated in the L2 design principles in Appendix B.1, each MAC needs be self-contained with all the control mechanisms, HARQ process, pilots, and signaling this implies – since different MAC behavior may require different type of control or information, it is easier that all are independent to each other.
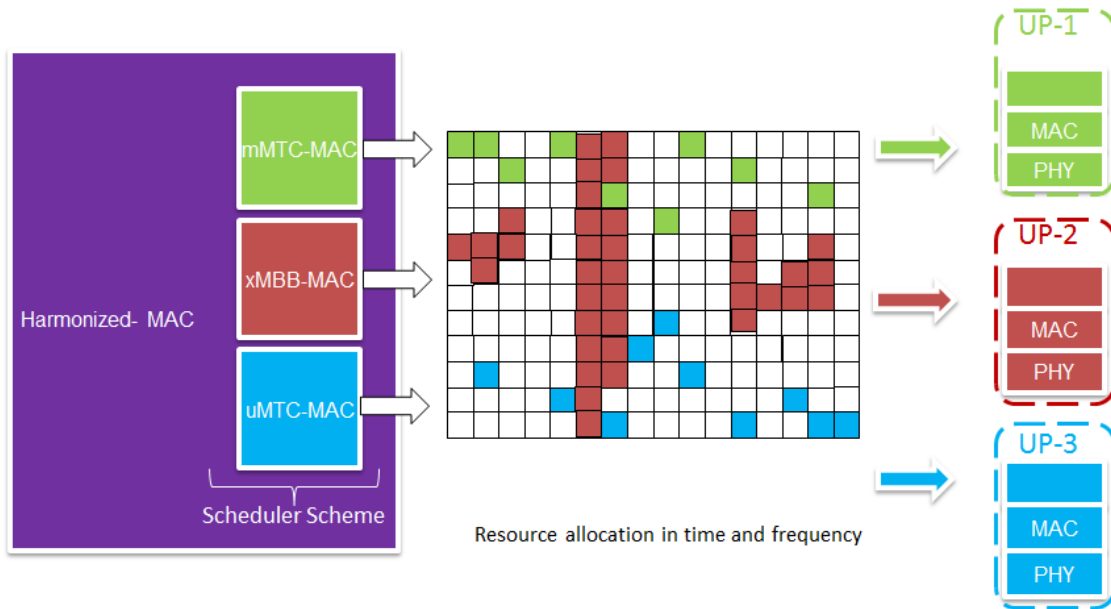


**Figure 4-23: Harmonized MAC scheme**

From a network perspective, the scheduling entity as part of the harmonized MAC will have to implement and process all the active MAC behaviors, but for each of these, behaviors can be processed independently. For instance, considering the case where a scheduled MAC and a contention-based MAC coexists, the contention based MAC scheduling is actually a distributed process, and not all the nodes will have direct access to the scheduled MAC information. Moreover, an example of resource partition can look like Figure 4-24, where the radio resources are partitioned in the time domain. The partitioning can be done in any domain (frequency, time, space, code…), although time domain may be the preferred option.
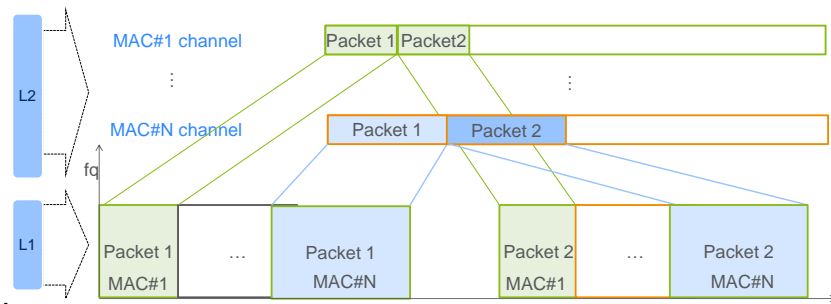
**Figure 4-24: Illustration of Harmonized MAC resource partitioning**

# 5        User Plane Aggregation

Two user plane protocol stack instances are said to be aggregated on a certain layer if they have one joint instance of each protocol stack layer on and above this layer. This is referred to as UP aggregation and it enables a UE to receive or transmit data flows via different links. These different links can either be from the same AIV, as in LTE, or from different AIVs as proposed by the RAN design in METIS-II. The benefits of UP aggregation include increased throughput, pooling of resources and support for seamless mobility, reduced complexity in the BSs and the end devices (as less functionalities may need to be implemented), lower delay in case of switching between AIVs (as this can happen on a rather low protocol layer), and less standardization and implementation effort.

One of the RAN design questions in METIS-II is how tight novel AIVs are expected to be integrated with each other and with legacy technologies (e.g. LTE evolution) and on which level different transmission forms should be aggregated. The loosest integration would occur in a flow level with IP as aggregation layer where each flow terminates in a common CN for the multiple AIVs, including the evolution of LTE.  In the case of RAN solutions, considering the definition of UP aggregation explained above, examples of protocol solutions are the following:

- PDCP as the aggregation layer on the top of multiple RLC/MAC/PHY layers.

- RLC as the aggregation layer on the top of multiple MAC/PHY layers.

- MAC as the aggregation layer on the top of multiple PHY layers.


## 5.1        Protocol aggregation alternatives

In LTE, two examples of protocol aggregation options are LTE-MAC as aggregation layer, enabling a feature called Carrier aggregation, and LTE-PDCP as aggregation layer, enabling a feature called Dual Connectivity.

Similarly to LTE, a MAC level aggregation would allow a single MAC scheduling, making it particularly suitable to deployments where the transmission points are co-located or connected with a high-speed backhaul. That could enable features such as cross-carrier scheduling. The MAC level aggregation techniques might require use of synchronous functions such as scheduling, link adaptation, channel state reporting, and power control. Some well-known examples of the lower layer multi-connectivity (MC) are LTE Coordinated Multi-Point (CoMP), which aims at improving the cell edge robustness, and LTE Carrier Aggregation (CA). The PDCP Level Aggregation is characterized by asynchronous UP, relaxed synchronization, distributed MAC layer scheduling, and relaxed fronthaul requirements. The prime higher radio layer MC example is the LTE Dual Connectivity (DC) [3GPP13-36300], [3GPP13-36843] which

splits a radio bearer in the RAN over multiple BSs and which uses a common PDCP layer. The LTE Dual Connectivity is regarded as the baseline for the higher-radio layer MC studies in METIS-II. The comparison and the pros/cons of MAC and PDCP level aggregation is shown by Table 7-4 in Appendix C.

For the 5G RAN, UP aggregation will continue to play an important role, with METIS-II envisioning some differences and/or enhancements compared to existing solutions. In LTE the multiple links are still LTE links, at least with exactly the same MAC/PHY protocols. In the 5G RAN, the multiple links for UP aggregation can either be from the same AIV or from different AIVs.

For the case where **multiple links are from the same AIV** (e.g. same waveform and numerology) solutions could be inspired by CA for co-located cases and/or DC for non-collocated cases. In other words, there could be both MAC level aggregation and/or PDCP level aggregation for non-collocated cases. As in LTE, the design of UP aggregation solutions may need some protocol design enhancements compared to the non-aggregated case such as the introduction of PDCP functions (in the case of dual connectivity) and/or MAC/PHY functions (in the case of carrier aggregation).

For the case where **multiple links are from different novel AIVs** additional constraints will likely exist especially when it comes to a MAC level aggregation. These constraints will depend on the differences between the AIVs supposed to be aggregated or in other words, how they are harmonized. Considering only the novel AIVs, some proposals for the overall AI (see Chapter 4) consider the same waveform but different numerology for the AIVs while other alternative proposals rely even on different waveforms. Further investigations will be performed in METIS-II in order to better understand the limitations of these proposals in order to enable lower layer UP aggregation.

One particularly important case is the study of UP aggregation between novel AIVs and the evolution of LTE. In that particular case, additional constraints exist compared to the aggregation of new AIVs. A solution based on lower layers (e.g. MAC level) would require additional constraint to the PHY/MAC design of new AIVs, which might not be desirable [SM+15]. An alternative being considered is to have PDCP as the aggregation layer for the UP aggregation of LTE and the new AIVs. To support at least the same DC alternatives as in LTE, a single PDCP instance is desirable (so that one can perform flow split aka bearer split) which would benefit from a common PDCP layer for the different AIVs, including the evolution of LTE. Since PDCP does not have access-specific function, it seems to be a reasonable design for aggregation to have at least a common PDCP for the AIVs that are envisioned to be aggregated. More details are provided in the next Section 5.2. The different alternatives for the UP aggregation are illustrated in Figure 5-1.
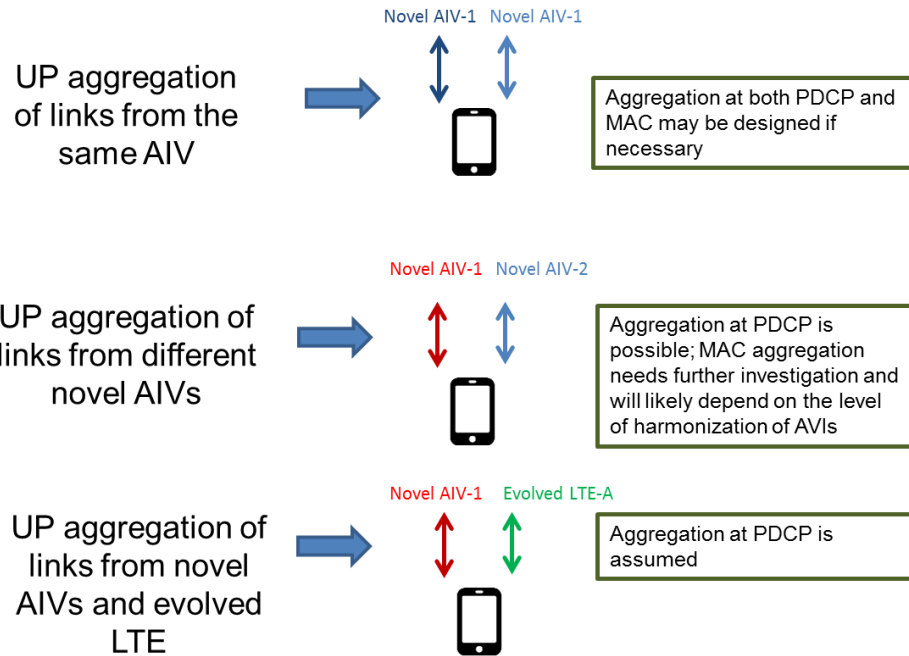
**Figure 5-1: UP aggregation alternatives for harmonized AIVs**

The previously described cases assume some level of harmonization among the AIVs, both for novel AIVs among themselves and the novel AIVs jointly harmonized with the evolution of LTE. However, in case it is preferred to design non-harmonized AIVs (i.e. in case some AIVs require very different RAN protocol stacks), UP aggregation could be achieved by a CN-based aggregation. The obvious disadvantage of that approach would be the difficulty to exploit the dynamics of the radio environment which can be even more important than in LTE considering the transmission in higher frequencies. In state of the art, with a CN-based aggregation on flow level, a UE simultaneously uses multiple flows where each flow runs a full UP protocol stack.

Different kinds of solutions may exist either for CN-based (for non-harmonized AIVs) and RAN-based UP aggregation. Option ①in Figure 5-2 shows the principle of flow based MC where the aggregation of the flows is located in the CN (i.e. multiple flows would lead to multiple S1* connections). Such flow based MC can already be achieved with the 3GPP Multi Access PDN Connectivity (MAPCON), IP flow mobility (IFOM) [3GPP14-23861] and Network based IP flow mobility procedures (NBIFOM) [3GPP15-23861]. In the example shown there would also be two PDCP entities, one per each BS the UE connects to. The solution in LTE relying on Master Cell Group (MCG) and Secondary Cell Group (SCG) would fall into that category.

Option ②shows the RAN-based option of the flow based MC with symmetric UL/DL. In this option, the switching/aggregation point is located in the RAN and this allows not only IP based flow routing as in option ① but also a flow routing/forwarding on PDCP layer.  The RAN based option allows faster reacting on changes in the radio environment compared to option ①.

Option ③ "Flow based MC, RAN based, asymmetric UL/DL" describes a case where the UL for a given flow uses a different network point than the DL.
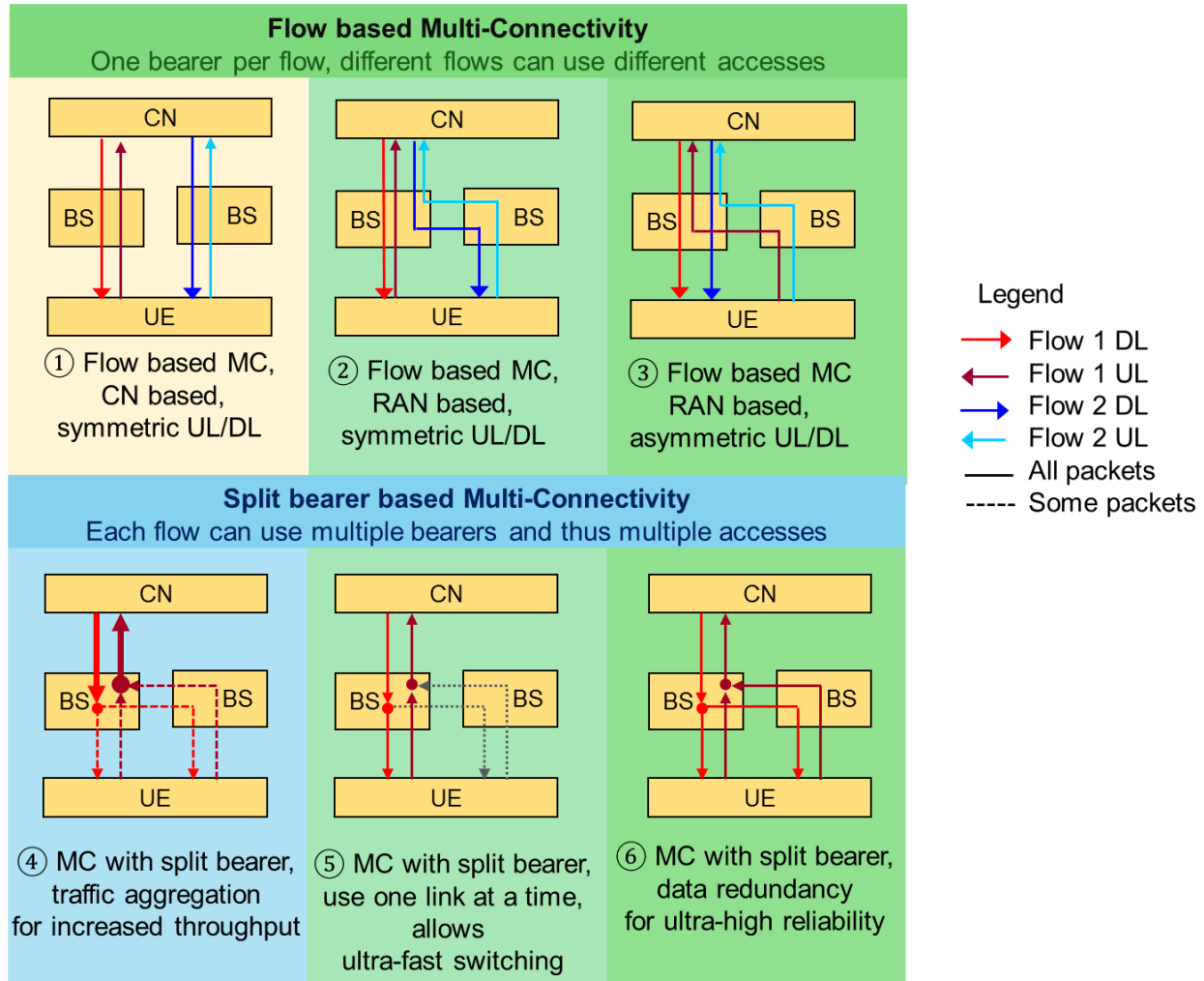


**Figure 5-2: UP aggregation alternatives**

Option ④ shows the case where MC is achieved by using a split bearer, e.g. by splitting a bearer on PDCP level and where then two links are used in parallel to achieve higher throughput (traffic aggregation).

Option ⑤ shows also a split bearer case but here only one link is used at a given time. This enables a fast switching between the links and thus enables to react very fast on changing radio conditions.

Option ⑥ shows a case where the user data is duplicated and the same data is sent on two radio links. This data redundancy is useful to achieve ultra-high reliability.

# 5.2 UP Aggregation of LTE-A and novel AIVs

In parallel with the 5G research activities such as METIS-II, 3GPP is continuously adding new features to LTE-A. At the time 5G reaches the market, LTE is expected to be widely deployed, so the interworking of new AIVs and LTE-A is important to consider. The evolved LTE-A (called in 3GPP LTE-A Pro) AIV is expected to be ***tightly integrated*** to the 5G architecture [MET2-WP]. Such an approach has also been endorsed by 3GPP [3GPP16-38913] where it is stated that "the new 5G radio interface should support high performing inter-RAT mobility and aggregation of data flows via at least dual connectivity" [3GPP13-36300] supporting both collocated and non-collocated site deployments. The densification of new AIVs might evolve continuously however, in order to leverage previous LTE investments, operators should have the flexibility to define their spectrum migration strategy (e.g. taking into account the density of new AIVs and/or LTE subscribers) and, at the same time, to efficiently use the radio resources in both AIVs e.g. the frequency bands allocated to LTE and the new AI. This would be facilitated by the above mentioned tight integration.

In the LTE architecture, the MAC layer provides services to the RLC layer in the form of logical channels, and performs mapping between these logical channels and transport channels. The main functions are: uplink and downlink scheduling, scheduling information reporting, Hybrid-ARQ feedback and retransmissions, multiplexing/demultiplexing data across multiple component carriers for carrier aggregation. In principle, the integration on the MAC level can lead to coordination gains, enabling features such as cross-carrier scheduling for both air interfaces. Major gains could potentially be possible for dual-radio UEs. The challenge to realize a MAC aggregation comes from the assumed differences in the time- and frequency-domain structures for LTE and the new AIVs. A high level of synchronicity would be needed between the common MAC layer and both the PHY layer of LTE and of the new air interface, even if assuming a harmonized numerology for both OFDM-based transmission schemes. This challenge would likely limit MAC level of integration to co-located deployments in which this high level of synchronicity can be achieved. RLC aggregation is also challenging due to the existing level of synchronicity between PHY, MAC and RLC. For example, in order to perform fragmentation/reassembly, the RLC needs to know the scheduling decisions in terms of resource blocks for the next TTI, which in consequence, is a function of PHY layer information. A joint fragmentation/reassembly for the two air interfaces would likely not work unless a common scheduler is deployed. This would also likely limit the possible deployments to the collocated case as described for common MAC layer.

In LTE-A, in contrast to PHY, MAC and RLC functions; the PDCP functions do not have strict constraints in terms of synchronicity with the lower layers. In other words, a specific design for PHY/RLC/MAC functionalities for both LTE and new AIVs would likely not impose problems to design the PDCP as the aggregation layer. In addition to this, such solution would work in both co-located and non-collocated network deployment scenarios, making it more universal and future-proof.

METIS-II envisions that such a solution for the UP aggregation should support at least the same scenarios as in LTE Dual Connectivity solutions, including the flow split case. The current working assumption is that this should be realized by a single PDCP layer for both the evolution of LTE and the new 5G AIVs (at least those where UP aggregation with LTE should be supported). The reasoning for that comes from the fact that existing PDCP functions are very much access/service-agnostic functions which can be confirmed by the fact that 3GPP assumes the same PDCP functions for non-MBB use cases such as MTC and more recently Narrow Band-IoT (NB-IoT). A common PDCP, as illustrated on Figure 5-3, would allow less constraints to the design of PHY/RLC/MAC functionalities for the new AIVs, as it would not need to be aligned with the lower layer design of LTE-A.
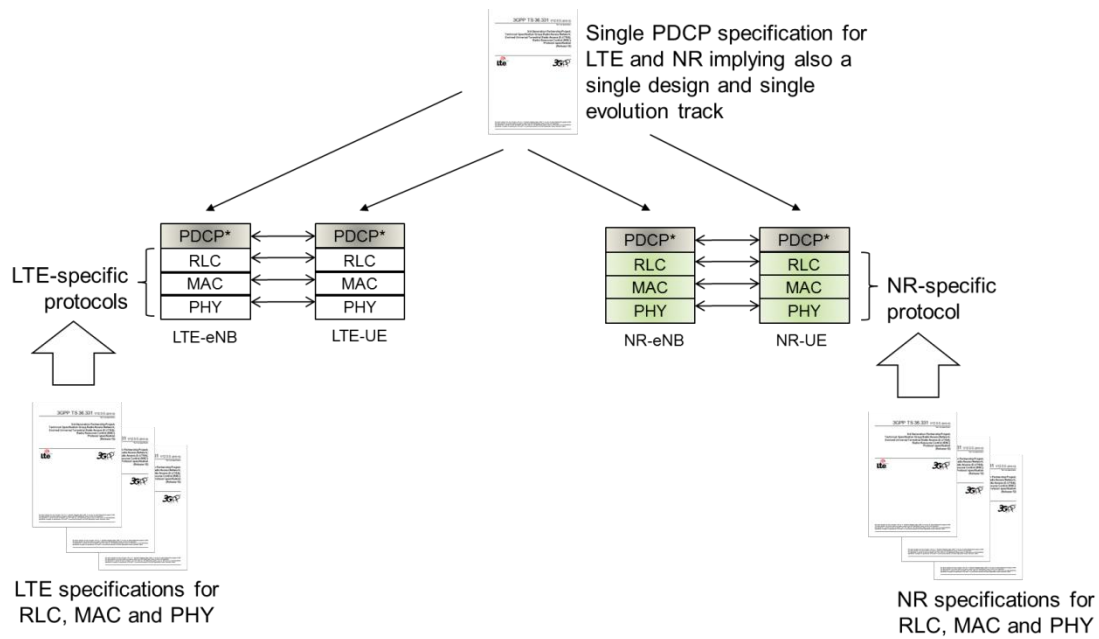


**Figure 5-3: Common PDCP framework for LTE-A and New AIVs**

In addition to the flexibility of PDCP as detailed in above, an advantage of a common PDPC specified for both LTE-A and the new AIVs is that it would support *high performing inter-RAT mobility* as required by 3GPP [3GPP16-38913]. In that case it would be possible to define a single PDCP instance when the UE moves from a new AIV to LTE-A that can be re-located and support the handling of potential issues from the lower layers such as duplicate detection and PDU reordering since the functionality is already available in current PDPC specifications. The inter-RAT mobility between LTE and the new AIV might happen quite often, especially in early deployments where full coverage of the new AIVs might not be available. A common PDPC is a CN transparent solution where the UE can move between LTE and new AIVs without notifying the CN. This reduces the signaling compared to current inter-RAT hard handover. As proposed in section 5.2.1, this is supported by a feature called *fast UP switching*.

Yet another advantage of having a single PDCP instance used for both AIVs providing UP aggregation / dual connectivity features (such as flow aggregation and flow routing) is illustrated in Figure 5-4. Therein, a single instance can be defined for both AIVs when dual connectivity is applied within a given service session. That would have two main advantages:

- It allows the reuse of existing re-location functions for the single PDCP instance, which might be beneficial not only for mobility but for solutions where a flow is moved from one access to another;
- It also allows more dual connectivity alternatives, including a split flow (which is not possible if two PDCP instances are defined);
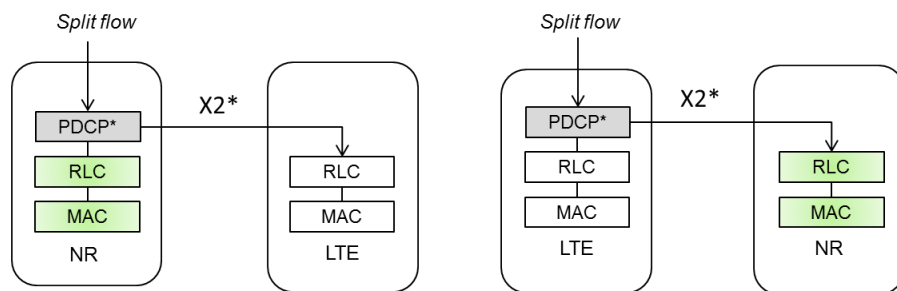


**Figure 5-4: PDCP layer aggregation solution for tight integration of LTE-A and new AIVs**

For the control plane solutions two alternatives are currently being considered: a single RRC or dual RRC [MET2-WP]. These will be further detailed in D6.2 to be published in June 2016.

## 5.2.1    PDCP aggregation features for LTE and novel AIVs

A common PDCP layer for the aggregation of LTE and novel AIVs has the potential to improve the hard handovers between LTE and the new AIVs. In addition to that, it enables UP aggregation features such as UP fast switching and flow aggregation. These features allow increased throughput, pooling of resources from multiple AIVs and support for seamless mobility. Figure 5-5 shows a more detailed illustration of the PDCP aggregation between LTE and 5G AIVs, where a single PDCP exists for both AIV types at the network and the UE side, and a single CoP instance exists.

### Hard handover between LTE-A and novel AI

In order to efficiently enable UEs to switch between coverage layers, high performing inter-RAT mobility solutions between the new AIVs and LTE should be designed. That is particularly important in scenarios with coverage islands where an active UE leaves new AIVs coverage layer and enters LTE coverage, or in scenarios with overlapping coverage layers but with new AIVs deployed in very high frequencies where coverage is more spotty. These solutions should target the following:

- High robustness against packet losses (lossless), handover failures and radio link failures ;
- Low interruption delays (seamless);
- Low signaling overhead:
  - Between the UE and both AIVs;
  - Between CN and RAN nodes of LTE and the new AIVs.

Inter-RAT mobility for active UEs is currently supported between LTE and UMTS. However, a handover from one RAT to another requires the full re-establishment of the UP protocol stack in the other RAT. Intra-LTE mobility, on the other hand, has the advantage of benefiting from existing LTE-PDCP functions to handle lossless mobility (through data forwarding and retransmission of PDCP SDUs during handovers) and the possibility to have the PDCP context being continued which might reduce the interruption delays. Intra-LTE mobility also benefits from the fact that a common Core Network connection (for both UP and CoP, S1-C and S1-U) exists so that intra-LTE handovers have also the possibility to be transparent to the CN. That would be an advantage especially in co-located deployments of LTE and NR.

The UP fast switching alternative assumes that the UP packets are switched at PDCP level to either LTE or new AIVs, as shown by Figure 5-5.  For this feature, the UP for one UE uses only a single AIV at a time, but a fast switching mechanism is provided between. Apart from providing resource pooling, seamless mobility and reliability, a main advantage is that it applies for UE with single transceivers. It is worth mention that the switching might require some signaling  between the UE and the Network, although it will be much lower compared to hard handovers (since it is transparent to the CN and relies on existing PDCP functions).
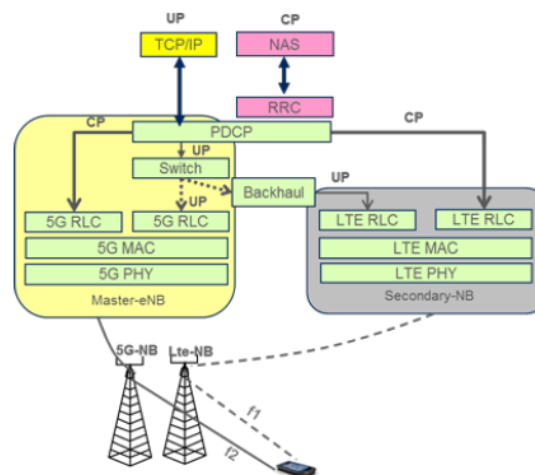


**Figure 5-5: LTE and new AIV protocol stack for fast switching case. The user plane (UP) is either transmitted over LTE-A or the new AIVs**

Flow aggregation and Flow Routing. Flow aggregation allows a single flow to be aggregated over multiple AIVs. In another variant, defined as flow routing, a given user data flow is mapped on a single AIV, so different flows of the same UE may be mapped on different AIVs. The benefits of this feature is increased throughput, pooling of resources and support for seamless mobility. The flow aggregation variant may have limited benefits when the AIVs provide different latency and throughput. The solution has also limitations to work only for dual transceiver devices. Differences for UL and DL variants shall also be studied in the future.

## Evaluation: UP aggregation of LTE-A and novel AI

In Appendix C, evaluation results for PDCP level user plane aggregation between LTE-A and 5G are presented. The user throughput performance is compared vs. the load (throughput per cell). LTE-A is here using 2.0 GHz and the novel 5G AI is using 2.6 GHz. In the flow aggregation case (similar to LTE dual connectivity), when the bandwidth is doubled the user throughput is also almost doubled at low load compared to stand alone deployments.

# 6　　Conclusions

This document – the first external deliverable from METIS-II WP4 – had the following ambitious goals:

**Objective 1**: to provide a first recommendation on which and how many novel air interface proposals are expected to be introduced in the 5G context;

**Objective 2**: to collate initial views on which forms of air interface aggregation and user plane provisioning are foreseen for 5G;

**Objective 3**: to open up the discussion on which protocol level novel air interfaces should ideally be integrated among each other and with legacy technologies, and give examples of various options and underlying trade-offs.

In this closing section we examine how these goals were achieved and what the key take-aways are from the work reported in this deliverable, and how they impact future work of METIS-II.

### Objective 1

With a view to achieving this objective, a unified way of describing the 5G air interface design proposals using a 5G service/frequency mapping was proposed. This was followed by the elaboration of METIS-II air interface evaluation criteria and key design principles, classified into the following 4 categories:

- The suitability of an AI proposal to meet the overall 5G KPIs and directly related UP design requirements
- Additional UP-related AI design principles as identified by METIS-II
- Requirements posed from CoP considerations on the design of AIs
- The extent of harmonization across AIVs in overall AI considerations

The most important PHY layer considerations were then presented on the underpinning technologies of future AI candidates. This was then followed by descriptions of different AI proposals being considered for 5G AI design within METIS-II.

### Objective 2

After the different AI proposals were presented, an analysis of commonalities was carried out with regards to a set of features extracted from AI proposal descriptions. Following this analysis, an initial assessment was performed of AI proposals (grouped around subjacent waveform technologies) using the harmonization KPIs conceived within METIS-II, where various forms of air interface aggregation were identified and their features discussed.

**Objective 3**

The examination of the extent of harmonization embedded within various AI proposals provided an initial overview of different User Plane aggregation approaches and various trade-offs each of these entails. This additionally set the scene for a wider discussion on the UP aggregation amongst the new AIV as well as between new AIVs and LTE and its evolution. While 5G AI proposals are not constrained to be backwards compatible with LTE-A, some benefits exist in harmonizing at least some 5G AI aspects with the LTE design, and these were examined in more detail.

A key outcome of the work presented in this deliverable is the specification of an evaluation framework for 5G AI candidates, setting its focus on the "extent of harmonization" across underpinning components in overall AI considerations. The "extent of harmonization" has been defined as a combination of features such as utilization of radio resources, implementation complexity, standardization effort, forward compatibility, and interaction with legacy systems. Additional criteria include UP-related design principles and requirements posed from CoP considerations. It is expected that the elaborated evaluation criteria, resulting from wide consensus reached within METIS-II, aligned with 3GPP while offering a long-term, integrated system view, will impact researchers and standards bodies in the technical and economic trade-offs they take into account when assessing new AI technologies.

# 7      References

[3GPP13-36300]      3GPP TS 36.300, "Evolved Universal Terrestrial Radio Access (E-UTRA) and Evolved Universal Terrestrial Radio Access Network (E-UTRAN); Overall description; Stage 2," (Release 12), v12.0.0,  Dec. 2013.

[3GPP13-36843]      3GPP TR 36.843, "Feasibility Study on LTE Device to Device Proximity Services; Radio Aspects," v1.0.0, Nov. 2013.

[3GPP-141865]      3GPP-141865, "Further LTE Physical Layer Enhancements for MTC," Edinburgh, Scotland, Sept. 2014.

[3GPP14-23861]      3GPP TR 23.861, "Network based IP flow mobility,"  (Release 12), Jun. 2014

[3GPP15-23861]      3GPP TR 23.861, "Network based IP flow mobility," (Release 13), Mar. 2015

[3GPP15-45820]      3GPP TR 45.820, "Cellular system support for ultra-low complexity and low throughput Internet of Things (CIoT)," (Release 13), Dec. 2015

[3GPP-160671]      3GPP TSG RAN RP-160671, "New SID Proposal: Study on Next Generation New Radio Access Technology," Mar. 2016

[3GPP-160846]      R1-160846, "Street microcell channel measurements at 2.44, 14.8, and 58.68 GHz," 3GPP TSG RAN WG1 #84, Feb. 2016.

[3GPP16-38913]      3GPP TR 38.913, "Study on Scenarios and Requirements for Next Generation Access Technologies," (Release 14), v0.2.0, Feb. 2016

[5GCM]      "5G channel models up to 100 GHz," available online: http://www.5gworkshops.com/5G_Channel_Model_for_bands_up_to100_GHz(2015-12-6).pdf

[5GN15-D31]      5GNOW Deliverable D3.1, "5G Waveform Candidate Selection," 2013.

[5GN15-D32]      5GNOW Deliverable D3.2,  "5G Waveform Candidate Selection," 2014.

[5GN15-D33]      5GNOW Deliverable D3.3, "Final 5GNOW Transceiver and frame structure concept," 2015.

 [ABS2011]      P. Achaichia, M. Le Bot and P. Siohan, "Windowed OFDM versus OFDM/OQAM: A transmission capacity comparison in the HomePlug AV context," IEEE Intl. Symposium on Power Line Comm. and its applications, 2011

[BTS +13]      G. Berardinelli, F. Tavares, T. Sorensen, P. Mogensen, K. Paujukoski, "Zero-tail DFT-spread-OFDM signals," IEEE Globecom 2013 Workshops, Atlanta, USA, Dec. 2013

[BTS +14]      G. Berardinelli, F. Tavares, T. Sorensen, P. Mogensen, K. Paujukoski, "On the Potential of Zero Tail DFT-s-OFDM in 5G Networks," IEEE VTC 2014 Fall, Vancouver, Sep. 2014

[DMF+16]       S. Dutta, M. Mezzavilla, R. Ford, M. Zhang, S. Rangan, M. Zorzi, "Frame Structure Design and Analysis for Millimeter Wave Cellular Systems", submitted to IEEE Transaction on Wireless Communications.

[Fou15]        Y. M. M. Fouad et al., "Time-Frequency Grassmannian Signalling for MIMO Multi-Channel-Frequency-Flat Systems", IEEE Communications Letters, vol. 19, no. 3, pp. 475-478, Mar. 2015.

[FZD+16]       R. Ford, M. Zhang, S. Dutta, M. Mezzavilla, S. Rangan, M. Zorzi, "A Framework for Cross-Layer Evaluation of 5G mmWave Cellular Networks in ns-3", WNS3 2016

[FZM+16]       R. Ford, M. Zhang, M. Mezzavilla, S. Dutta, S. Rangan, M. Zorzi, "Achieving Ultra-Low Latency in 5G Millimeter Wave Cellular Networks", submitted to IEEE Communication Magazine.

[HL05]         Seung H. Han and Jae H. Lee, "An overview of peak-to-average power ratio reduction techniques for multicarrier transmission," IEEE Wireless Communications, 2005.

[HS00]         B. M. Hochwald and W. Sweldens, "Differential Unitary Space-Time Modulation", IEEE Trans. on Communications, vol. 48, no. 12, pp. 2041–2052, Dec. 2000.

[Hyu14]        Hyungju Nam, et.al., "A New Filter-Bank Multicarrier System for QAM Signal Transmission and Reception," in Proc. IEEE Intern. Conf. Commun. (ICC'14), pp. 5227–5232, Jun. 2014.

[ITU14]        IMT Vision, "Framework and overall objectives of the future development of IMT for 2020 and beyond", ITU, Feb. 2014

[KP11]         F. Khan, and J. Pi, "mmWave mobile broadband: unleashing the 3-300GHz spectrum," presented at IEEE Wireless Commun. Netw. Conf., Mar. 2011.

[L+14]         E. Lahetkangas et al., "Achieving low latency and energy consumption by 5G TDD Mode Optimization", ICC Workshops, 2014

[LENA_ns3]      "The LENA ns-3 LTE Module Documentation," CTTC.

[M+14]         P. Mogensen et al., "Centimeter-wave concepts for 5G ultra-dense small cells", VTC Spring 2014

[MDZ+15]       M. Mezzavilla, S. Dutta, M. Zhang, M. R. Akdeniz, S. Rangan, "5G mm Wave Module for the ns-3 Network Simulator", ACM MSWiM 2015.

[MET15-D24]    METIS Deliverable D2.4, "Proposed Solutions for New Radio Access", Feb. 2015.

[MET215-R11]   METISII Report R1.1, ''Preliminary refined scenarios and requirements, and consolidated use cases'', Sep. 2015.

[MET215R41]    METISII Report R4.1, "Preliminary air interface analysis and user plane design considerations," Nov. 2015.

[MET216-D11]   METISII Deliverable D1.1, "Refined scenarios and requirements, consolidated use cases and quialitative techno-economic feasibility assessment," Jan. 2016

[MET2-WP]       METISII White Paper "5G RAN Architecture and Functional Design," March 2016. Available at: https://metis-ii.5g-ppp.eu/documents/white-papers/

 [mmW_ns3]       Available online: https://github.com/mmezzavilla/ns3-mmwave

[NGMN15-WP]     NGMN White Paper 2015, v1.0, Feb. 2015.

[RCC+14]        S. Roger, J. Cabrejas, D. Calabuig, J. F. Monserrat, Y. Fouad, R. H. Gohary, and H. Yanikomeroglu, "Non-coherent MIMO Communication for the 5th Generation Mobile: Overview and Practical Aspects," Waves Journal, 2014.

[SM+15]         I. Da Silva, G. Mildh at al., "Tight integration of new 5G air interface and LTE to fulfill 5G requirements," Vehicular Technology Conference (VTC Spring), IEEE 81st, pp. 1-5, Glasgow, May 2015.

[SW14]          F. Schaich, T. Wild, "Relaxed Synchronization Support of Universal Filtered Multi-Carrier including Autonomous Timing Advance," IEEE ISWCS'14, Barcelona, Aug. 2014

[SW15]          F. Schaich, T. Wild, "Subcarrier spacing – a neglected degree of freedom?" IEEE SPAWC 2015, Stockholm, Jun. 2015

[SWA16]         F. Schaich, T. Wild, R. Ahmed, "Subcarrier spacing – how to make use of this degree of freedom," accepted for IEEE VTC spring 2016, Nanjing, May 2016

[SWC14]         F. Schaich, T. Wild, Y. Chen, „Waveform contenders for 5G - suitability for short packet and low latency transmissions," IEEE VTCs'14, Seoul, May 2014

[VV16]          S. Venkatesan and R. A. Valenzuela, "OFDM for 5G: Cyclic prefix vs. zero postfix, and filtering vs. windowing," IEEE ICC 2016 (to appear)

[WBK+16]        P. Weitkemper, J. Bazzi, K. Kusume, A. Benjebbour, and Y. Kishiyama, "Adaptive Filtered OFDM with Regular Resource Grid," to be published in Proc. Intl. Workshop on 5G RAN Design in co-location with IEEE Conf. Comm. (ICC 2016), Kuala Lumpur, Malaysia, May 2016.

[WS14]          T. Wild, F. Schaich, "A Reduced Complexity Transmitter for UF-OFDM," IEEE VTC Spring 2015, Glasgow, Jul. 2015

[WS15]          T. Wild, F. Schaich, "A Reduced Complexity Transmitter for UF-OFDM," IEEE VTC Spring 2015, Glasgow, Jul. 2015

[WWS+15]        X. Wang, T. Wild, F. Schaich, S. ten Brink, "Pilot-aided Channel Estimation for Universal Filtered Multi-Carrier," IEEE VTC Fall 2015, Boston, Sep. 2015

[ZHL+16]        J. Zhang, C. Huang, G. Liu, and P. Zhang, "Comparison of the link level performance between OFDMA and SC-FDMA," in Proc. Netw. China, 2016.

[ZSW+15]        Z. Zhao, M. Schellmann, Q. Wang, X. Gong et al., „Pulse shaped OFDM for asynchronous uplink access," Asilomar Conference on Signals, Systems and Computers, Monterey, USA, Nov. 2015

# A     Waveform details

## A.1     Harmonized / flexible CP-OFDM

The sensitivity to phase noise and Doppler can be adjusted via a proper choice of sub-carrier spacing. The impact of phase noise increases as a function of frequency. In order to make an OFDM system robust to phase noise, larger subcarrier spacing can be used at higher oscillator frequencies. In Figure 7-1 and Figure 7-2 we show that sufficiently high SNR can be achieved in presence of phase noise, by proper choice of sub-carrier spacing in OFDM even at very high frequencies, while keeping low CP overhead. For example, 40 dB SNR can be achieved with 30 KHz subcarrier spacing at 20 GHz oscillator frequency, 60 KHz subcarrier spacing at 40 GHz oscillator frequency, and 500 KHz subcarrier spacing at 60 GHz oscillator frequency.
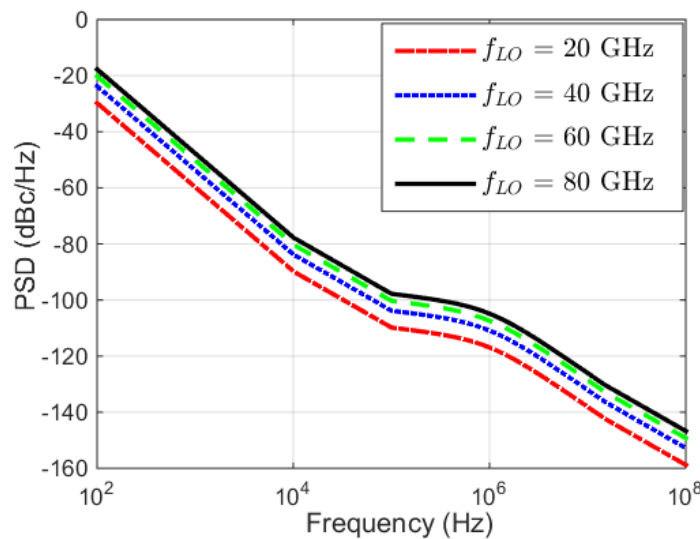


**Figure 7-1: Phase noise power spectral density at different oscillator frequencies**
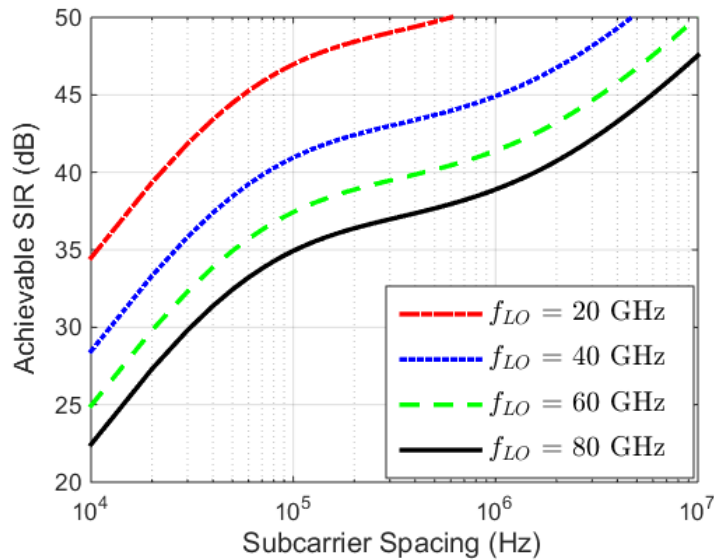
**Figure 7-2: Achievable Signal-to-Interference ratio subject to phase noise at different oscillator frequencies.**

For a fixed CP overhead in an OFDM symbol, larger subcarrier spacing implies smaller CP. CP has to be greater than the delay spread of the channel. Therefore, channel delay spread sets an upper limit on the subcarrier spacing. Some recent channel measurements at different carrier frequencies (2.44 GHz, 14.8 GHz, and 58.8 GHz) have shown that delay spread is similar at different frequencies, see Figure 7-3 [3GPP-160846]. Similar conclusion is made in a recent white paper [5GCM]. It is also important to note that the observed delay spread of the channel depends on few other factors such as deployment scenario and beam forming. Delay spread is usually smaller in indoor environments and use of narrow beams may reduce delay spread as well.
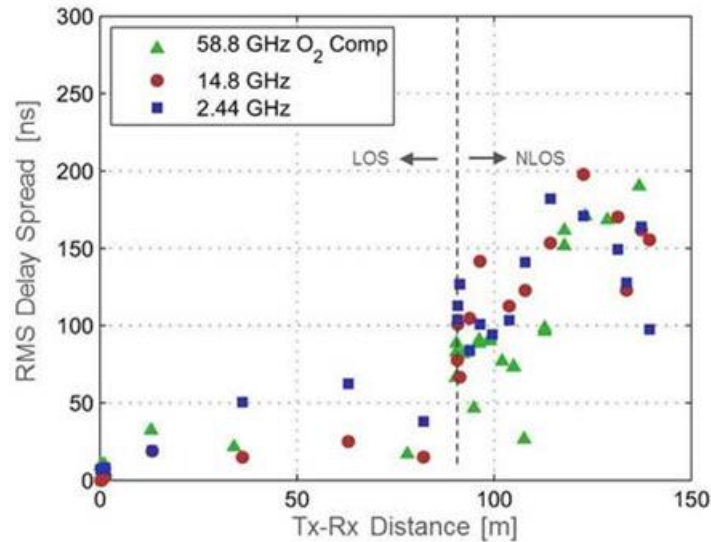
**Figure 7-3: Delay spread has a weak dependency on carrier frequency.**

High PAPR in OFDM can also be substantially reduced via various well-known PAPR reduction techniques with only minor compromise in performance [HL05]. Low PAPR is important in situations where higher power amplifiers efficiency (lower power back-offs) are desired such as for UL and D2D transmissions to improve the coverage. Currently, LTE uses DFTS-OFDM for both UL and D2D link due to its lower cubic meter.  However, DFTS-OFDM has certain drawbacks in comparison with OFDM such as less flexible scheduling and more complex MIMO receiver with reduced link level and system level performance [ZHL+16]. Since MIMO will be a key also component for UL and D2D link in 5G radio access technology, DFTS-OFDM may not be a preferred solution.  The use of one waveform for all link types (uplink, downlink, D2D link, backhaul link) will also make transceiver designs and implementations symmetric for all transmissions. It is important to note that due to the use of small sized low cost base stations in the future, the requirements on PAPR for uplink and downlink would also be similar.

There are different ways of improving frequency localization in OFDM. In most situations, especially at high frequencies envisioned for 5G radio access, frequency localization is not a major concern. The spectrum is not as specious at high frequencies. However, if necessary, the frequency localization can be improved by windowing or filtering, which will be discussed in the section related to Filtered-OFDM, Windowed-OFDM, and Universally Filtered-OFDM. It is important to note that windowing is a lower complexity operation than filtering.

# A.2    Advanced SC-FDMA schemes

The block diagram of ZT-DFTs-OFDM is shown below.  ZT-DFTs-OFDM is a modified version of SC-FDMA. The basic idea of zero tail and zero head insertion is to realize smooth transitions between OFDM symbols, which will in turn produce a waveform with low out of band emissions

in the frequency domain. One of the appealing properties of ZT-DFTs-OFDM is good time and frequency localization, where the time-domain symbol does not extend into the next symbol. This makes ZT-DFTs-OFDM quite useful for dynamic TDD so that flexible downlink-to-uplink or uplink-to-downlink switching can be enabled without altering the numerology of the system. Because of the good spectral containment, ZT-DFTs-OFDM is seen a good candidate for massive MTC where devices may not perform tight synchronization with the network. The same spectral containment and time localization property makes it highly useful for device-to-device communication with potential applications to V2V/V2I communications, where for very long distances of V2V/V2I communication, asynchronous scenarios may result in the communication.

For flexible TDD as in Figure 7-4, the intention is to make use of a sub-frame structure with bi-directional control embedded as below for CP-OFDM, SC-FDMA and extensions such as ZT-DFTs-OFDM. The data and control symbols are then well localised
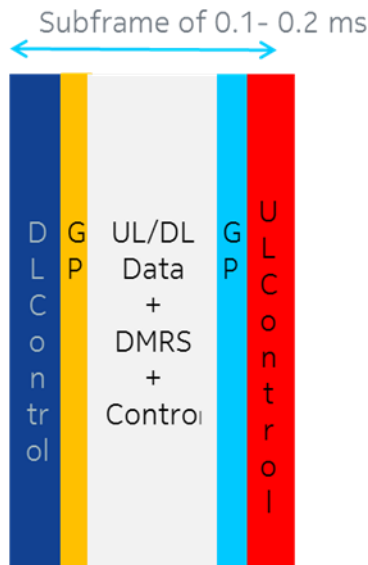


**Figure 7-4: Flexible TDD sub-frame structure optimized for small cell.**

The block diagram for generating a ZT-DFTs-OFDM signal is shown below. Figure 7-5 shows a multi-carrier modulation framework. The guard insertion may insert guard subcarriers (or guard band) between physical resource blocks to mitigate inter-carrier interference. The multi-carrier modulation may realize CP-OFDM and SC-FDMA (DFTs-OFDM) (along with optional windowing) with cyclic prefix. The multi-carrier modulator can also realize ZT-DFTs-OFDM along with UFMC filter with optional cyclic prefix for scenarios which require better spectral containment.
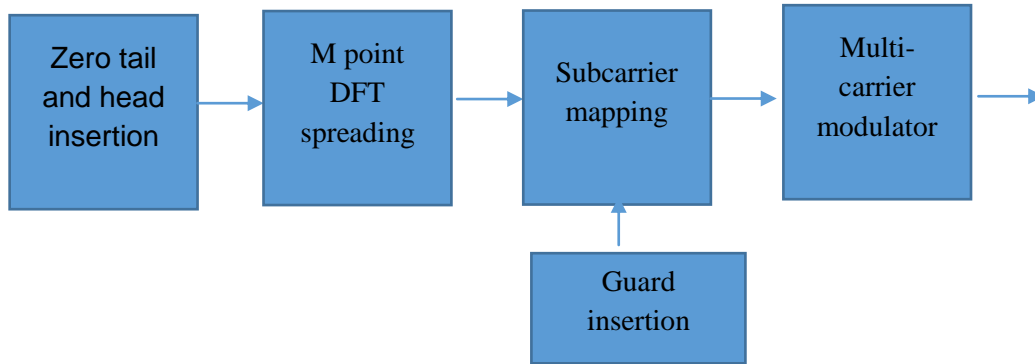
**Figure 7-5: ZT-DFTs-OFDM, with parameterization for flexible waveform realization.**
**Filtering, guard subcarriers and windowing can be included in the same framework. The zero head and zero tail are parameterizable. The multi-carrier modulator can use an N-point IFFT and in addition may use filtering (using zero-tail filter, UFMC) or windowing along with CP-insertion.**

Figure 7-6 shows spectral containment for in-band multiplexing of two users in adjacent PRBs over a transmission bandwidth of 100 MHz.

- Two users in multiplexed in adjacent PRBs, where each PRB consists of 256 subcarriers. ZT-DFTs-OFDM signals are then generated by the two users.

- The signals are then transmitted over a 100 MHz bandwidth.

- The two users who are thus multiplexed in frequency, can be asynchronous to each other thus motivating a possible MTC scenario

- The performance is measured by the so-called interference to signal ratio (ISR), where the interference from the asynchronous user is measured on an intended user. The average interference to signal ratio is then shown for the two users.
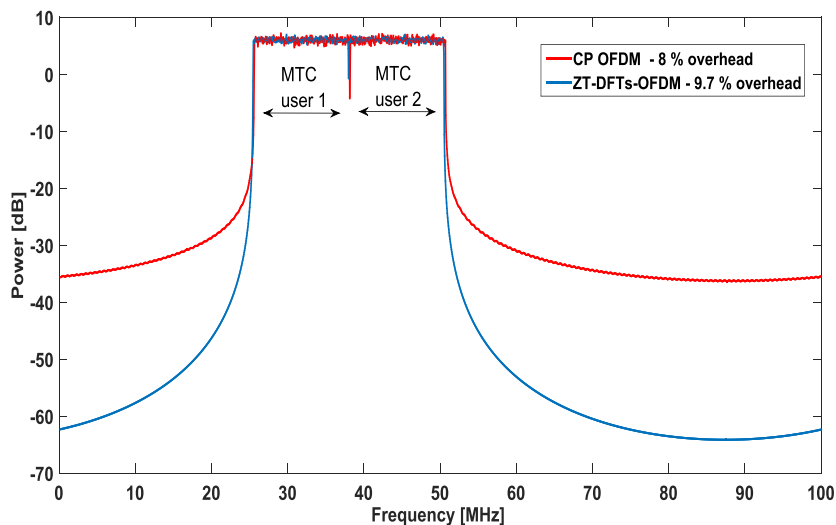


**Figure 7-6: Spectral containment of ZT-DFTs-OFDM.**

Spectral containment property of ZT-DFTs-OFDM is shown in Figure 7, where reduced in-band emissions are shown within a transmission bandwidth of 100 MHz. Reduced in-band emissions thus mean reduced leakage to adjacent PRB(s), mitigating interference between adjacent PRBs. The system numerology for ZT-DFTs-OFDM is the same as CP-OFDM, thus utilizing the sub-frame duration and sub-carrier spacing as in CP-OFDM. As seen in Figure 7, the enhanced waveform shows better spectral containment at the cost of slight overhead of around 1.7 % more than CP-OFDM, which is because of the additional zero overhead in pre-DFT samples, while there is no necessary symbol duration extension because of the DFT filtering before IFFT operation for ZT-DFTs-OFDM.

# A.3    Filtered OFDM based solutions

## A.3.1    Universal Filtered OFDM (UF-OFDM)

UF-OFDM, a.k.a. UFMC, transceiver is depicted in Figure 7-7, illustrating the principles of UF-OFDM. Actual implementations most likely follow the approach given in [WS15] using frequency domain filters or even apply look-up-tables for being used in low-end devices.
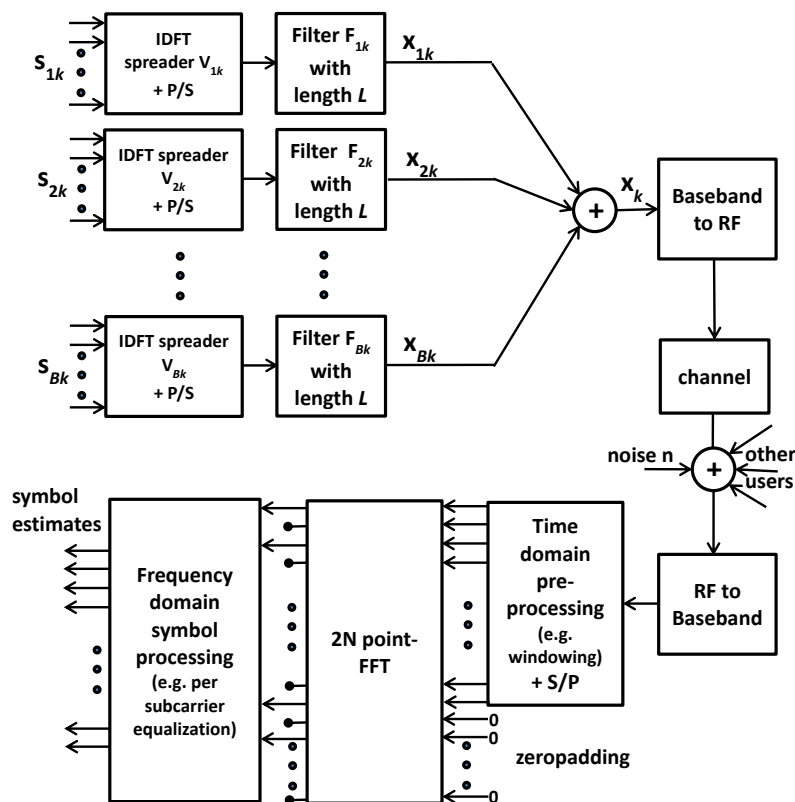


**Figure 7-7: UF-OFDM transceiver**

The time-domain transmit vector $\mathbf{x}_k$ for a particular multicarrier symbol of user $k$ is the superposition of the sub-band-wise filtered components $\mathbf{x}_{ik}$ ($i=[1\ldots B]$ with $B$ is the number of sub-bands being allocated to the user) with filter length $L$ and FFT length $N$. For the $i$-th subband, the $n_i$ complex QAM symbols are transformed to time-domain by the tall IDFT matrix $\mathbf{V}_{ik}$, which includes the relevant columns of the inverse Fourier matrix according to the respective sub-band position within the overall available frequency range. $\mathbf{F}_{ik}$ is a Toeplitz matrix, composed of the FIR filter impulse response, performing the linear convolution. $\mathbf{F}_{ik}$ is a design parameter, adjustable to propagation conditions and time-frequency offset requirements. For $L$=1, UF-OFDM converges to (non-CP-)OFDM. For $n_i$=1 and $L$>>1, UF-OFDM converges to FBMC-FMT.

The filtering per block of subcarriers (e.g. physical resource block - PRB - or sub-band in the LTE terminology) results in filters which are spectrally broader in pass-band than FBMC and thus shorter in time, e.g. in the order of the CP-OFDM cyclic prefix length. Short bursts will be supported well with that, as well as operation in fragmented bands. The side-lobe suppression now works in between resource blocks, instead of in between subcarriers. The filter ramp-up and ramp-down in time domain provides a symbol shape which has inherent soft protection against inter-symbol interference (ISI), as well as robustness for supporting multiple access users which are not perfectly time-aligned. It is recommended to pre-equalize the frequency domain filter impact by multiplying the transmit symbols with a pre-compensation factor in order to transmit with a flat pass-band.

The receiver processing can still be frequency-domain (FD) FFT-based: The receive time window gets zeros appended to the next power of two, an FFT is carried out where each second frequency value corresponds to a subcarrier main lobe. Note that there exists an equivalent alternative based on an N-point FFT: The tail of the symbol (N-th sample to sample number N+L-1) is added to the beginning and so the overall FFT size will be no larger than regular CP-OFDM. Similar to CP-OFDM, single-tap per-subcarrier frequency domain equalizers can be used which equalize the joint impact of the radio channel and the respective sub-band filter. This leads to similar complexity order [WS14] as CP-OFDM. Before performing the FFT at the receiver, the time- domain signal optionally is weighted with a window, e.g. with raised-cosine shape at the symbol edges see e.g. [SW14]. Various publications have analyzed UF-OFDM and compared its performance with CP-OFDM and OQAM-FBMC (e.g. [SWC14]).

## A.3.2 Filtered OFDM (F-OFDM)

The schematic of an F-OFDM transceiver is shown in the Figure 7-8. It can clearly be seen that the original OFDM transmission chain has merely been extended by the sub-band filtering component f(n) at TX and RX side.
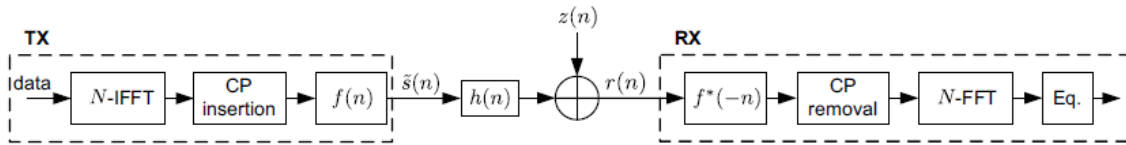
**Figure 7-8: F-OFDM transceiver structure**

The choice of the filter is quite flexible, and it may be chosen with the aim to minimize OOB radiation and in-band distortion. Also, the actual performance of the different filters for F-OFDM highly depends on the considered scenario and the particular filter design. In case the filter tails exceed the CP length, there will be certain amount of ISI even for frequency flat fading channels, but this can be kept rather small by a proper choice of the filter. The well-known tradeoff between time and frequency localizations can be observed here; the shorter the filter time response is, the broader the occupied spectrum will be, which leads to higher OOB radiation. When the filter has longer time response, the OOB leakage can be made much lower; however, ISI may become large unless large guard times are inserted. Therefore, the careful design of the filter is important in order to allow for low OOB distortion while limiting in-band distortion owing to filtering and possibly increased ISI.

# A.4    OFDM with windowing / pulse shaping

## A.4.1    Windowed-OFDM (W-OFDM)

In this section we describe both transmitter and receiver windowing.

**TX windowing:**

With TX windowing the boundaries of each OFDM symbol are multiplied with a smooth slope in time-domain, increasing smoothly from 0 to 1 (increasing slope) or 1 to 0 (decreasing slope), see Figure 7-9. The increasing slope is applied at the beginning of the cyclic prefix while the decreasing slope is applied after the end of the core OFDM symbol within an extra added cyclic suffix.
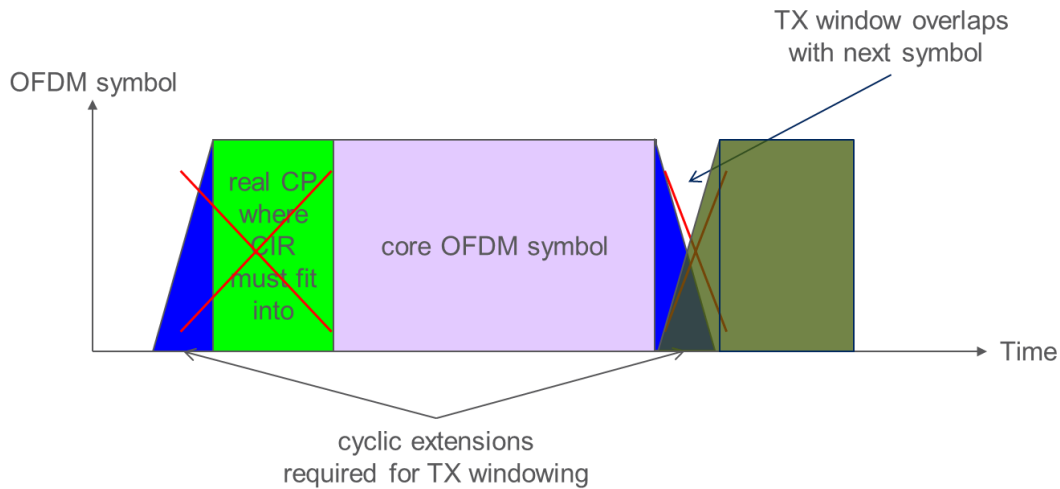
**Figure 7-9: TX windowing**

Figure 7-9 also shows that the increasing slope of the next OFDM symbol overlaps with the decreasing slope of the previous OFDM symbol. This is possible since the receiver discards the windowed samples (it only keeps the core OFDM symbol) and overlapping reduces overhead. Since the receiver keeps only the samples of the core OFDM symbol TX windowing is transparent to the receiver.

The remaining cyclic prefix length to cover linear dispersions created by multi-path propagation, filtering operations, etc. is reduced by the duration of a single slope (the decreasing slope is done within an extra added cyclic suffix that overlaps with the increasing slope of the next OFDM symbol and cyclic prefix reduction is thus already encountered for) compared to non-windowed OFDM system with the same cyclic prefix overhead.

**RX windowing:**

A standard OFDM receiver "cuts out" the desired OFDM symbol period by applying a rectangular window in time-domain to the received signal and subsequently applies an FFT (the rectangular window is part of the FFT operation). Application of a rectangular window in time-domain corresponds to convolution in frequency-domain with a sinc-like function. The sinc-like function leads to high interference pick-up from adjacent non-orthogonal signals such as OFDM signals with other numerologies. To reduce interference pick-up the rectangular window must be replaced by a smooth window function. To this end a smooth increasing window slope is applied at the boundary between cyclic prefix and core OFDM symbol (half within cyclic prefix and half within core OFDM symbol); a decreasing smooth window slope is applied at the boundary between core OFDM symbol and added cyclic suffix, see Figure 7-10.

This operation corresponds in frequency-domain to a convolution with the Fourier transform of the RX window (cyan-coloured window function in Figure 7-10a, which spectrum decays faster than that of a rectangular pulse and thus leads to reduced interference pick-up. If the applied window slopes fulfil the Nyquist criteria (i.e. they are centre asymmetric) the signal part cut away

by the decreasing windowing slope (indicated by the upper-right orange triangle in Figure 7-10b is the same as the remaining signal part after application of the increasing window slope within the cyclic prefix (indicated by the lower-left orange triangle in Figure 7-10b since the cyclic prefix is a copy of the last part of OFDM symbol. If the windowed cyclic prefix part (lower-left orange triangular in Figure 7-10b is added to the last part of the core OFDM symbol the core OFDM symbol is restored at its second boundary. The core OFDM symbol can also be restored at the first symbol boundary by applying the same trick, i.e. adding windowed cyclic suffix (lower-right red triangle in Figure 7-10b to the beginning of the core OFDM symbol. Now the complete OFDM is restored and subcarriers are orthogonal again. The FFT is applied to the restored core OFDM symbol as indicated in Figure 7-10b. Interference pick-up remains reduced as long as the interference does not have a periodicity equal to the OFDM symbol duration.
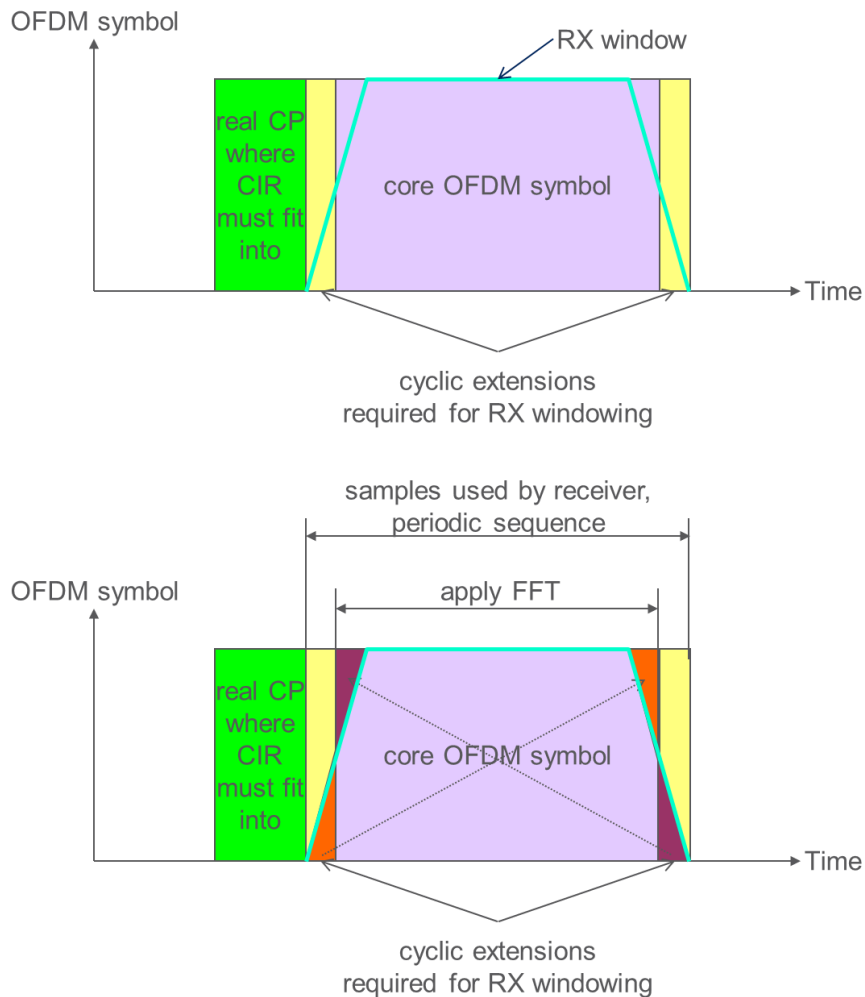


**Figure 7-10: Schematic illustration of RX windowing.**

**Top: Smooth window slopes are applied at the boundaries between cyclic prefix/core OFDM symbol and core OFDM symbol/cyclic suffix. Bottom: If the RX window slopes fulfil the Nyquist criteria the core OFDM symbol can be restored by adding the windowed cyclic extensions to the core OFDM symbol.**

Windowing has extremely low complexity. Only the windowed samples must be scaled and overlap-and-add over the windowed periods must be performed.

In an OFDM system with different numerologies (subcarrier bandwidth and/or cyclic prefix length) multiplexed in frequency-domain, only subcarriers within a numerology are orthogonal to each other. Subcarriers from one numerology interfere with subcarriers from another numerology since energy leaks outside the subcarrier bandwidth and is picked up by subcarriers of the other numerology. Windowed-OFDM can be used to reduce inter-numerology interference due to improved frequency localization. Figure 7-11 compares SIR in an OFDM system without windowing and with TX and RX windowing. The simulation parameters for both setups are provided in Table 7-1. It can be observed that windowing substantially increases the achievable SIR. SIR is averaged across subcarriers within one resource block which is assumed 12 subcarriers. All resource blocks except 3 wideband and 2 narrowband experience an SIR of 30 dB and above with combined TX/RX windowing of length 12.

**Table 7-1: Simulation parameters**

| Parameter | Numerology 1 | Numerology 2 |
|---|---|---|
| Numerology | $\Delta f = 15$ kHz, $T_{cp} = 4.7\ \mu s$ | $\Delta f = 30$ kHz, $T_{cp} = 2.4\ \mu s$ |
| FFT size | 2048 | 1024 |
| Sum of all cyclic extensions | 144 samples | 72 samples |
| Length of cyclic suffix | Number of samples of TX window slope plus half the samples of RX window slope | |
| Length of overlap between symbols | Number of samples of TX window slope | |
| TX and RX window slope length | 0 (no windowing), 12, 24 | 0 (no windowing), 6, 12 |
| TX and RX window function | $1/(N_{win} + 1) \cdot (1{:}N_{win})$ and $1/(N_{win} + 1) \cdot (N_{win}{:}{-}1{:}1)$ for increasing and decreasing window slope, respectively. $N_{win}$ is the window slope length. | |
| Resource allocation | $\{600 \dots 1199\}$ | $\{0 \dots 299\}$ ($\{0{:}2{:}598\}$ narrowband subcarrier) |
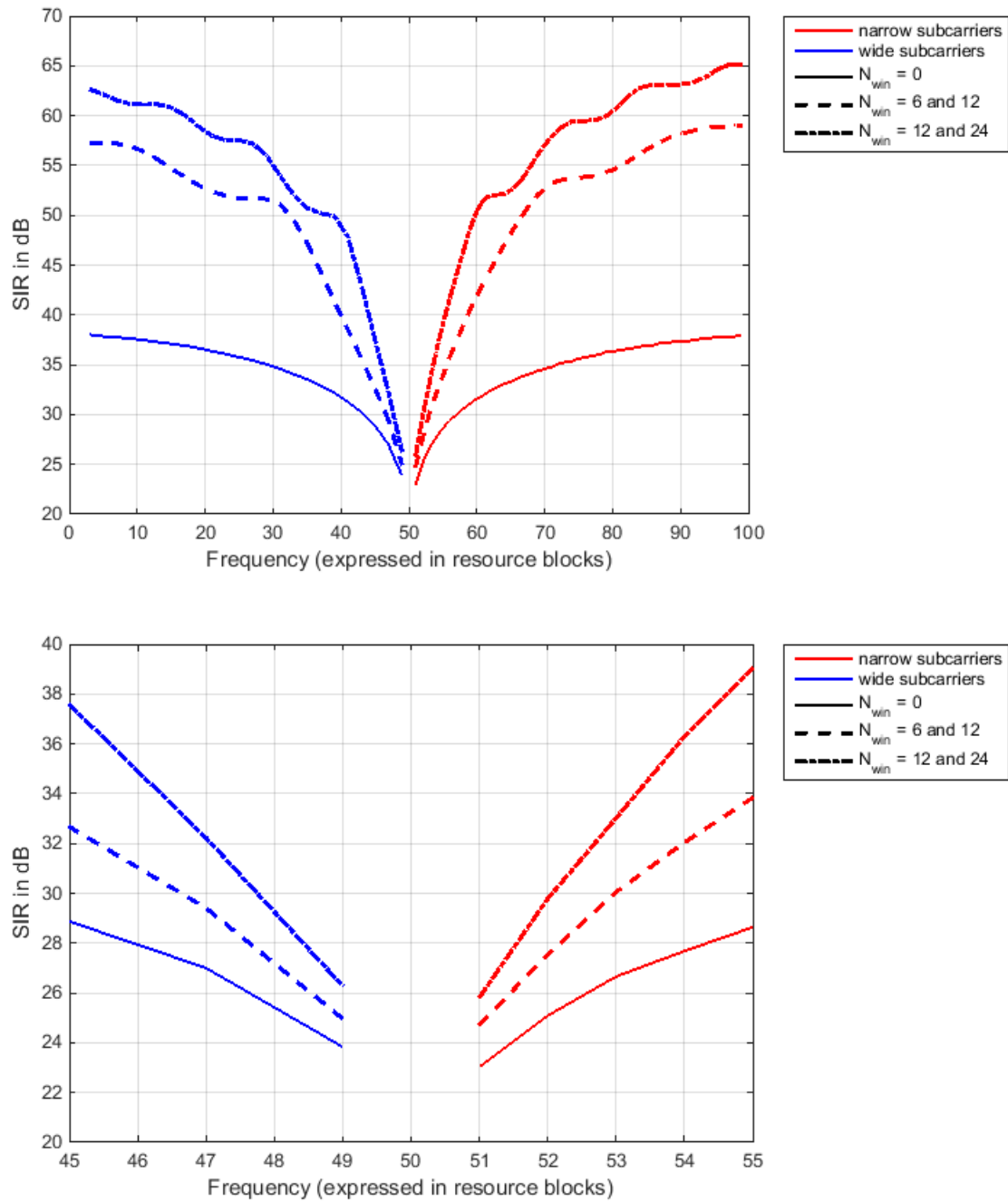
**Figure 7-11: Top - Comparison of SIR without windowing and with TX/RX windowing. Bottom - Zoomed into the centre resource blocks.**

## A.4.2　　P-OFDM

Following the general definition of multi-carrier modulation, the time-frequency rectangular lattice is defined by the symbol interval $T = N\,T_s$ and the subcarrier spacing $F = (MT_s)^{-1}$, where $T_s$ is the sampling rate of the baseband signal, N is the number of signal samples constituting one symbol interval, and M is the number of subcarriers. For the system design of P-OFDM, we assume $N > M$, translating to an overhead in form of a cyclic prefix. This overhead can be characterized by $\vartheta = TF\text{-}1 = \frac{N}{M} - 1 > 0$.

The general description of the OFDM transmit signal s(t) using an arbitrary (orthogonal) pulse g(t) is given as:

$$s(t) = \sum_{n=-\infty}^{+\infty} \sum_{m=0}^{M-1} a_{m,n} g(t - nT) e^{j2\pi mF(t-nT)}$$

where $a_{m,n}$ is the (complex-valued) information bearing symbol with sub-carrier index m and symbol index n, respectively. The orthogonal transmit pulse shape g(t) shapes the frequency response of the individual subcarrier signals, whereas the orthogonal property ensures that there is no inter-carrier and inter-symbol interference between the signals transmitted successively along the time/frequency rectangular lattice. The general description of the OFDM signal as above does not constrain the length of the pulse shape g(t) to the symbol interval T as known from CP-OFDM; it only sets the orthogonality constraint as requirement. That means, the pulse shape g(t) may indeed have a length of $L = KT$ with $K \geq 1$ being a rational number, translating to overlapping pulse shapes in the time domain for a certain fractional number of symbols. Respecting the orthogonality constraint in the pulse shape design will still ensure a reconstruction of the signals at the receiver without interference from preceding and succeeding symbols for any choice of K.

CP-OFDM can be consider a special case of P-OFDM, where K = 1 and g(t) is the rectangular pulse shape realizing the "add CP" operation, which is given by

$$g_{cp}(t) = \begin{cases} \dfrac{1}{\sqrt{T}} & t \in \left[-\dfrac{T}{2}, \dfrac{T}{2}\right] \\ 0 & \text{otherwise.} \end{cases}$$

At the receiver, the receive pulse shape $\gamma(t)$ is used for the signal reconstruction. For CP-OFDM, $\gamma(t)$ realizes the "remove CP" operation, which is given by

$$\gamma_{cp}(t) = \begin{cases} \dfrac{1}{\sqrt{T - T_{cp}}} & t \in \left[-\dfrac{T - T_{cp}}{2}, \dfrac{T - T_{cp}}{2}\right] \\ 0 & \text{otherwise.} \end{cases}$$

Furthermore, if $K \approx 1$ and a pulse shape with smoothened edges is used, we obtain a windowed-OFDM system as described in [ABS2011].

The P-OFDM transceiver for arbitrary rational overlapping factor K can be efficiently realized by a poly-phase network (PPN), which is plugged into the OFDM transmission chain after the IFFT

at the transmitter and before the FFT at receiver, as shown in Figure 7-12. All other algorithms for channel estimation, MIMO, etc. remain the same as for CP-OFDM. For the short pulse shape where K≈1, the PPN structure can be simplified to the "CP", "zero-padding" or "windowing" operations. For a general choice of K, the PPN requires KM complex multiplications and storage for approximately (K-1)M complex numbers in the register memory. For a pulse shape with K = 4, for example, the overall modulator complexity of P-OFDM increases by 10% to 30% compared to CP-OFDM.
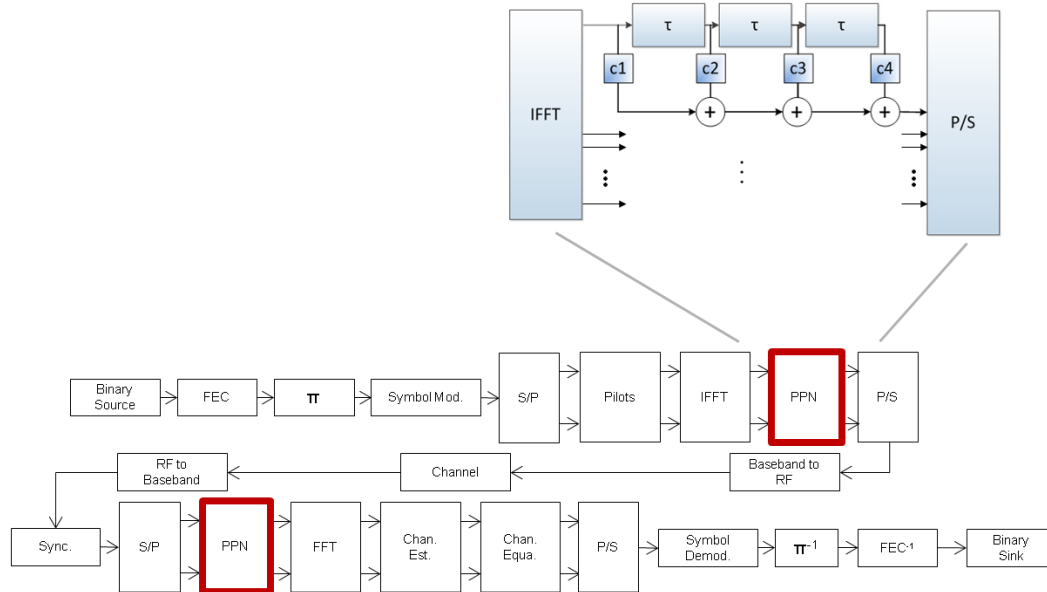


**Figure 7-12: P-OFDM transceiver with efficient implementation of pulse shaping by a polyphase network**

From the general description of the OFDM signal given above, we can thus conclude that there are in total three degrees of freedom for the design of a multi-carrier system, which are given by the triple (F, T, g(t)). As the pulse shape g(t) in CP-OFDM is fixed to the rectangular window, the degrees of freedom are effectively reduced. Hence, by optimizing the pulse shape g(t), we therefore exploit a novel degree of freedom for the waveform design compared to CP-OFDM, enabling us to attain performance improvements in selected scenarios without altering the signal structure inherent to CP-OFDM.

**Better coexistence properties thanks to spectral containment**

To enable flexible spectrum usage, low out-of-band (OOB) power leakage is desired. For the comparison of P-OFDM with CP-OFDM, we consider again the two cases TF = 1.07 and TF = 1.25. From the power spectral density (PSD) analysis shown in Figure 7-13, we can observe that P-OFDM with an appropriately designed pulse shape filter achieves a much lower OOB power leakage with the than CP-OFDM does. Note that, in practice, a subband-wise low pass filtering can be adopted for CP-OFDM to shape the signal and make it fit into the spectral

mask, as long as the shaping does not invoke a huge loss in error vector magnitude (EVM). Such condition holds if sufficient guard subcarriers are applied in CP-OFDM.

### CP-OFDM          P-OFDM with K=1.07          P-OFDM with K=4
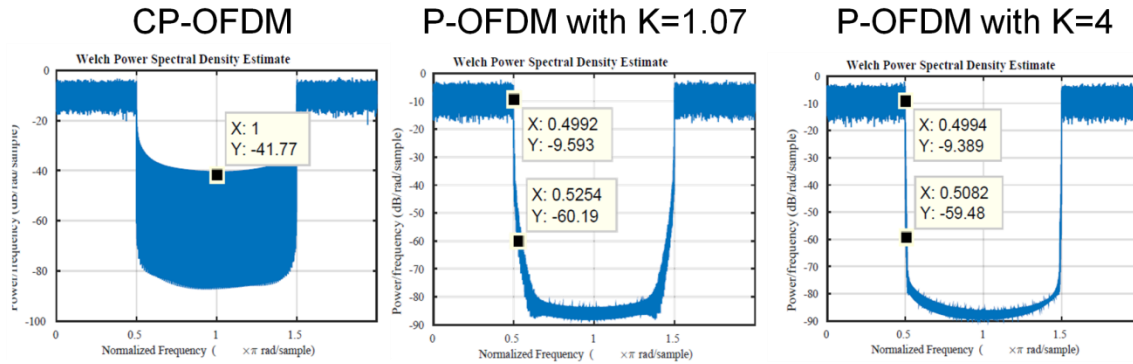


**Figure 7-13: PSD of CP-OFDM and P-OFDM for TF = 1.07 (i.e. 7% CP overhead)**

**Table 7-2: Required guard carriers to obtain power suppression of -50 dB**

| | | *K = 4* | *K = 1.07* |
|---|---|---|---|
| *TF = 1.07* | Guard Subcarriers | 9 | 27 |
| | Guard Subc. overhead (compared to 20MHz) | 0.7% | 2% |
| | EVM for Edge Subc. | -48.9 dB | -57.2 dB |
| | EVM for Central Subc. | -48.9 dB | -57.3 dB |
| *TF = 1.25* | Guard Subcarriers | 7 | 14 |
| | Guard Subc. overhead (compared to 20MHz) | 0.53% | 1.05% |
| | EVM for Edge Subc. | -56.8 dB | -55.8 dB |
| | EVM for Central Subc. | -56.8 dB | -55.8 dB |

In the above figures, we used an LTE-typical setting of 15 KHz subcarrier spacing for 20 MHz bandwidth. To meet a desired spectral leakage of -50 dBc/Hz, the required number of guard subcarriers for P-OFDM (without any additional subband filtering) is given in Table 7-2. Note that the linearity of the RF unit should be considered for meeting the actual spectral mask requirement.

The spectral containment of the signal power enables P-OFDM to support individual configurations of sub-bands within the system bandwidth, as illustrated in Figure 7-14 (note that this feature holds similarly also for other filtered waveforms). These individual configurations

also allow for the use of individual signaling and independently designed frame structures to be used in each of the sub-bands.
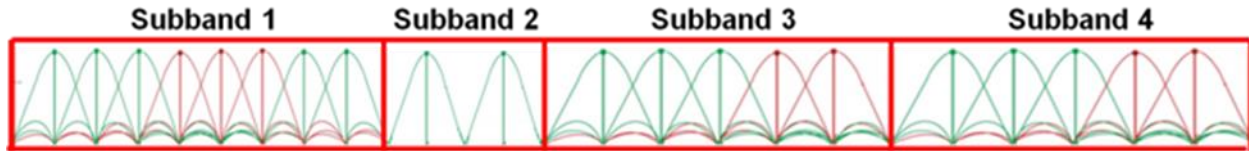


**Figure 7-14: Sub-bands with individual numerologies enabled by filtered waveforms**

# A.5      FBMC based solutions

FBMC represents a multi-carrier system where the single subcarrier signals are individually pulse shaped with a pulse that may extend over several symbol intervals of duration T, yielding an excellent spectral containment of the multi-carrier signals. The use of such a pulse results in overlapping pulses if several FBMC symbols are transmitted successively in time. Practical values for the overlapping factor $K$ reach up to 4, where $K$ specifies the number of symbol intervals T which the time domain pulse spans. For an illustration of overlapping pulses with $K = 4$, see Figure 7-15, where the selected division of the x-axis represents the symbol interval T.



Time
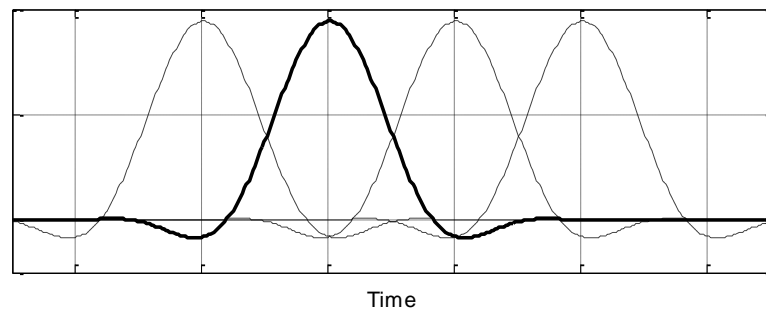
**Figure 7-15: Impulse response of the filter.**

Figure 7-16 shows the power spectral density of a notched FBMC signal in comparison to an OFDM signal. It clearly highlights the steep slopes of the FBMC frequency localized signal, which can be realized thanks to the long durations of the overlapping time-domain FBMC symbols.
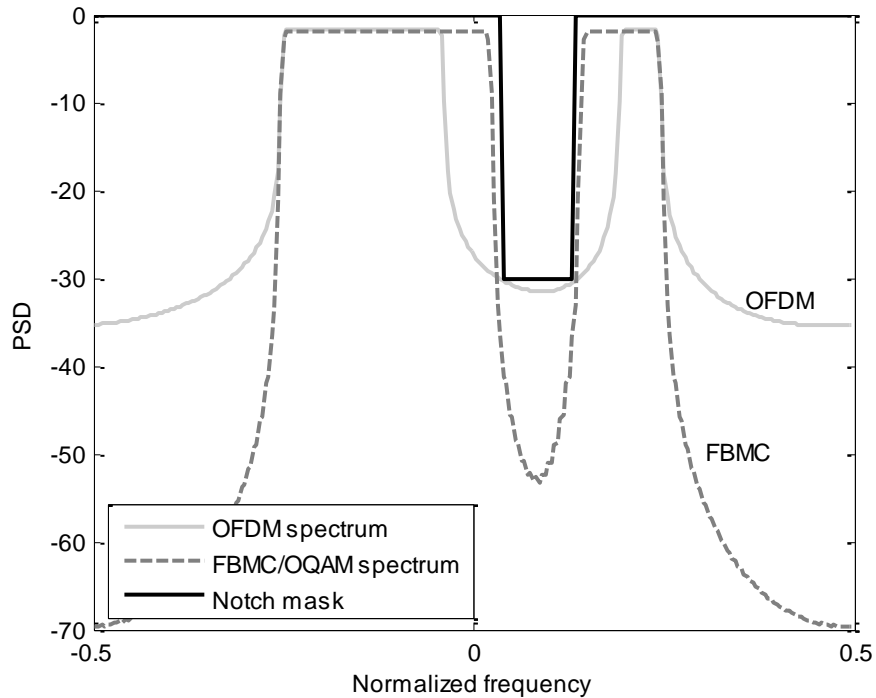
**Figure 7-16: Power spectral density of FBMC signal and OFDM signal with spectrum notch**

Main FBMC candidates under discussion for 5G are OQAM-FBMC and QAM-FBMC, which are presented in more detail in the following subsections.

## A.5.1 OQAM-FBMC

For achieving maximum spectral efficiency, OQAM signaling has been proposed in the literature. In this case, no guard bands or guard intervals are required; consequently, the maximum spectral efficiency yields TF = 1 (with F being the subcarrier spacing). However, the orthogonality in OQAM is in the real signal field only, which means that some algorithms developed for OFDM cannot be directly transferred, but require redesign of some signal processing procedures.

The schematic of an FBMC transceiver is shown in Figure 7-17, where the signal blocks that differ from an equivalent OFDM transceiver are given in grey shaded color. As seen in the figure, instead of CP adding/ removal, FBMC requires filter banks realizing the prototype pulse other than rectangular. The overall framework of FBMC modulation/demodulation can be efficiently realized with FFT and polyphase filtering. Comparing transceiver complexity of general FBMC with the specific OFDM approach, latest research results have shown that the additional complexity required for implementing the subcarrier filtering is only moderate, amounting to u up to a factor of two for OQAM signaling.
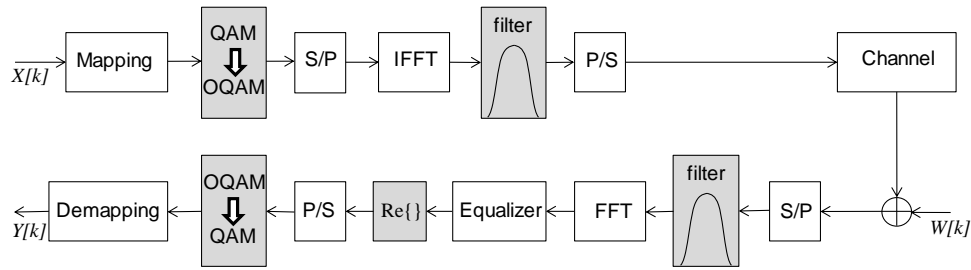
**Figure 7-17: FBMC transceiver**

## A.5.2    QAM-FBMC

Regarding the spectral efficiency of the waveforms, several parameters play an important role, e.g. the block length. For OFDM (as well as F-OFDM), the efficiency in time and frequency does not depend on the block length as a fixed overhead in time (either CP or zero padding) is added to each symbol, whereas for OQAM-FBMC a guard time corresponding to the filter tail may be needed for uplink to avoid ISI, but it is only added once per block. Consequently, OQAM-FBMC may not be very efficient for very short blocks. On the other hand, for long blocks OQAM-FBMC may have a higher efficiency compared to CP-OFDM and F-OFDM as the overhead due to the CP or guard period gets larger than the fixed overhead of OQAM-FBMC due to the filter tails. Furthermore the guard bands at the edges of the spectrum (and between users in case of asynchronous uplink) can be made much smaller for OQAM-FBMC due to the lower OOB radiation.

In FBMC, the effectively increased symbol duration is suitable for handling the multi-path fading channels even without CP overhead. Consequently, the FBMC system can reduce the inherent overheads such as CP and guard-bands in CP-OFDM. FBMC is also attractive in specific asynchronous scenarios, where CoMP and DSA in a fragmented spectrum are employed to support the much higher traffic demand in 5G.

However, to maintain the transmission symbol rate, the conventional FBMC system generally doubles the lattice density either in time or in frequency compared with OFDM while adopting OQAM. In OQAM, in-phase and quadrature-phase modulation symbols are mapped separately with half symbol duration offset. Thus, OQAM-FBMC causes intrinsic interference that makes it not straightforward to apply conventional pilot designs and corresponding channel estimation algorithms as well as MIMO schemes as in CP-OFDM systems. In this regard, QAM-FBMC system which can transmit the QAM symbols is proposed to enable fundamental spectral efficiency enhancement whilst keeping the signal processing complexity low.

With a base-filter that takes the spectrum confinement and the orthogonality among adjacent subcarriers into consideration, the QAM-FBMC system performs comparable to the CP-OFDM system even without the CP overhead, while the guard-band overhead reduction is also available from the well-confined spectrum as shown in Figure 7-18. Improved receiver

algorithms including channel estimation and equalization can further mitigate the multi-path fading channel impact without the CP.
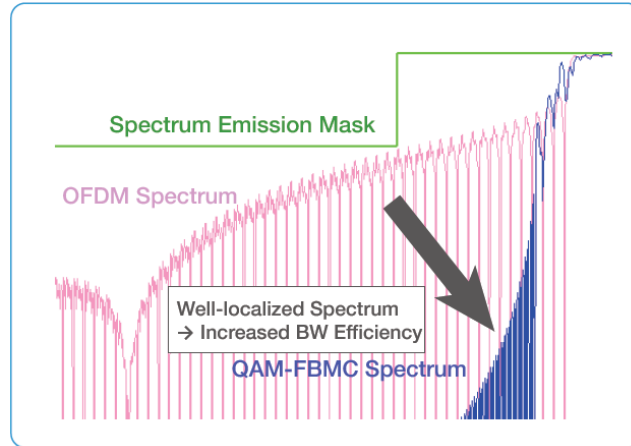


**Figure 7-18: Well-localized QAM-FBMC Spectrum.**

An examplary QAM-FBMC system with two different prototype filters for the even- and odd-numbered subcarriers is illustrated in Figure 7-19. The information symbols are divided into the even-numbered sub-carrier symbols and the odd-numbered sub-carrier symbols. Then the symbols are IFFT transformed and repeated. Finally pulse shaping with two prototype filters are performed to the symbols by means of windowing (element-wise multiplication) and added. The symbol transmission rate of QAM-FBMC is the same that of CP-less OFDM. The received symbols are FFT transformed and equalized in frequency domain. Then the received symbols are filtered by the Rx filter for even-numbered sub-carrier symbols and due to certain orthogonality conditions, the odd-numbered sub-carrier symbols are filtered out. The same procedure is applied in the Rx filter for odd-numbered sub-carrier symbols. By doing this, the received symbols are divided into the even-numbered symbols and the odd-numbered symbols. Each symbol is filtered by the prototype filter and then demodulated. It has been shown that such a QAM-FBMC system can achieve comparable performance to CP-OFDM in multipath fading channels.
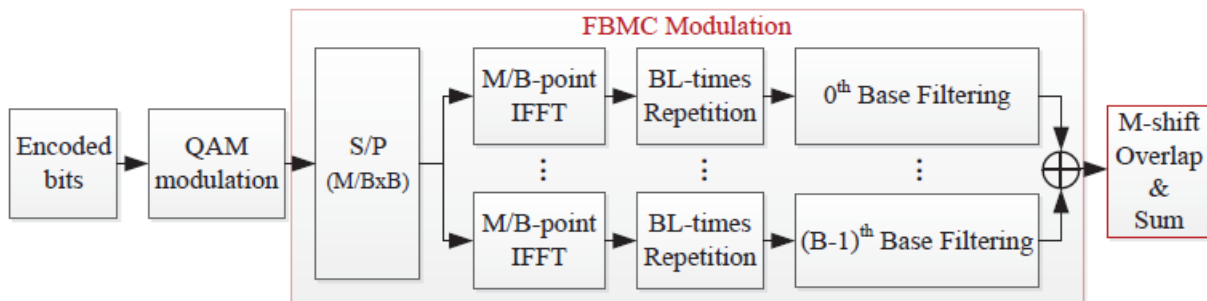


**Figure 7-19: Transmitter and receiver of a QAM-FBMC system.**
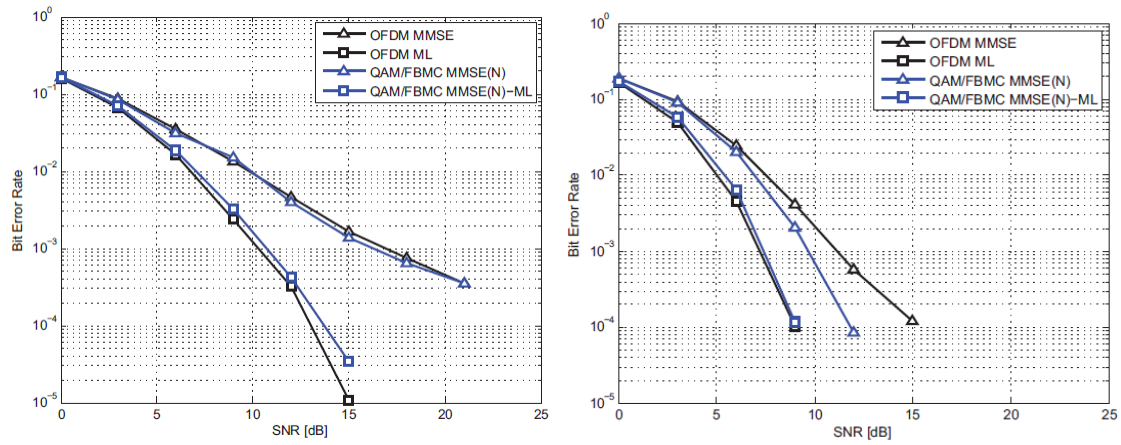
**Figure 7-20: BER for 2×2 MIMO over EPA and ETU channel (left: EPA, right: ETU)**

# B  Harmonized air interfaces

## B.1  Layer 2 Design Aspects

**L2 Design Principles of the harmonization approach used in section 4.2.1.**

The key design principles have impact the L2 design as explained as follows:

**Service agnostic design allowing flexible service centric configurations:** The different 5G use-cases will have vastly diverse requirements as mentioned in the introduction and in the key requirements of Chapter 2. The 5G standard should provide a large set of service agnostic features which the network may configure and enable to fulfill the service specific requirements. This is supposed to enable co-existence of multiple services while maintaining low complexity and high efficiency for each service.

**Stay in the box:** A key feature of LTE is that all traffic is mapped dynamically to a single pair of shared channels (PDSCH/PUSCH). This maximizes statistical multiplexing and allows a single UE to get instantaneous access to all radio resources of a carrier or even multiple carriers. Appropriate RLC configurations and scheduling policies ensure that QoS requirements are met. Therefore, we want to stick with this design principle while designing 5G as well.

**Flexibility for control plane** : 5G shall have a lean and scalable design to cope with various latencies on the transport and radio interface as well as with different processing capabilities on UE and network side. To ensure scalability, one should for example avoid fixed timing relations between control messages such as HARQ (MAC), ARQ (RLC) and RRC signaling.

**Layers of coordination**: When the cost of observation and control is too high, e.g. in terms of delay or overhead, scheduling decisions can be delegated to nodes and UEs to realize a suitable coordination when the coordinator collects sufficient information. The centralized resource scheduler still has the full right to use radio resources but in situations where observation and control is more efficient to maintain in another node (e.g. in multi-hop relaying or D2D) the momentary decisions on how to assign resources should be distributed.

**Lean and thereby future-proof:** Please see Chapter 2, design principles and control plane requirements. For example, the 5G terminal should not expect control messages at specific time/frequency resources (as is the case today for HARQ feedback in LTE).

# B.2 Harmonized CP-OFDM for multiple bands with enhancements for multi-service support

We show the performance of multiplexing in asynchronous cases in Figure 7-21, where a timing misalignment is captured between two ZT-DFTs-OFDM signals. The scenario is characterized as follows:

- Two users are multiplexed in adjacent PRBs, where each PRB consists of 256 subcarriers. ZT-DFTs-OFDM signals are then generated by the two users.
- The signals are then transmitted over a 100 MHz bandwidth.
- The two users who are thus multiplexed in frequency, are asynchronous to each other
- The performance is measured by the ISR, where the interference from the asynchronous user is measured on an intended user. The average ISR is then shown for the two users.
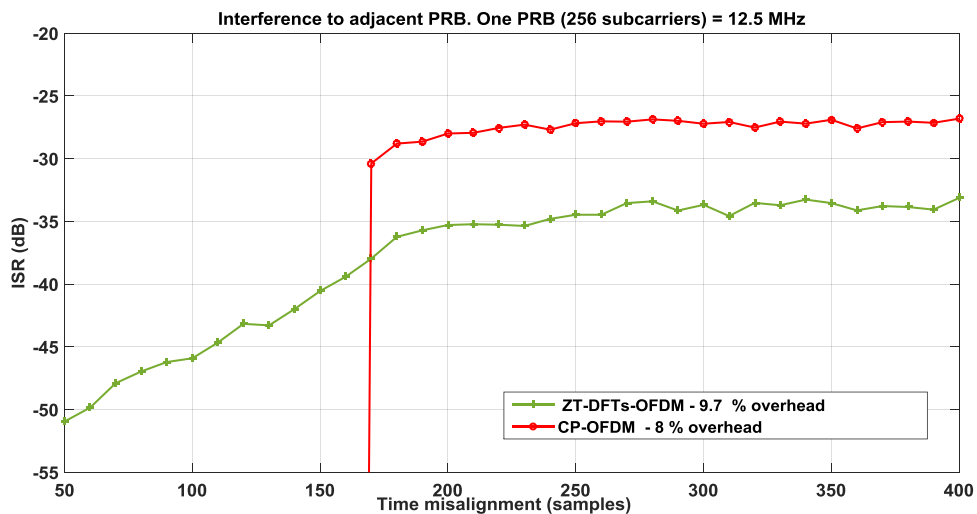


**Figure 7-21: Performance with time misalignment**

# B.3 Air interface design based on P-OFDM

**Selected scenarios with favorable performance improvements for P-OFDM**

In this section, we take a look at selected scenarios where P-OFDM can provide significantly better performance than conventional CP-OFDM. We use the LTE-based setting for CP-OFDM and assume that the P-OFDM scheme has the same overhead as CP-OFDM (i.e. TF = 1.07, if not stated otherwise). Meanwhile, the same pilot structure and transceiver algorithm for

equalization and channel estimation are used. Therefore, we focus on the performance gain achieved solely by the optimized pulse shaping.

**Asynchronous TA-free transmission**

We first focus on the scenario of uplink transmission where no closed-loop TA adjustment is applied, yielding an asynchronous transmission. Due to the radio propagation latency, the timing misalignment is present upon the arrival of the uplink signal at the BS. Assuming a cell radius of 2 km, TA misalignment is calculated according to the propagation delay of the round trip, i.e. it will lie approximately in the range of [0, 13]μs.

We consider Turbo-coded BLER performance for two users accessing the same frequency sub-band, which are then separated at a multi-antenna BS by using a linear MMSE receiver. Figure 7-22 depicts the results for the asynchronous transmission of two users to one BS equipped with four antennas. Since the normal CP length in OFDM of LTE systems is 4.7 μs, it cannot fully cover the time misalignment caused by the asynchronous transmission. Therefore, a performance degradation is observed for CP-OFDM for all modulation and coding schemes (MCS). P-OFDM uses an optimized pulse shape with K = 4, which shows significantly higher robustness to timing misalignment compared to CP-OFDM.
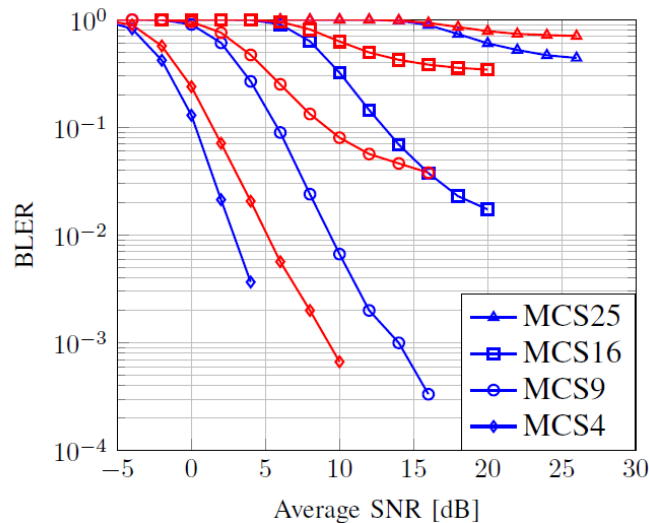


**Figure 7-22: BLER performance for asynchronous multi-user uplink (ETU channels, timing offset uniformly distributed in [0, 13]μs). Blue: P-OFDM, red: CP-OFDM**

**High mobility scenarios**

High mobility has been recognized as a key requirement for the next generation radio technology to support a variety of new services, e.g., high speed train and V2V communication. For both cases, we apply the designed pulse shape with K = 4, TF = 1.25. For the HST scenario, LTE based CP-OFDM (with identical TF = 1.25) is taken as baseline. Figure 7-23

depicts the BLER performance for P-OFDM and CP-OFDM, both with least square (LS) based channel estimation. It is shown that P-OFDM outperforms CP-OFDM due to its robustness to time and frequency distortions caused by high mobility, which is facilitated by the optimized pulse shape.
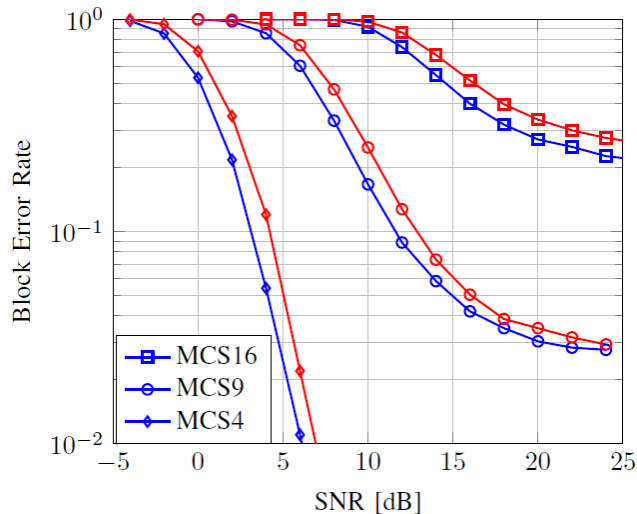


**Figure 7-23: Link level performance for high speed train (SISO in EVA channel, 500km/h, 15kHz subcarrier spacing, LS channel estimation). Blue: P-OFDM, red: CP-OFDM**

# B.4 Adaptive Filtered OFDM with Regular Resource Grid

**Impact of guard bands on regular resource grid**

Now, if we consider new waveforms that may be intended to work in asynchronous scenarios, filtering together with certain amount of guard bands may be beneficial. We consider the impacts on the regular resource grid. It is often proposed in the literature to go for a limited number of filters to be used for the subbands in order to keep the system complexity and possible extra signaling low. Therefore, it may be reasonable to choose a limited set of filters covering a certain set of numbers of resource blocks similar to the PRB in LTE. The problem that may then occur is that when introducing the guard bands between the subbands, the subbands will be shifted apart in frequency domain and therefore violate the regular resource grid as illustrated in Figure 7-24. The resulting irregular grid leads to a tremendously increased overhead for signaling the shifted subband locations. In the next section we discuss new approaches to address this issue and also provide numerical analysis in detail.
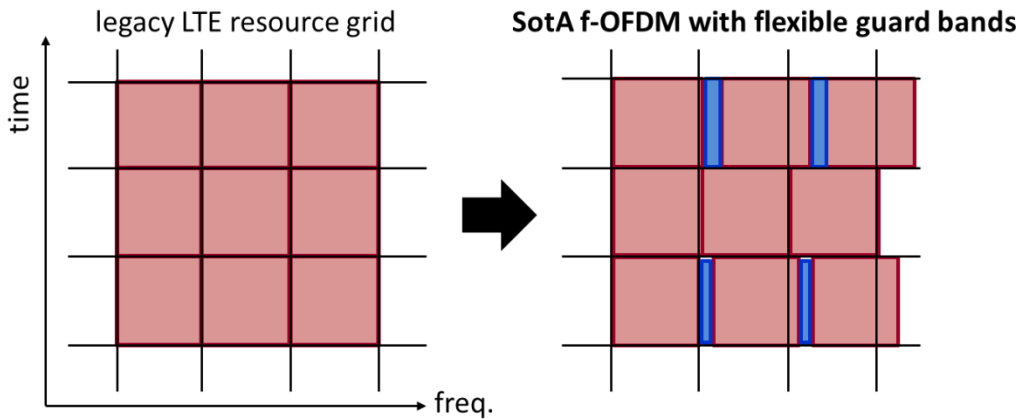
**Figure 7-24: Guard bands violating regular resource grid**

**Proposed regular resource grid with guard bands for F-OFDM [WBK+16]**

To circumvent the violation of the regular grid by introducing guard SCs that we discussed earlier, one can allocate guard bands within the regular resource grid as illustrated in Figure 7-25. To implement this while supporting flexible choices of guard bands, we further consider two approaches: either to define multiple filters, each of which referring to one subband size tailored with a pair of particular passband and guard bandwidth where allocating the guard band outside the filter passband bandwidth, or to keep the filter fixed with a constant passband bandwidth independent of the guard bandwidth where allocating the guard band within the filter passband bandwidth. These two approaches are illustrated in Figure 7-26. The first approach (Figure 7-26, left) would make the system much more complex as more filters would have to be defined and possibly signaled, whereas the latter (Figure 7-26, right) keeps the system simpler but may lead to a degradation of the OOB suppression. In the following sections we will investigate this effect in more detail and it will be shown that the latter approach performs even better in practically relevant interference scenarios regardless of the simplicity.
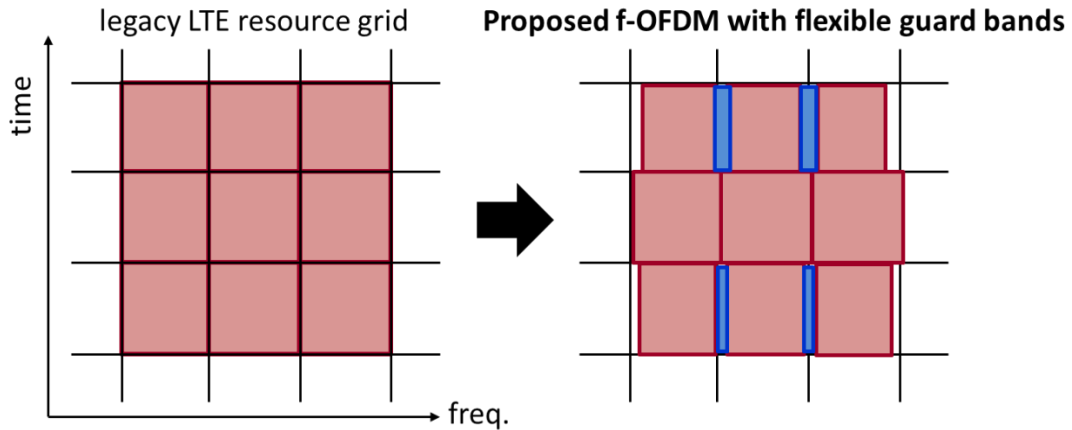
**Figure 7-25: Guard bands keeping regular resource grid**
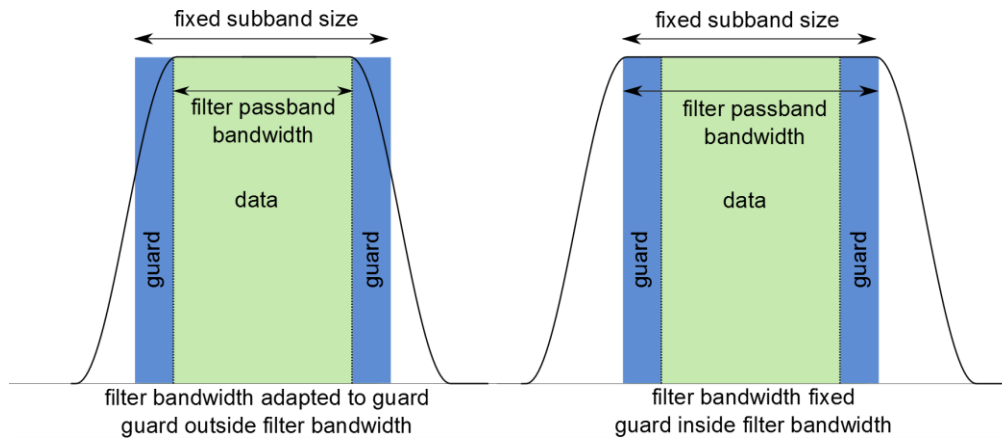


**Figure 7-26: Two approaches to keep regular resource grid**

**Simulation results**

In this section we will show and discuss simulation results for two different approaches in Figure 7-26 and the state-of-the-art (SotA) approach to include guard SCs. The two users are allocated resources next to each other in the frequency domain, only separated by 2 guard SCs, which are located either inside or outside the filter. The subband size is 48 SCs for both users, in the SotA case the guard SCs are outside the subband which destroys the regular resource grid, for the new proposal they are inside and keeps the regular grid, i.e., they are contained in the subband of 48 SCs. We consider half a symbol transmission timing misalignment between the two users to account for a worst case timing offset. The power ratio of the two users' signals observed at the receiver is varied as a parameter in order to investigate how the performance of the user of interest is affected by the different relative strengths of the interfering signal.
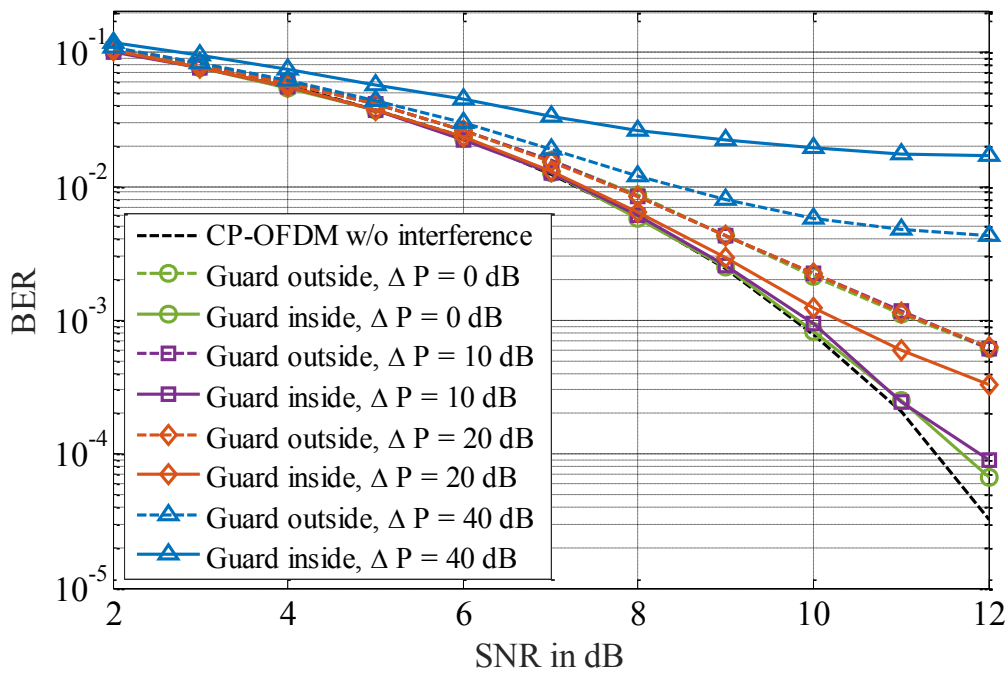
**Figure 7-27: Uncoded BER performance of F-OFDM on an AWGN channel with 2 guard SCs and QPSK modulation**

Figure 7-27 compares the SotA and new approaches in terms of uncoded bit error rate (BER) performance of F-OFDM versus SNR on an AWGN channel using QPSK modulation. As a reference the single user performance of CP-OFDM without interferer is also plotted. We can observe that the new approach (guard SCs inside subband) outperforms the SotA (guard SCs outside subband) for the interference power of up to 20 dB higher than the user of interest although the new approach keeps the system design simpler. For extremely high interference of 40 dB higher than the user of interest the performance of the new approach degrades and the SotA performs slightly better, but overall the performance is not satisfactory for such strong interference. The observations can be understood by considering the two effects of the OOB suppression and inband distortion that are introduced by the filtering. The new approach experiences the lower inband distortion because the edge SCs that are distorted by filtering are used as the guard SCs located inside the passband and do not carry data. That leads to the better performance of the new approach although the amount of interference from the neighbor user is slightly increased. High interference exceeding a certain level, however, starts dominating the overall degradation and thus, the performance is better for the SotA, which experiences lower interference from the neighboring user.

The observations and conclusions that are made for QPSK basically remain the same for 16QAM as illustrated in Figure 7-28 with slightly more pronounced differences in performance for 16QAM due to its increased sensitivity to the interference as compared to QPSK.
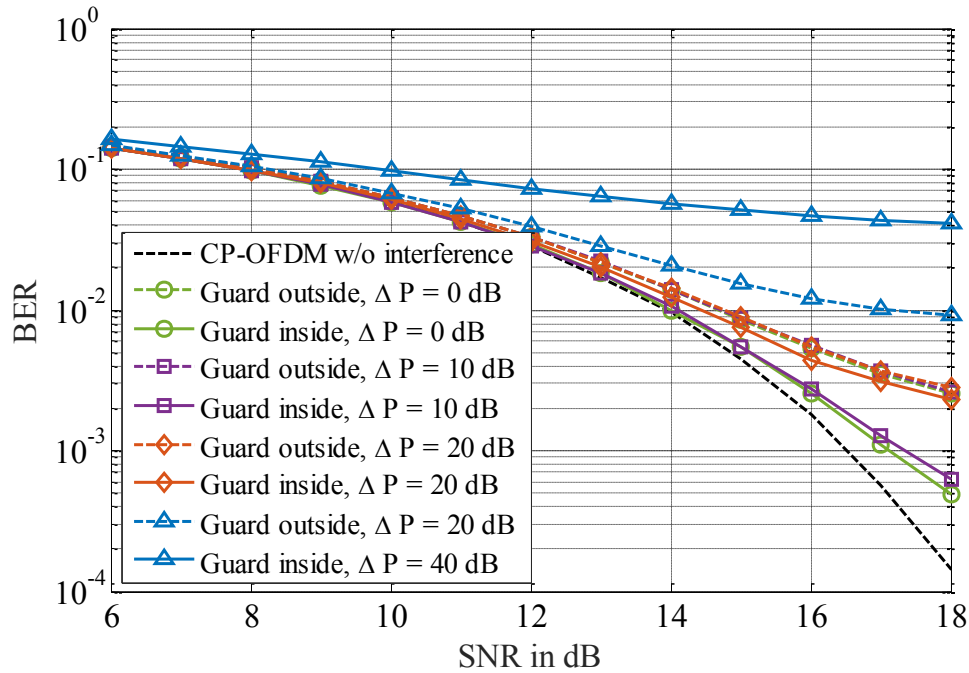
**Figure 7-28: Uncoded BER performance of F-OFDM on an AWGN channel with 2 guard SCs and 16QAM modulation**
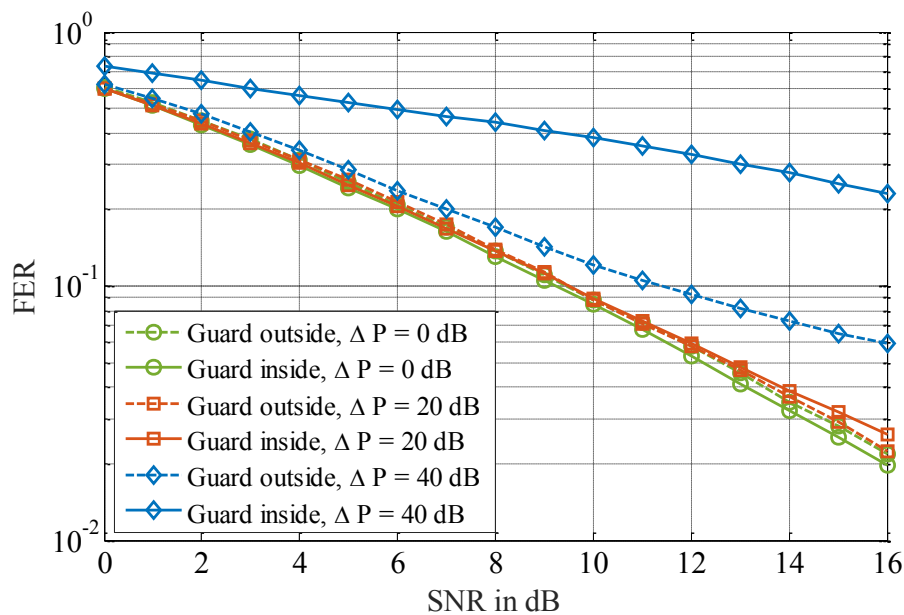


**Figure 7-29: FER performance for F-OFDM with different power offsets, EPA channel, 3 km/h, QPSK, Rc = 0:32, 2 guard SCs**
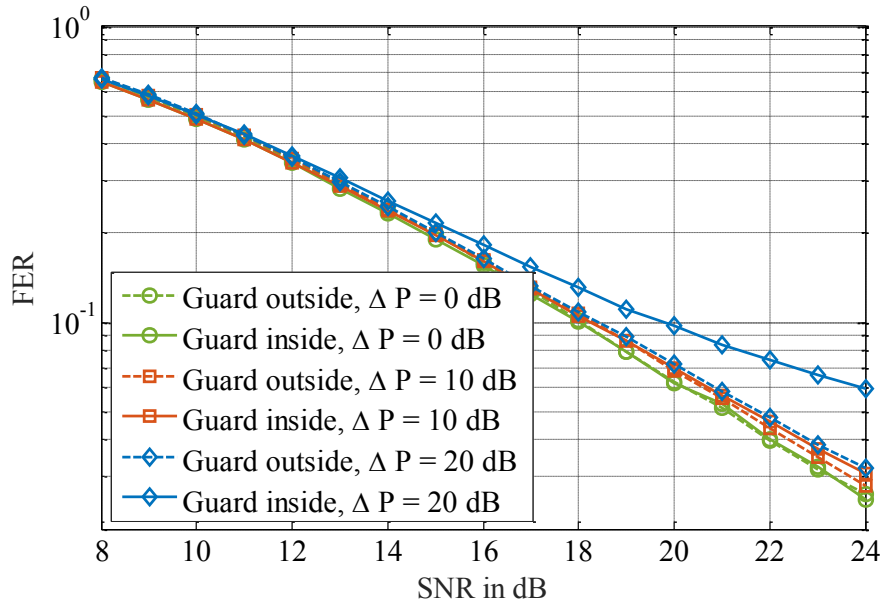
**Figure 7-30: FER performance for F-OFDM with different power offsets, EPA channel, 3 km/h, 16QAM, Rc = 0:55, 2 guard SCs**

Figure 7-29 and Figure 7-30 show the performance versus SNR over an EPA channel with mobility of 3 km/h where QPSK and 16QAM modulations are used, respectively. For a fading channel frame error rate (FER) evaluation makes more sense than uncoded BER and we apply LTE compatible turbo codes with code rates of 0.32 and 0.55, respectively, for QPSK and 16QAM. We can make the observations in FER performance similar to the uncoded BER over an AWGN channel with the smaller performance differences between the SotA and new approaches. Although results were shown for a specific filter design proposed in the literature, the results for other filter designs and respective conclusions are expected to be similar. Therefore, despite its system design simplicity our new approach allocating guard SCs within a constant passband with a fixed filter bandwidth is an attractive solution to accommodate diverse services by adaptive F-OFDM with regular resource grid, which may be seen as a candidate for future mobile communications systems.

# B.5 End-to-end evaluation of CP-OFDM and flexible sub-frame structures

## CP-OFDM performance at 28 GHz

As described in [FZM+16, DMF+16] we report the end-to-end performance trends at a specific CP-OFDM numerology designed for the 28 GHz band, as proposed in [KP11].

**Table 7-3: Numerology at 28 GHz.**

| Sub-carrier bandwidth | 270 KHz |
| --- | --- |
| Clock frequency | $f_s$ = 1 GHz |
| $N_{ofdm}$ | 4096 |
| $N_{cp}$ | 512 |
| $T_{sf}$ in µs | 500 |
| $T_{ofdm}$ in µs | 3.70 |
| $T_{cp}$ in µs | 0.46 |
| $T_{ofdm} + T_{cp}$ in µs | 4.16 |

First of all, we propose and OFDM-based flexible frame design, and report in Figure 7-31 some performance trends, in terms of data rate per UE at varying transmission packet size.
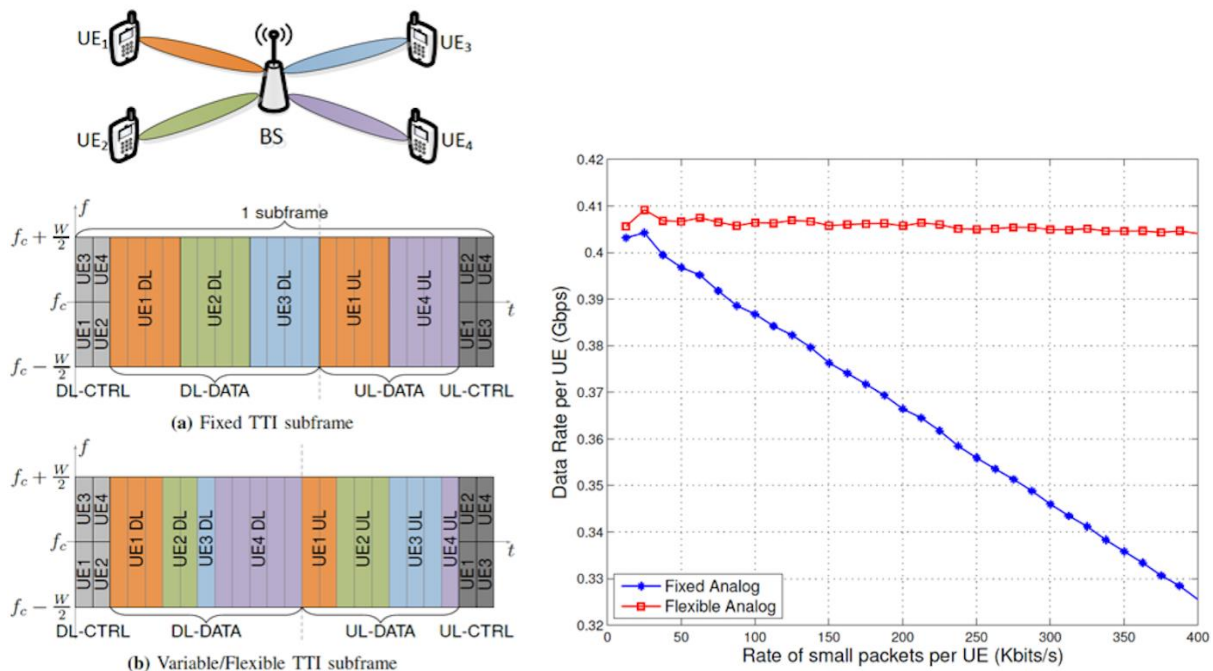


**Figure 7-31: Flexible frame design and results.**

Additionally, we report in Figure 7-32 the comparison of data latency trends for a fixed TTI vs. flexible TTI structure.
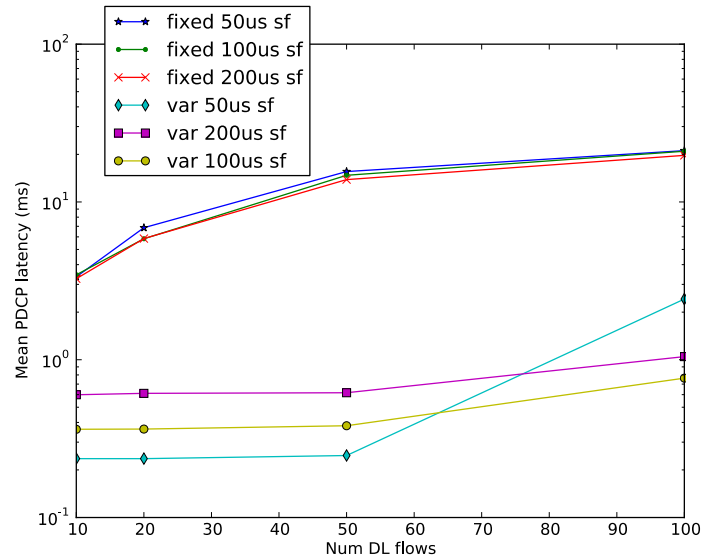
**Figure 7-32: DL Data latency.**

It is well known how critical latency is in 5G networks. This motivated us to carefully design fundamental procedures such as RLC segmentation/concatenation, RLC UM/AM, MAC HARQ (see Figure 7-33) and so forth, in order to capture the performance of a more realistic system.
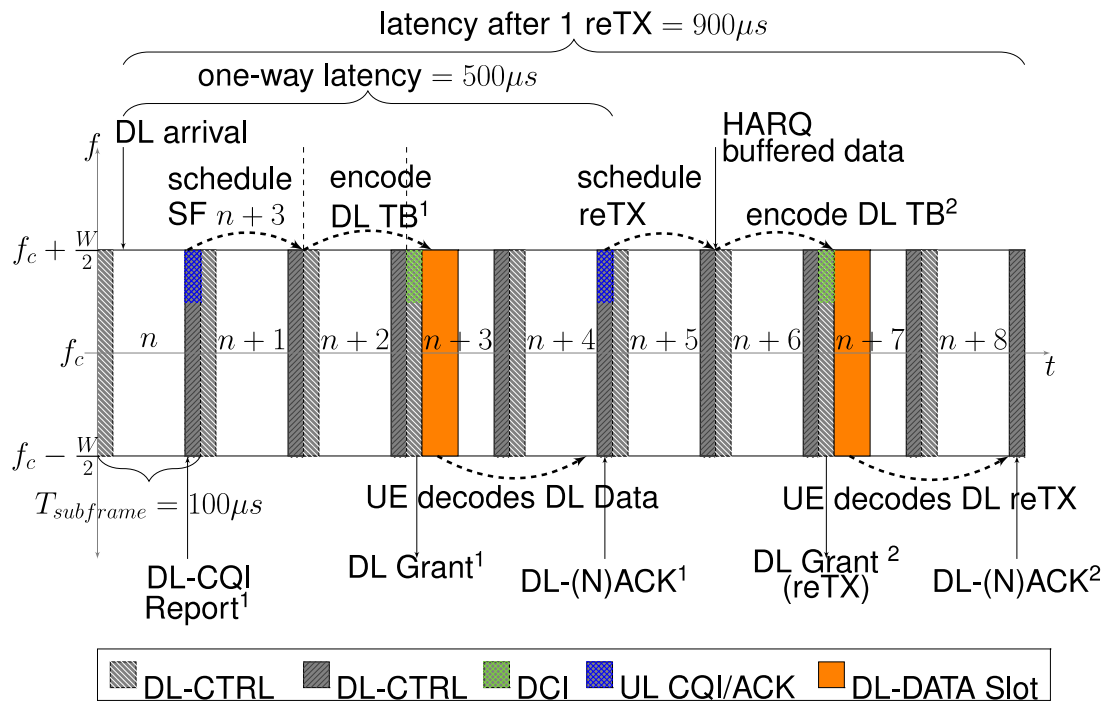


**Figure 7-33: HARQ process**

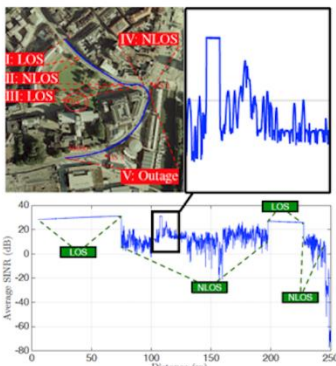As shown in Figure 7-34 and Figure 7-35, we analyze the performance trends of the upper layers while plugging both mmWave statistical channel models and mmWave realistic traces.
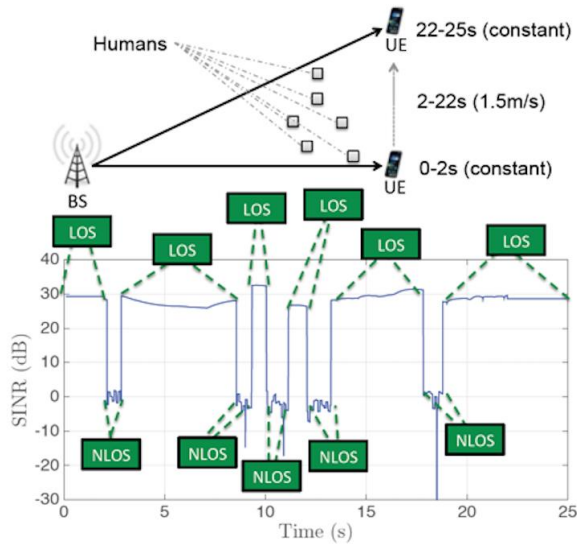


(a) SINR trend for Scenario 1.
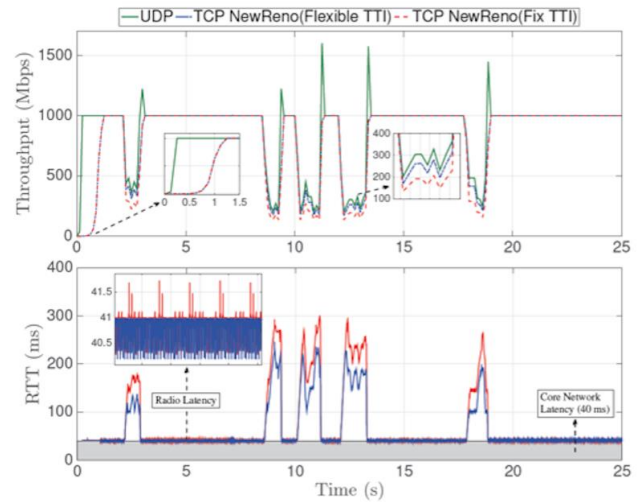
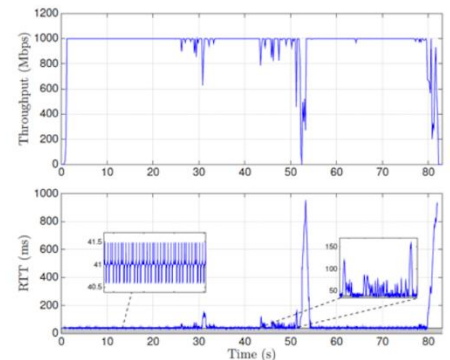(b) Performance comparison at 1 Gbps data rate.

**Figure 7-34: Performance evaluation of current transport protocols over statistical channels.**



(a) SINR
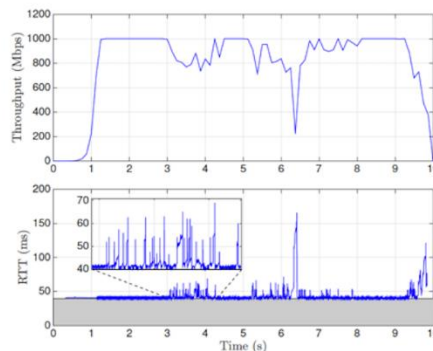
(b) TCP performance (25 m/s)

(c) TCP performance (3 m/s)

**Figure 7-35: Performance evaluation of current transport protocols over realistic traces.**

# C        User plane aggregation

**Table 7-4**: **Comparison of MAC- and PDCP level aggregation**

| | MAC level aggregation | PDCP level aggregation |
|---|---|---|
| **UP & CoP synchronicity** | Synchronous | asynchronous |
| **Synchronization Requirements** | accurate synchronization between transmission points needed | Relaxed |
| **MAC scheduling** | single MAC instance | multiple MAC instances |
| **Front-haul requirements** | Limited to co-located deployments or high-speed front-haul | Relaxed |
| **Usability examples** | -<br>Only AIV1 <-> AIV2 | AI1 <-> AI2<br>AIV1 <-> AIV2 |
| **Technology Example** | LTE Carrier Aggregation,<br><br>LTE CoMP | LTE Dual Connectivity |

## C.1.1        Clustered Multi Communications

Recall that clustered multi-connectivity can be seen as an extension of dual connectivity standardized in LTE as illustrated and the cluster concept proposed for mmW.

However, different from LTE DC the multi-connectivity in 5G needs to be more powerful and more flexible due to the given challenges in section 5.1. In LTE DC, UE connects to only one Master eNB (MeNB) and one Secondary eNB (SeNB) concurrently; different frequencies are used between MeNB and SeNB; and the target is mainly to improve user throughput. In cluster for mmW, UE can only connect to one eNB at the same time and there is only one frequency used in the cluster; and the target is mainly to improve robustness. For multi-connectivity in 5G, UE can connect to one MeNB and more than one SeNB. The frequency used in cluster in 5G can be either one or less than or the same as the number of network nodes in the cluster which depends on deployment. Multi-connectivity in 5G need fulfill the requirement of both robustness and throughput increase.

As in LTE DC, the focus in this report is on relaxed backhaul between MeNB and SeNBs, the techniques for fast backhaul is out of scope.

## Clustered Multi Connectivity UP architecture

The user plane architecture is illustrated by Figure 7-36, where clustered multi-connectivity is an enhanced version of LTE dual connectivity where more than one SeNB can be supported in the cluster.
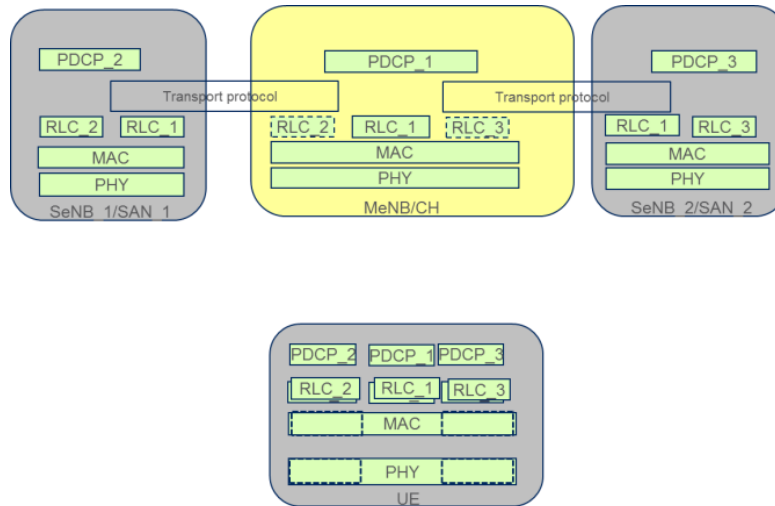


**Figure 7-36: Multi-connectivity user plane protocol architecture**

## Clustered Multi Connectivity CoP architecture

Note that the Control plane scope is examined by WP5 though it is worth to consider while we are describing the overall system architecture. There are two alternatives for multi-connectivity for control plane as illustrated by **b** in Figure 7-37.
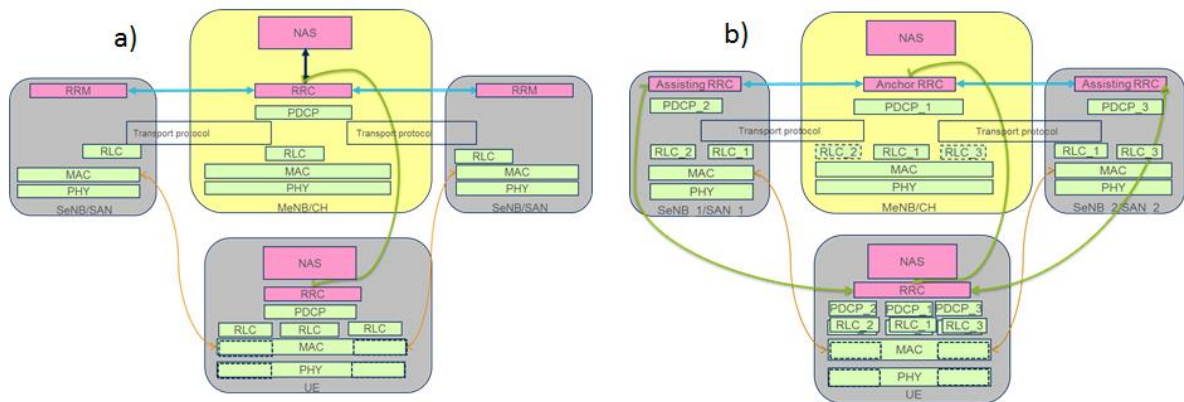


**Figure 7-37: Clustered Multi Connectivity CoP alternatives**

On the other hand, the clustered multi connectivity works in different modes to meet different network configurations which are depending on UE capability and application requirements. The modes can be classified into two types,

- robustness oriented mode and

- throughput oriented mode.

## Clustered Multi Connectivity Architecture and interfaces

The clustered multi connectivity architecture, as illustrated on Figure 7-38: Clustered Multi Connectivity Architecture and Air interfacesFigure 7-38, and interface for multi connectivity in 5G is as below. For the control plane, still only MeNB has interface with CN (core network), MeNB and SeNB reuse existing interface between them for cluster management purpose. It is not decided whether there is any cluster management related signaling between SeNB and MeNB. The responsibility for MeNB is that it is the single contact to core network. It is responsible for add, remove, change other SeNBs in the cluster. Beam switching within MeNB, beam switching between MeNB and SeNB, beam switching between one SeNB to another SeNB is under the control of MeNB. SeNB is responsible for beam switching within SeNB and may also be responsible for beam switching from it to another SeNB.
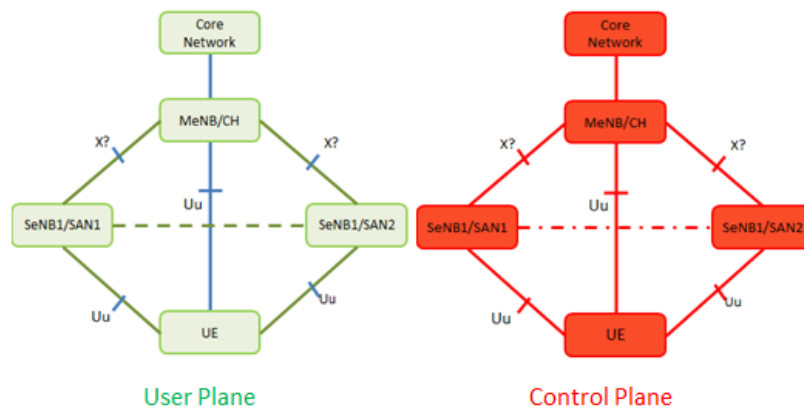


**Figure 7-38: Clustered Multi Connectivity Architecture and Air interfaces**

## Clustered Multi Connectivity CoP architecture

Note that the Control plane scope is examined by WP5 though it is worth to consider while we are describing the overall system architecture. There are two alternatives for multi-connectivity for control plane as illustrated by Figure 7-37.

a. Alternative **a** is only one RRC entity at MeNB/CH which can communicate with the RRC entity at UE. When SeNB/SAN needs to configure its local radio resources between it and UE, SeNB/SAN needs to first encapsulate its RRM message into an X2 message and transmit it via backhaul to MeNB/CH. And then MeNB/CH delivers that RRM message from SeNB/SAN to UE. Similarly, when UE sends measurement report, even this measurement report is SeNB/SAN related this message is received by MeNB/CH. MeNB/CH then checks the measurement report, if some of the information is related to SeNB/SAN, composes a new message and forwards it to SeNB via backhaul.

b.  The protocol architecture of alternative **b** is shown in Figure 7-38, where both MeNB/CH and SeNB/SAN have its RRC entity which can communicate with the RRC entity at UE. There is only one RRC state between UE and the network/cluster which is determined by the RRC connection between UE and MeNB/CH. The advantage of this alternative is that it can react fast to local radio resource configuration events between SeNB/SAN and UE.

### Mode selection in Clustered Multi Connectivity

The clustered multi connectivity works in different modes to meet different network configurations which are depending on UE capability and application requirements. The modes can be classified into two types,

- robustness oriented mode and

- throughput oriented mode.

Robustness oriented mode has two sub-mode, fast switching or diversity. Fast switching means UE only communicate with one eNB in the cluster at one TTI. Which eNB serves UE is according to the instantaneous channel quality between UE and different eNB in the cluster. The eNB with the best channel quality will serve UE. Diversity means more one than eNB communicates with UE concurrently in one TTI, and they transmit the same packets to UE. Throughput oriented mode means more than one eNB communicate with UE concurrently in one TTI with different packets.

For user plane message transmission, robustness oriented mode and throughput oriented mode are all possible which depends on many factors. If different frequencies are used in the cluster, throughput oriented mode can be selected. Then over the backhaul, MeNB will transmit different packets to different SeNB. And correspondingly, each eNB in the cluster will transmit different packets to UE so that throughput is increased. If single frequency is used in the cluster, i.e. different eNBs in the cluster interfering each other, then robustness oriented mode should be selected. Similar as user plane signaling message transmission, if resources over backhaul is not a problem, then use diversity mode over backhaul, i.e. MeNB transmit same packets to all SeNB in the cluster. If resource over backhaul is an issue, MeNB only transmit packet to one SeNB when it knows that SeNB has good channel quality with the UE. If resource over air interface is not an issue, use diversity mode over air interface. That is, more than one eNB serve UE concurrently. If resource over air interface is limited, use fast switching mode over air interface. That is, only one eNB serves UE in one TTI.

# C.2      Evaluation: UP aggregation of LTE-A and novel AI

In this section, a simulation study is presented, where we compare throughputs of two user plane aggregation PDCP solutions in DC (dual connectivity) scenarios between LTE-A and

novel 5G: *flow aggregation and flow routing*. The standardization of the new AVIs has just started but early consensus on certain aspects have been assumed within METIS-II such as shorter TTI and larger subcarrier spacing see section 4.1.1.

## Simulation assumptions and deployment models:

The parameter settings are given below. Table 7-5 summarizes the most important parameters used in the simulation experiments. The deployment model is the 3GPP case 1 with typical urban channel model, as illustrated by Figure 7-39. The LTE and new AIV nodes are co-sited and a number of different potential 5G frequency bands are investigated which are 2, 2.6, and 15 GHz. Note that all signaling is ideal, i.e. all RRC signaling is always received correctly. This means that there are no handover failures.

**Table 7-5: Simulation parameters**

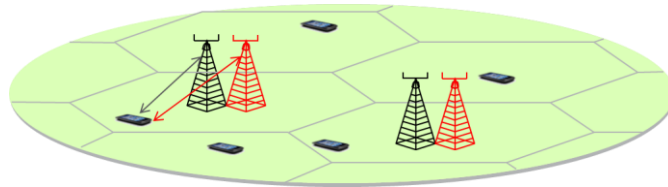| Parameter | LTE-A | New AIVs |
|---|---|---|
| Carrier Frequency | 2 GHz | 2.6 and 15 GHz |
| Bandwidth | 20 MHz | 20 MHz |
| TTI | 1 ms | 0.2 ms |
| Subbands per 20 MHz | 100 | 20 |
| Deployment | Lte and 5G co-sited | Lte and 5G co-sited |
| Traffic | FTP download of one 10 MB packet. | FTP download of one 10 MB packet. |
| User speed | 10 m/s | 10 m/s |
| Backhaul | Ideal | Ideal |
| RAT selection | RSRP | RSRP |
| DC selection | RSRQ | RSRQ |
| BS Tx power | 40 W | 40 W |

**Figure 7-39: 3GPP case 1 hexagonal cell layout, LTE and 5G is co-sited deployment.**

## Simulation Results:

Recall that, the results associated to the new 5G AIVs which are described in Section 4.1.1, where a CP-OFDM based AIV with flexible numerology is proposed. The simulation results compares following three options;

- *Flow routing* (flow switch) is modeled with UP switches between the radio links happening with zero delay, since there is no need to signal when one AIV or the other is being used.
- *Flow aggregation* packets are simply transmitted simultaneously over both AIVs.
- *Hard handover* is used as our baseline case, modeled as a 300 ms service interruption delay.

Figure 7-40 shows the user throughput performance vs. the load (throughput per cell). LTE-A is here using 2.0 GHz and the new AIV is using 2.6 GHz. The 90th percentile user throughput gain at low load for flow aggregation is around 80% compared to flow routing (named dual connectivity in figure) or hard handover and around 100% gain for the 10th percentile. Thus, in DC case, when the bandwidth is doubled the user throughput is also almost doubled at low load compared to stand alone deployments.

Apart from providing resource pooling, seamless mobility and reliability, a main advantage is that it applies for UE with single transceivers. It is worth mention that the switching might require some signaling although much lower compared to hard handovers (since it is transparent to the CN and relies on existing PDCP functions). Figure 7-41 compares the user throughput performance vs. the cell throughput when reducing the TTI from 1 ms (as in LTE-A) to 0.2 ms for the flow routing alternative. There is a clear benefit due to the benefit of lower TTI since the congestion window size which increases much faster with 0.2 ms, which in turn increases the user throughput. That can be explained by Figure 7-42.

The top sub-figure of Figure 7-42 shows the total user throughput in time and the bottom sub-figure shows the TCP congestion window size. The bottom congestion window size sub-figure clearly shows the benefit with lower TTI since the congestion window size increases much faster with 0.2 ms, which in turn increases the user throughput. Since the reduced TTIs leads to a smaller round-trip time, the TCP congestion window will grow more rapidly which can be clearly seen in Figure 7-42, which in turn increases the user throughput.
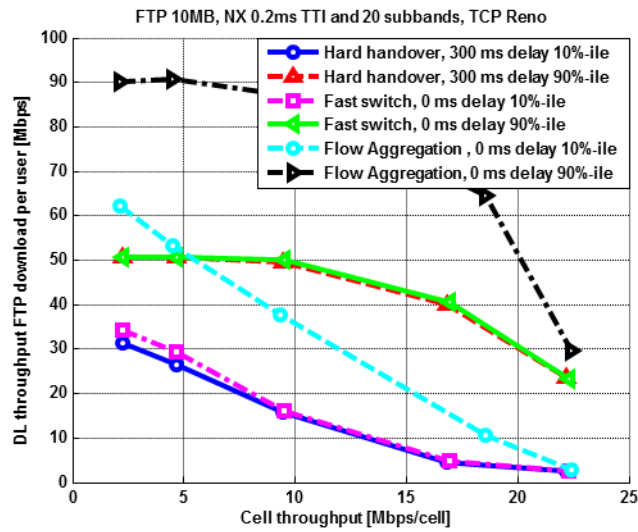
**Figure 7-40: User throughput vs. cell throughput (load) for different features enabled by the tight integration: LTE on 2 GHz and novel 5G AI on 2.6 GHz.**
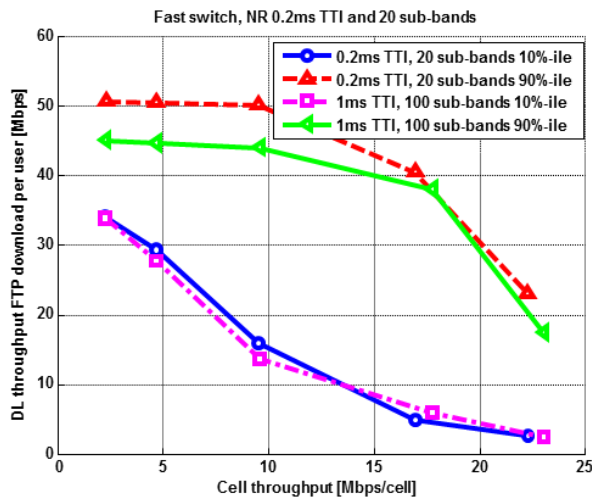


**Figure 7-41: Difference between LTE-A and novel 5G AI (i.e. LTE with 0.2 ms TTI and fewer sub bands) for fast user plane switch. LTE is using 2 GHz and new AIV with 2.6 GHz**
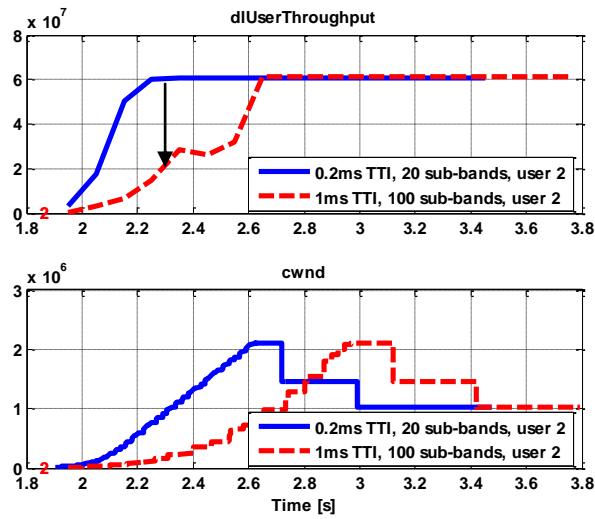
**Figure 7-42: Time-plot of LTE-A and novel 5G AI performances after user switches access. a) User throughput. b) TCP congestion window. The reduced TTI allows the user to reach the maximum congestion window and finish the slow start.**